Ruben Patel

Surveillance of marine resources by use of stationary platforms and Autonomous Underwater Vehicle (AUV)

Thesis for the degree doktor ingeniør

Trondheim, December 2006

Norwegian University of Science and Technology
Faculty of Information Technology, Mathematics
and Electrical Engineering
Department of Electronics and Telecommunications

NTNU
Norwegian University of Science and Technology

Thesis for the degree doktor ingeniør

Faculty of Information Technology, Mathematics and Electrical Engineering
Department of Electronics and Telecommunications

ISBN 978-82-471-0203-9 (printed version)
ISBN 978-82-471-0217-6 (electronic version)
ISSN 1503-8181

Doctoral theses at NTNU, 2007:10

Printed by NTNU-trykk

Contents

Preface

This dissertation is written for the degree of Doctor Engineer. The work has mainly been carried out at the Institute of Marine Research (IMR) in Bergen and at the Acoustic Group of the Department of Telecommunications at the Norwegian University of Science and Technology (NTNU). During the working period, 2001-2005, I have been involved in other interesting projects at the IMR. Although this has slowed the dissertation, the effort has been worthwhile. The following institutions have worked as partners during this work: SIMRAD, Norwegian Defence Research Establishment (FFI), Norwegian Underwater Intervention (NUI), Nortek AS and the Institute of Ocean Sciences (IOS). This work was financed by the Norwegian Research Council grant No. 143539/431, No. 130889/122 and by the IMR.

Acknowledgements

During my work I have had the privilege to meet many people. Firstly, I would like to thank my co-supervisor Dr. Olav Rune Godø for help, advice, letting me into other interesting projects and giving me great freedom during the work. I will also thank my supervisor Professor Jens Martin Hovem for introducing me to acoustics, going through the work and taking care of the administrative processes. John Kristensen, Dr. Per Espen Hagen and Bjørn Hjalving are thanked for help and cooperation while working with the Hugin software system during and after my stay at Kongsberg Simrad (KS) in Horten and at the Norwegian Defence Research Establishment (FFI) at Kjeller. Ole Bernt Gammelsæter, the late Erik Stenersen and Are Johansen thanked for helping in running the EK60s at the observatory. I am grateful to Geir Lasse Kaldestad, John Seim and the rest of the former NUI Explorer team for hardware implementation and piloting the NUI Explorer during testing and experimentation. I am particularly thankful to Terje Torkelsen for his excellent field-working and engineering abilities, and for establishing and maintaining the observatory in Ofoten. Lene Vestrheim is thanked for help in establishing and maintaining the Ethernet connection between the Institute and observatory.
Egil Ona is thanked for interesting discussions, good advice and his contagious enthusiasm. Some of the experiments were done using RV “Johan Hjort” and RV “G.O. Sars”, and I would like to thank the crew, engineers and scientists participating on these cruises for making it possible to perform the fieldwork and collecting necessary data. I would like to thank Dr. Svein Vagle and Grace Kamitakahara-King for taking care of me during the stay at the Institute of Ocean Science in Canada and Dr. David Farmer for scientific help, great hospitality and letting me live at his house during the stay at the University of Rhode Island in USA.

Morten Kvamme is thanked for his artistic work. The idea was to make one illustration for each article in this thesis. All the illustrations are based on the artist’s view of the articles and have been created without any consultation from me. I also want to thank my mother and father for unconditional support and believing in me. My brother is thanked for interesting discussions and always making me go a step further. Åse is thanked for always making me laugh and giving me energy. Hege and Eva Lene are thanked for the effort in correcting Paper 2.

Ruben Patel Bergen, 2006

List of papers

1. Patel, R., Jalving, B., Godø,O. R. 2001.The Hugin concept, Hugin as a multi platform for marine research. I Congreso International de Ciencia y Tecnologia Marina, Pontevedra, abril, 2001, 8 pp. (Published)
2. Patel, R. 2004. Remote Controlling Windows Applications. Dr. Dobb's journal, June 2004, pp 12-20. (Published)
3. Patel, R., Handegard, N. O., Godø, O. R. 2004. Behaviour of herring (*Clupea harengus* L.) toward an approaching autonomous underwater vehicle. ICES Journal of Marine Science. 61: 1044-1049. (Published)
4. Patel, R., Ona, E. 2005. Calibration and data correction on stationary bottom mounted transducers. Manuscript, 18 pp. (Manuscript)
5. Patel, R., Godø, O. R. 2005. Diel variation in acoustic density of overwintering Norwegian spring spawning herring (*Clupea harengus* L.*)* as observed from a moving vessel and stationary bottom mounted platform. Manuscript, 19 pp. (Manuscript)
6. Patel, R., Godø, O. R. 2005. Observing behaviour of overwintering herring (*Clupea harengus* L.) in Ofoten with Acoustic Doppler Current Profiler. Manuscript, 18 pp. (Manuscript)

My contribution to the attached papers

Paper 1
The HUGIN concept, HUGIN as a multi purpose platform for Marine Research.
Authors : R.Patel, B. Jalving and O.Godø.

Own originality
Implementation of EK60MK1 into the HUGIN AUV. Work done on the plugin manager and EK60MK1 plugin.

Beyond the state of the art
Design of an IPC/TCP bridge that enables us to remote control the EK60MK1 while it is integrated in the HUGIN AUV.This is the fist attempt in integrating an EK60MK1 into the HUGIN AUV system.

Paper 2
Remotely controlling windows applications.
Author: Ruben Patel

Own originality
Software development, design and testing. Experiment design and supervision.

Beyond the state of the art
Implementing and using a transmission protocol to the EK60MK1 while integrated in the HUGIN AUV. Transmitting commands and receiving data trough an acoustic link from the EK60MK1. Viewing real-time echogram from the EK60MK1 in the HUGIN AUV while on mission.

Paper 3
Behaviour of herring (Clupea harengus L.) towards an approaching autonomous underwater vehicle.
Authors: Ruben Patel, Nils Olav Handegard, and Olav Rune Godø

Own originality
Experiment design and supervision. Methods and calculation of avoidance distances.

Beyond the state of the art
Remote navigation of a acoustic sensor platform during *in situ* data collection.
Calculations of avoidance distance form the HUGIN AUV.

Paper 4
In-situ calibration of deep bottom mounted echo sounder systems.
Authors : Ruben Patel and Egil Ona

Own originality
Data comparisation, correction formulas and calculations.

Beyond the state of the art
Remote calibration setup and calibration with ROV of cabled acoustic sensors.

Paper 5

Diel variation in acoustic density of overwintering Norwegian spring spawning herring (*Clupea harengus* L.*)* as observed from a moving vessel and stationary bottom mounted platform.

Authors : Ruben Patel and Olav Rune Godø.

Own originality

Methods, calculations and data analysis.

Beyond the state of the art

Mapping of herring vertical stratification with stationary echo sounders. Comparing acoustic data between a stationary system and a moving vessel. Establishing biological diurnal variation and connection with local time and sun height. Show that there is less difference between day-night from the stationary system than there is from a moving survey vessel.

Paper 6

Observing behaviour of over-wintering Herring (Clupea harengus L.) in Ofoten with Acoustic Doppler Current Profiler

Authors : Ruben Patel and Olav Rune Godø

Own originality

Experiment setup. Methods and calculations.

Beyond the state of the art

Integration of echogram and ADCP information. Fish mainly move with the water mass. An additional movement away from the shore and vertical sinking indicate a circular movement of the herring mass.

Summary

In this thesis I investigate, describe and demonstrate new platform technology and its application in fisheries research. The first task was to prepare an Autonomous Underwater Vehicle (AUV) for payload integration (Paper 1). The instrument to be integrated into the AUV was a SIMRAD EK60 scientific echo sounder. Space limitations of the AUV demanded physical modifications. The EK60 software was designed for manual operation. To overcome the associated problem for remote control in accordance with the communication protocol of the AUV, a new version of the EK60 had to be designed and implemented (Paper 2). A field trial was performed to test the payload integration, including steered and autonomous runs; communication between the topside mother vessel and EK60 in the AUV, and the avoidance of the target species in the area (Paper 3).

The application of observation technology, with continuous recordings over time, gives a true representation of the temporal dynamics of density and vertical distribution without spatial resolution. This approach is complementary to snapshot research vessel surveying with area coverage assuming nil temporal effect. It may be particularly useful in areas of high dynamic activity, such as the Ofoten fjord area. An acoustic observatory was established in this area. Calibration of the main transducers needed special attention due to the expected depth effects on performance (Paper 4). The stationary transducers give the collected data an excellent temporal resolution at the sacrifice of spatial resolution. This makes it an ideal tool for studying vertical migration patterns. It is also important to compare these data with those collected from a moving research vessel (RV) (Paper 5). The lack of spatial resolution made it difficult to get any information about the fish school movements. Deploying an Acoustic Doppler Current Profiler (ADCP) as a unit of the observatory (Paper 6) gave this information including the potential of assessing biomass flux in and out of the fjord.

1. Introduction

Traditionally, scientific surveys have been done through quasi-synoptic coverage of the geographical distribution of the organisms of interest. Scientific surveys using acoustics and bottom trawl are described by Simmonds and MacLennan (2005) and Doubleday and Rivard (1981). Surveys are repeated annually using the same methodology at the same time of the year. Standardisation is assumed to improve reliability of estimates of marine populations from one year to the next.

Nevertheless, present methodology may suffer from inappropriate handling of temporal processes. In addition to diurnal variation the duration of a survey is long enough for the horizontal and vertical fish movements to significantly affect results. If the fish follow an annual cycle other than the fixed calendar schedule of the survey, the picture will not be comparable from survey to survey. New survey conditions may arise if environmental conditions change over time. Godø and Wespestad (1993) show that at low stock abundance and when a population is comprised of young fish, cod are distributed close to the bottom. In contrast, when abundant year-classes attain an age of 2-3 year, their distribution is more likely to be pelagic.

An ecosystem approach in the management of marine resources, demands detailed information on the dynamics and interaction among fish species and fish-plankton interactions. Scientific surveys of today are not designed for this complex task. The focus has been to assess abundance of individual stocks by area. There is a demand for a more advanced coherent and holistic approach. This requires models that perform well and are able to tackle the temporal dynamics of the organisms, including correct predator-prey distribution overlap and relevant migrations. These models need better representation of the in-situ biology in time and space. To gain forecasting abilities there is a need for appropriate continuous observation systems, which provide the required data to the models.

Due to the technological advances in underwater observation and communication technology the time is overdue to reconsider the methodology and technology to meet the challenges of the ecosystem approach. The objectives here are to demonstrate that AUV and observatory techniques may become important tools for the ecosystem approach. The motivation for this thesis is biological, but the problems are of a technological nature. This thesis will demonstrate technological solutions that respond to the challenges set by the ecosystem approach.

More specifically, the goal of this work is primarily to implement and test the performance of acoustic sensors operated from two different platforms; an AUV and a stationary observatory. Papers 1 and 2 describe the technical solutions associated with the implementation of these sensors in the AUV while Paper 3 describes the application of AUV with sensors in a biological context. Paper 4 describes some of the technical challenges to be overcome in operation of sensors at deep water, while Papers 5 and 6 demonstrate results from studies of herring.

This synthesis try to see the six paper in a larger context. First I give a short historic overview of AUV and observatories. This is followed by a more general discussion on

properties of AUV and stationary systems and potential for combination of data from these two technology regimes. The results from Papers 1 to 6 is revisited under this perspective. Lacks and limitations for routine applications in marine science are discussed. The synthesis is ended with some concluding remarks.

1.1 History

Stationary sampling stations (observatories) has a longer history than AUVs. Observatories have gone from ship-based sampling stations to fully automatic samplers sending their data to shore through different telecommunication links. A few pioneering ocean observatories over the last 30 years have allowed scientists and engineers to gain valuable experience in maintaining and running them and have demonstrated the scientific value of data from such systems. The Ocean Weather Stations (OWS) were established after World War II to guide ocean-going vessels (Committee on the Implementation of a Seafloor Observatory Network for Oceanographic Research, 2004). Hydrographical station "S" was implemented in 1954 and is one of the world's first significant ship-based sampling stations, and supports The Bermuda Atlantic Time-series Stations (BATS) which focuses on characterizing, quantifying and understanding the carbon biochemistry (Michaels and Knap, 1996). The SOund Surveillance System (SOSUS) was built in late 1950's to detect, follow and classify Russian submarines. The end of the Cold War rendered the possibility of using the hydrophone array in scientific research and it has now been used for acoustic thermometry and seismic (Fox et al., 1995) and marine mammal monitoring.

The first AUVs were developed for oceanographic research and military exploration in the late 1960's and successfully tested in the early 1970's. The development of AUVs speeded up in the 1980's and 1990's (Fernandes et al., 2003). This was due to development of underwater communication, underwater positioning systems and Inertial Navigation System (INS). Other factors include battery technology, the shrinking size of electronic components and low powered electronics.

1.2 AUV and observatories

Traditionally abundance estimation is done by mapping the horizontal density distribution of the stock e.g. by acoustics or bottom trawling. An acoustic assessment can in theory be done automatically using an AUV, but is normally not directly possible using a stationary system. Observatories gives good temporal resolution and the data can be used to study small-scale processes. Combining observatory data collection and AUVs gives an autonomous spatio-temporal coverage that is not yet utilized.

Properties of AUVs

The advantage of using AUVs is associated with the freedom of no physical attachment to the mother vessel. Compared to using a towed body, survey speed is increased by 60-70% and line turn is reduced from hours to minutes (Chance and Northcutt, 2000). The ability to do more advanced survey tracks can reduce survey time and reduce the amount of redundant data collected (Sonnier, 2004).

The unique ability of AUV's to follow bottom topography is a big advantage for surveying the near bottom fish species. The acoustic dead zone (Ona and Mitson, 1996) is reduced the closer the echo sounder transducer gets to the bottom and this is further reduced by aligning the transducer with the bottom slope. The surface dead zone can also be reduced by using an upward pointing transducers. When running the AUV too close to the target organisms a platform effect may occur as exemplified in Paper 3 when approaching herring with the NUI Explorer .

The untethered and autonomous nature of AUVs allow them to survey and measure in areas otherwise unavailable. Under ice surveys have been performed for marine research studies (Fernandes and Brierley, 1999) and for laying fibre optical cables (Ferguson et al., 1999). The platform stability is independent of the weather conditions so high quality data are collected under all conditions. The weather limitation for AUV's lies in the recovery system not on the AUV itself.

The surface limitation of traditional Research Vessels makes it necessary to collect deep-sea data remotely. Using an AUV enables the researchers to bring their instruments close to the objects of interest and collect high quality data.

Major drawbacks of using AUVs are their limited range, power capacity and speed. These three factors are connected and associated with the size of the power banks that take a vast amount of valuable space in the AUVs. Size and weight of the AUV are limited by costs that increase with these two factors. The energy that can be drawn from batteries varies with water temperature, which is normally dependent on water depth and geographic location. Prediction of AUV range may also be difficult due to varying currents.

The untethered and autonomous nature of AUV's makes them vulnerable to damage and loss. During autonomous operation Autosub was stuck beneath a sub sea overhang (International Ocean Systems, 2000) but was later rescued by an ROV from the mother vessel. The large high speed military AUV Marlin was lost during a test run in the English channel due to an initialization error (International Ocean Systems, 2001). This AUV was recovered after a couple of days when found on a beach. NUI Explorer was lost twice when trapped by a sub sea hydrographical boundary layer at 15 meters depth. Its last mission ended at 3000 m outside the coast of Angola when damaged during recovery after a bottom-mapping mission. The AUV was located, but the insurance company cancelled the rescue operation due the high cost.

Properties of Stationary observatories

Automatic observatories has low running costs and can be served by a small crew. Data are sampled continuously and can, in many situations, be accessed in real-time. When the infrastructure is established, sensors can share power sources and communication lines, which means sharing expensive underwater cables, surface buoys or other equipment. Establishing an observatory represent a onetime investment in instrumentation, deployment and infrastructure, followed by reduced running costs. In budget terms this means difficult to establish but easy to run.

An observatory might include instrumentation located from the sea floor to surface. Subsurface observatories take measurements unbiased by weather conditions, while surface or near surface instrumental observations are susceptible to wind and waves. The necessary robustness makes them operative in virtually all weather conditions and long operational duration, their stationary and autonomy makes them ideal for establishing long term detailed time series at a low cost. The excellent temporal resolution gives researchers the possibility to study the process and nature of dominating incidents and when they occur. Another important quality in observatories that deliver real-time data is that phenomena can be studied when they occur (Lashkarin and Lowder, 1996). This gives researchers a unique chance to adjust the sampling effort according to special incidents. The lack of spatial resolution makes it impossible to calculate geographical gradients that are essential to study complex dynamical interactions (Schofield and Glenn, 2004).

It is important to know the characteristic of the actual deployment area and some historical knowledge should exist. It is also important to know how the observation point reflects the surrounding area and to which geographical extent these gathered data could be used. Local effects, as for instance, small local maelstroms, temperature anomalies and biological aggregations, should be mapped.

The observatory presented in this thesis focuses on monitoring characteristics if the biology in the water column by means of acoustic sensors.

2. Implementation

In this thesis I equipped an AUV (Papers 1 and 2) and an observatory (Paper 4) with acoustic sensors for application in marine research. Some results are presented in papers 3, 5, and 6, but additional data are presented in the following sections to underline the technological advantages represented by the development.

2.1 AUV and earlier work

AUV varies in size and shape, which are normally determined by the assigned type of task. The PURLII is a small and portable AUV and was used to get a snapshot of the temperature structure within a small lake (Laval et al., 2000). Some AUVs have the ability to hold position. This makes them more suitable for close inspection tasks. The Cetus 1 is used for mine searching and automatic classification and uses three vertical thrusters when in hovering mode (Trimble, 1999). The ABE AUV is used for stereo photography of the seafloor and has the ability to hover and manoeuvre in all three axes independently (Singh et al., 2000). AUVs for rapid inspection of large underwater structures are described in Yu and Ura (2004). Here they use a system of several AUVs linked with a “smart cable”. This is a cable that can report its 3D structure and hence the relative position of all AUVs is available. The linked AUVs navigate by recognized landmarks. Although most of today’s AUVs are driven by electrical power, some AUVs use other means of propulsive energy. One example is the R-One AUV (Ura and Obara, 2000). This is a full submersible AUV driven by a closed cycle diesel engine system. This means that it has to transport fuel, oxygen and absorption tanks for the exhaust gas. Solar driven AUVs have been developed and

tested for experimental purposes (Ageev, 1999). Their problem is the low utilization of the potential power from the sun.

There are two main structural configurations for AUVs. The flooded structure has internal pressure containers with underwater cables between containers. In the second main configuration the pressure container is used as the hull. This reduces the waste space and weight, which in turn affect the operational cost according to Smith et al., (2001). The AUV used in this research has a flooded structure.

Many basic systems in AUVs remain the same, independent of operations. In many scenarios only payload sensors have to be changed. Therefore AUVs are normally divided into: Payload, navigation and control systems. In Paper 1 these three systems are described for the Hugin vehicle.

Some marine biology studies using AUVs have been described. Fernandes and Brierley (1999) demonstrated an AUV in autonomous mode operated from a mother ship. The same AUV was also used to study Antarctic krill beneath sea ice (Fernandes et al., 2003), and Brierley and Thomas (2002) found three times more krill under ice than in the open water. The launch and recovery of AUVs in harsh weather conditions might be a problem due to waves. Using a sheltered harbour as a launch and recover site for a survey will extend the weather conditions for AUV operation, as was done with the Autosub (Griffiths et al., 1998; Millard et al., 1998).

The AQUA EXPLORER 2000 was fitted with small-scale passive sonar. Using the sonar the AUV could detect whale sounds and from this information in one experiment could follow and study the Humpack whale (*Megaptera novaeangliae*) around the Kerama Islands in Okinawa (Iwakami et al., 2002).

The Hugin class AUV, which is used in this research (Paper 1,2 and 3), has been used extensively in bottom mapping for the oil industry and for mine hunting. In this thesis I investigate avoidance distance for the Norwegian Spring Spawning Herring (NSSH) towards an approaching AUV (Paper 3). The study done by Fernandes et al., (2002) report passing herring schools by 7 m and 10 m using the Autosub-1 AUV. It is important to notice that this study was focusing on fish avoidance form the survey vessel.

2.2 Stationary observatory and earlier work

Existing observatories have to our knowledge not been equipped with scientific echo sounders for assessing fish and plankton. Rather than going through observatories in general I will focus on challenges and opportunities in using scientific echo sounders in observatories. These sounders need to be calibrated in order to compare data trough time, between instruments and for absolute biomass estimation. In our case thus a new challenge was apparent. How can a bottom-mounted system be calibrated remotely and routinely? The Simrad EK60 scientific echo sounder is used in our stationary system. A standard method for calibrating hull mounted transducers is suggested by Foote et al. (1987). But different approaches are used depending on the measurement set-up and platform holding the transducer. Ona and Vestnes (1985) physically tilted RV Eldjarn in order to measure the equivalent beam angle on a hull-mounted single beam transducer. Dalen et al. (2003) calibrated a transducer mounted on a towed body

relying on the random pendulum movements of suspended calibration sphere. MacLennan and Simmonds (1992) used a fixed calibration sphere while tilting the towed body and recording the tilt angels. A similar procedure was used in Paper 3 where the AUV was manually tilted over a fixed calibration sphere. In Paper 4 we use an ROV to get our calibration sphere closer to the transducer. Due to the depth and currents it would be impossible to suspend the sphere from the surface mounted winches as suggested in Foote et al. (1987).

The calibration data (Paper 4) was used to correct previously recorded acoustic data before the analysis in Paper 5. The stationary system has a better temporal resolution then the data from the moving RV. The layer depth and thickness, biologically determined diurnal periods and duration is therefore studied from this system (Paper 5). Huse and Korneliussen (2000) and Fréon et al. (1996) studied diurnal variability from a moving vessel. Some of the methods in this work are used in Paper 5. It is assumed that the bottom-mounted system produces temporal unbiased data in contrast to the vessel data due to vessel avoidance as reported in (Olsen, 1990; Olsen et al., 1983; Olsen, 1971; Soria et al., 1996; Fréon et al., 1992). Due to the lack of spatial resolution in the stationary double counting of will occur. In order to perform biomass estimation, the swimming speed of the fish schools must be known.

Using the split beam information from the EK60 swimming speeds and directions can be estimated for single fish by tracking the target through the acoustic beam (Ona and Hansen, 1991; Handegard et al, 2005). Because this method relies on non-over lapping echoes, the technique is limited to more dispersed fish aggregations. Earlier studies shows that for denser schools an Acoustic Doppler Current Profiler (ADCP) can be used. Roe and Griffiths (1993) demonstrate that different biological information can be obtained from routine ADCP operation. Zedel et al. (2003) used a moored downward looking ADCP to observe swimming speed of over-wintering and migrating herring in the Vestfjorden and Ofotfjorden in northern Norway. Paper 6 uses an EK60 and ADCP to measure swimming speed of over-wintering herring in Ofotfjorden in northern Norway, in addition an algorithm to remove speed anomalies is implemented.

2.3 AUV ; Methods and Results

The HUGIN class is a series of AUVs originally intended for detailed bathymetric seabed surveying and for mine hunting. In collaboration with the partners it was my first task to turn the vehicle into a flexible multi-sensor platform where sensors could be easy to added or removed. To add this functionality a redesign of the software architecture was needed. Paper 1 gives an overview of the HUGIN system and describes the basic system architecture and operation. In order to get an indication of the underwater radiated noise from the AUV, noise measurements were made at a military measurement station used for measuring combat submarines and other military vessels. The noise measurements showed that the AUV radiated less noise than the mother vessel, RV “Johan Hjort” did at a distance of 2 nautical miles while laying still. This was evident since the noise from the AUV could not be detected due to the noise from the RV at the measurement station (Paper 1).

The next step was to implement the main sensor, an EK60 scientific echo sounder, into the AUV. This sensor can only be controlled through a graphical user interface (GUI). The goal was to be able to control it from the mother vessel and view real-time data from the sensor under AUV survey operation. Due to the slow acoustic communication link between the AUV and the mother vessel data had to be compressed before transmission. In Paper 2 a detailed description and the practical solution to the problem of remote controlling such a system is presented as program code.

The final objectives were to test the AUV in steered and autonomous modes. In the steered mode, the AUV was run directly underneath the mother vessel so that there is continuous communication between the two vessels. In this mode a direct comparison of the AUV EK60 data recorded by the mother vessel is possible. In Autonomous mode a pre-programmed survey is downloaded into the AUV and the AUV runs a survey without communication to the mother vessel. The measurements are used to calculate the avoidance distance from the AUV. Paper 3 describes the autonomous and steered survey in addition to the avoidance analysis.

The first survey was planned in the winter of 2001 immediately after a bottom mapping survey for the oil industry. During this survey the NUI Explorer was wrecked by the stern propeller of the mother vessel due to miss-communication on the bridge. This halted the project for one year.

Some field testing was done in the waters outside Bergen. These tests revealed some problems of electrical and acoustic interference. The electrical interference was traced to the power source; this was reduced by connecting electrical filters on the power cable to the EK60. The acoustic interference was due to other acoustic equipment on the AUV, the only way to avoid this was to turn off the interfering equipment. Since the source came from the AUV's basic sensors used for safe navigation this could not be done.

The new software architecture implemented a payload processor into the AUV (Paper 1). The payload processor is a dedicated computer where all the communication between payloads and the rest of the AUV is handled. Since each new payload has its own communication language, there has to be written a specific piece of code for each payload. These small programs, called payload plug-ins, act as the bridge between sensors and the payload processor. All the payload plug-in connect to a payload manager which acts as a container and administrator, routing messages from the AUV to the correct plug-in.

Since the EK60 scientific echo sounder could only be controlled through a GUI a special program was designed. The program taps directly into the Windows message queue (Pietrek, 2001). This technique can in principle be used to control other windows applications. The program listened for messages from the EK60 plug-in running on the payload processor. These messages were translated to Windows events, which is a message generated when a user presses a button or enters text in a text box on an application. When the correct Windows messages were sent into the Windows message queue, the parameters of the EK60 program were changed accordingly and the program could thus be remotely controlled.

When the AUV was run in steered mode the parameters of the EK60 could be altered and real-time data from the sensor could be viewed onboard the mother vessel. The autonomous mode demonstrated that the AUV could be used in parallel with the mother vessel activities. Analysis of data gathered by the EK60 revealed that the over-wintering herring showed an avoidance distance of 5-10 m from the AUV (Paper 3).

With modern software design, new sensors are easier to connect to the AUV, although there might be some physical problems due to size and form of the instrumentation. The plug-in design hides the complexity of the AUV architecture for the developer. This makes it easier to focus on the functionality of the payload to be integrated.

The remote controlling mechanism for the EK60 worked well. Care should be taken when controlling programs remotely that are not designed for this. In principle, one needs to know all the different responses the application could deliver as a result of user interaction. One error could freeze the whole application as the application waits for users to acknowledge its warning or error box. GUI objects can take some time before they appear, or close but this is usually not a problem since the user is many times slower than the GUI.

When running the AUV in steered mode the manoeuvrability is restricted by the mother vessel. In addition, the mother vessel is focused around the AUV and there is little room for other tasks to be performed. This is the cost of being able to steer the AUV and retrieve real-time data. In Autonomous mode no real-time data can be obtained, but the mother vessel is available for other tasks.

The 5-10 m is a relatively short avoidance distance shown by the fish. It confirmed the indication from the radiated noise measurements that the HUGIN AUV is a quiet vessel (Paper 3) taking into account the reactive behaviour of herring (Vabø, 1999). This is a promising result when considering using the AUV for detailed close-up studies of marine life.

2.4 Stationary observatory; Methods and Results

The observatory focuses on recording data on Norwegian Spring Spawning Herring during their over-wintering including the immigration and emigration. The two bottom-mounted EK60 scientific echo sounders were wired to shore to give continuous access to the data. This is the same instrumentation as used for RVs during annual herring surveys in this area (Foote et al., 1997). Additional instrumentation has been added for shorter or longer periods for testing specific features.

To secure quality scientific data from the bottom-mounted transducers there was a need to establish methodology to calibrate them. Due to the depth of the transducers it was not possible to use standard echo sounder calibration methods as used for ships (Foot et al., 1987). Paper 4 describes the methodology developed and demonstrates how to verify the resulting measurements. To the authors' knowledge, a ROV was used for the first time ever, to bring the calibration sphere into the acoustic beam of a transducer. The method opens for routine calibration to secure stable performance of the instrumentation over time.

EK60 data hold information on migration speed and direction of fish movement when echoes are resolved and target-tracking methods can be used (Handegard et al., 2005). In order to obtain this information when fish echoes overlap, an Acoustic Doppler Current Profiler (ADCP) was deployed as part of the observatory (Paper 5). Data from the EK60 were used to verify that the ADCP could adequately reflect the signal strength of the schools. Fish speed inside the schools was calculated and analyzed. This gave the migration speed of the schools.

Using stationary EK60 sensors gives a different view of the herring stock compared to the quasi-synoptic surveys carried out annually in the Ofoten area (Røttingen and Tjelmeland, 2003). In Paper 5 these differences are studied. The stationarity of the bottom-mounted EK60 gives data with excellent temporal resolution. This has proved efficient in studies of distribution and migration dynamics, uncovering details not available from conventional surveys. Some examples are presented below.

Three different instruments were connected during the main study period: an ADCP, a sidescan sonar and an EK60. Figure 3 shows a more detailed map pinpointing the geographic location of each instrument.

Due to heavy fishery activity there have been incidences of cable rupture most likely from illegal bottom trawling in the area or hooking by gillnet moorings. The harsh weather conditions have resulted in power failure due to waves smashing the fuse box and physical movement of the cabin resulting in disconnecting power cables to computers.

Nortek AS contributed with a Continental Current profiler (Nortek, 2001). This is a 193.5 kHz ADCP with a range of 200 m, used to observe the migration speed of herring in the upper layer (Paper 6).

The Institute of Ocean Science (IOS) in Canada provided a 12 kHz side-scanning sonar (Farmer and Trevorrow, 1999). This sonar has the potential for fish detection out to horizontal ranges of up to 7 km, providing spatial coverage significantly greater than that achieved with conventional echo sounders or net trawls. The data was not analysed in this thesis due to lack of sound speed profiles during the measuring periods.

The basic acoustic system consists of a 40-element (20λ), 12 kHz sidescan array. The 12 kHz operating frequency was selected as a compromise between low acoustic absorption while maintaining modest transducer directivity. Additionally, 12 kHz components were readily available commercially. The sidescan array has a total length of 2.49 m, yielding a horizontal transducer beamwidth of 2.8° (to -3dB) and is made up of model TR-229 Tonpilz piston elements assembled in a linear array and calibrated by EDO/Western. In the vertical plane, the array elements have a beam width of 122° and a front-to-back ratio of -6 dB. The transmitting power response of the array on the forward axis is unknown because of undetermined losses in the 300 m cable used to connect the array with the transceiver unit and logging computer back on shore. The array and sonar transceiver has a bandwidth of approximately 10%, or 1.2kHz.

SIMRAD designed two identical 38 kHz EK60 split-beam systems (Simrad, 2001) whose transducers are depth rated to 1500 m. The main task of this instrumentation is to measure the dynamics of herring in density by depth and time in the observatory area.

The connection point of the infrastructure are sheltered in a cabin on land. At the first attempt to run the ADCP, a radio link to the cabin was established. This tended to fail due to antenna movements caused by waves. Instead, data were stored internally in the instrument. This again reduced the amount of data collected and deployment time due to storage limitations.

The sonar and the EK60 units are connected to computers in the cabin through underwater cables. The sonar transceiver was placed in the cabin. This transceiver and array were connected to a Pentium PC-based system for data acquisition, processing, display, and data storage. Data acquisition and logging operations were performed within a program developed by the IOS. This also provided a graphic user interface for real time data display. Figure 1 shows a block diagram of the sonar system.

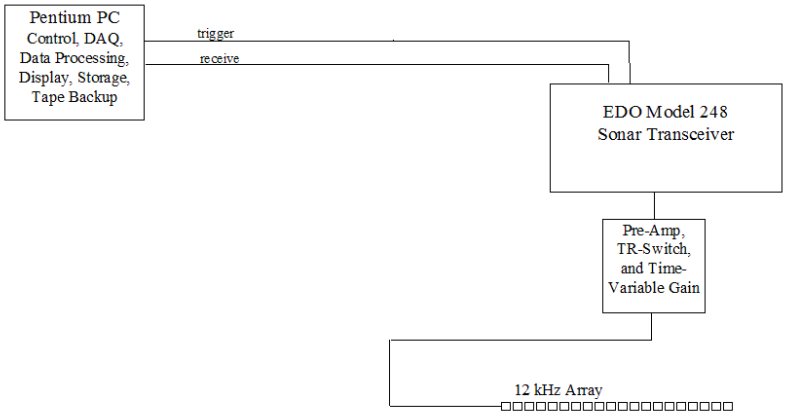

Figure 1. Block diagram of the components and connections for the sonar.

The EK60 general-purpose transceivers (GPT) were placed in an underwater unit connecting them to the transducer with a one-meter long cable. Such short transducer cables reduce the noise, which is estimated to vary between –120 dB to –130 dB for the outer transducer and between –118 dB to –126 dB for the inner transducer. The underwater cable delivers power to the GPTs and transmits digital data to and from the PC in the cabin. Power is delivered through an UPS, Variac and over-voltage protection to secure against short-term power failures; remove some noise interfering with the data gathering and to protect equipment connected to the power net. Figure 2 shows the power and data infrastructure.

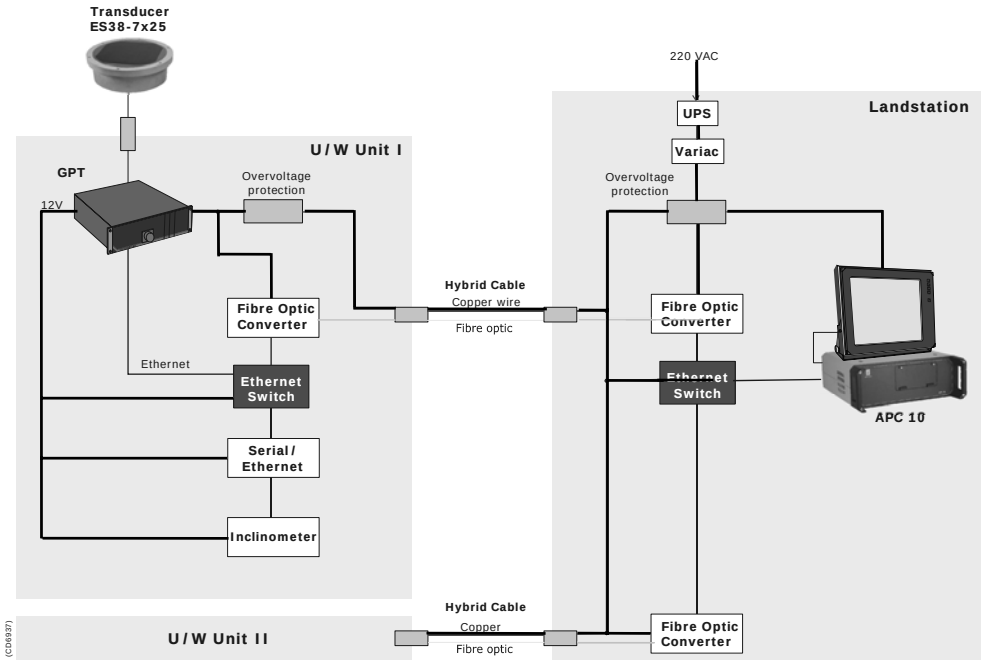

Figure 2. Block diagram of the echo sounder system. Thick lines indicate power lines and thin lines indicate data lines. The diagram for Underwater (U/W) unit II is identical to U/W unit I.

In order to get the correct time stamp on all data and synchronize time between the instruments a GPS unit was mounted in the cabin. This was connected to the EK60 PC and the PC's time was corrected according to GPS time every 10th minute to avoid time drift. The sonar PC updated its time every 15 minutes from the EK60 PC through the Ethernet connection.

To access data a threadless Ethernet connection was established between the cabin and the nearest broadband connection at Løddingen, which is a town located in sight across the fjord. A connection point to the Ethernet was established. This gave access to one of the instrumentation computers and the Ethernet of the cabin from IMR. Using terminal emulator software, the screen from the EK60 computer could be accessed directly giving full control over the instrument data collection software. A data-streaming server was established using the Microsoft media encoder software. This enabled users all over the world to view real-time data from some of the instrumentation. The EK60 system gathers around 1.5 MB/min and the Sonar gathers around 1.7 MB/min. Total data rate is then 2.2 MB/min.

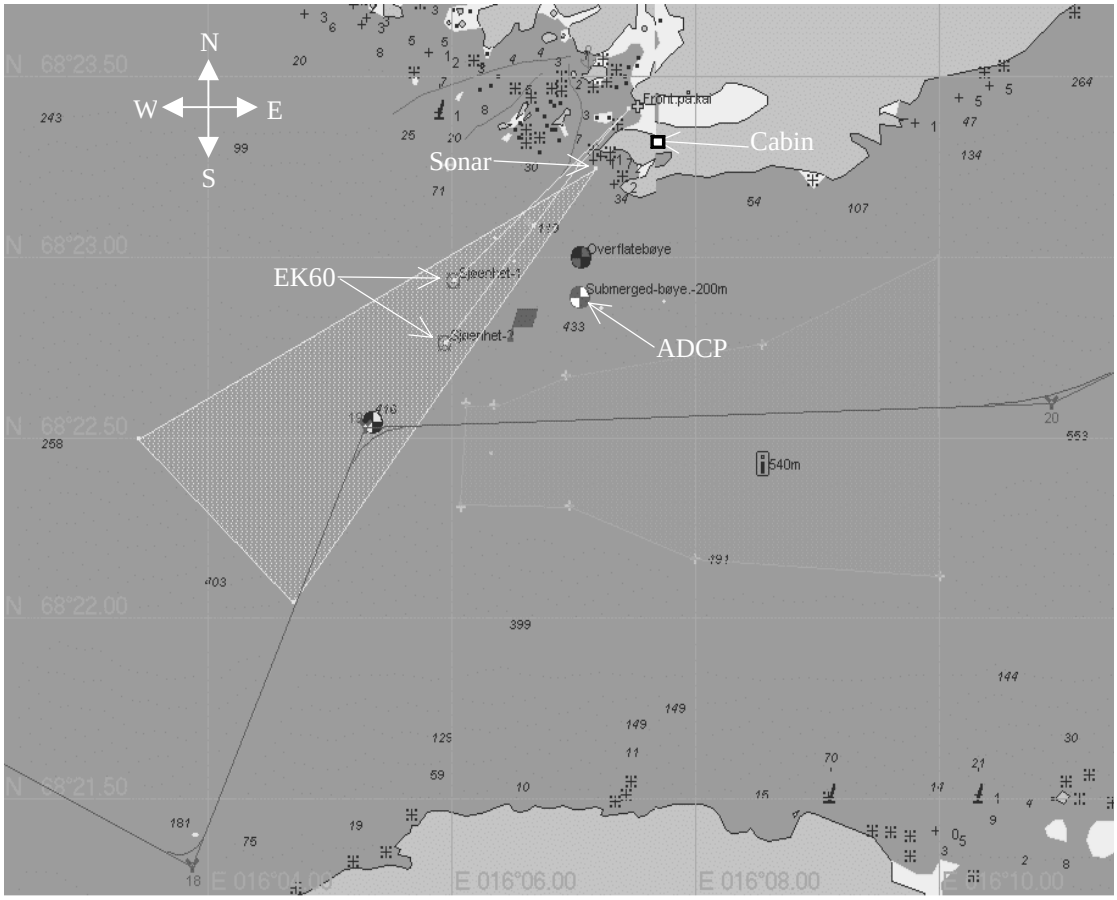

Figure 3. Geographic location of the instrumentation. Triangle grid indicates the horizontal coverage of the sonar.

The inner EK60 transducer was placed at a depth of 400 m and the outer at a depth of 500 m with the transducers separated by a distance of 415 m. The ADCP was lowered to a depth of 150 m. Distance from the outer transducer to the ADCP was 800 m and the distance from the ADCP to land was 600 m. Due to restriction in the cable length and bottom topography the sonar was placed at a depth of 12-15 m. Distance from the inner transducer to the sonar was 1000 m. Bottom topography along the sonar direction is shown in Figure 4. The horizontal sound propagation of the sonar is affected by the sound speed profile in the water. Figure 5 shows the sound ray path for two typical sound speed profiles during wintertime. Calculations show that there is a tendency for a sound channel in the upper layer. This is especially true for the lower panel in Figure 5.

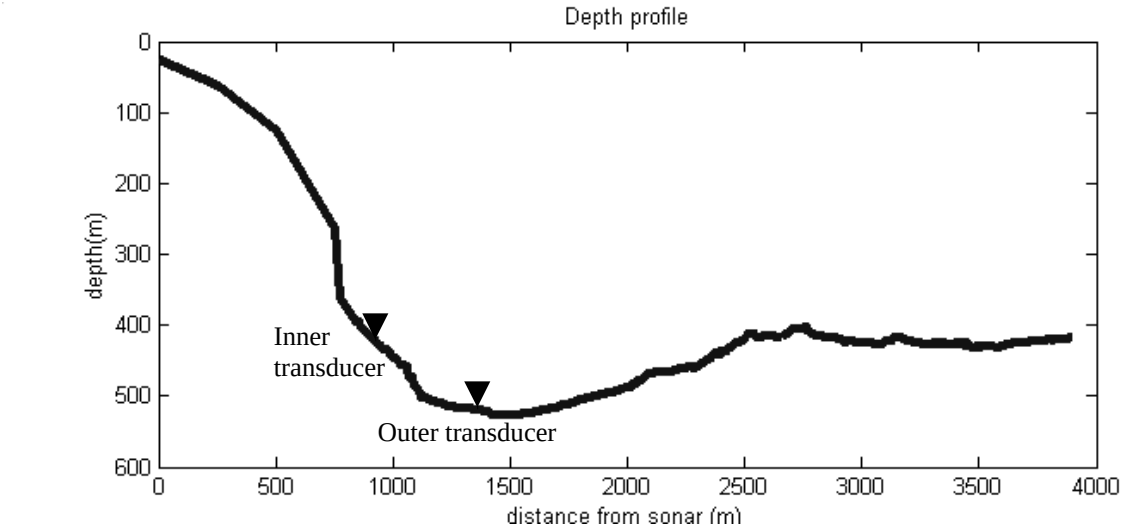

Figure 4. Bottom topography along the sonar beam direction. The sonar is positioned at a distance of 0 meters. Triangles indicate position of the two EK60 units.

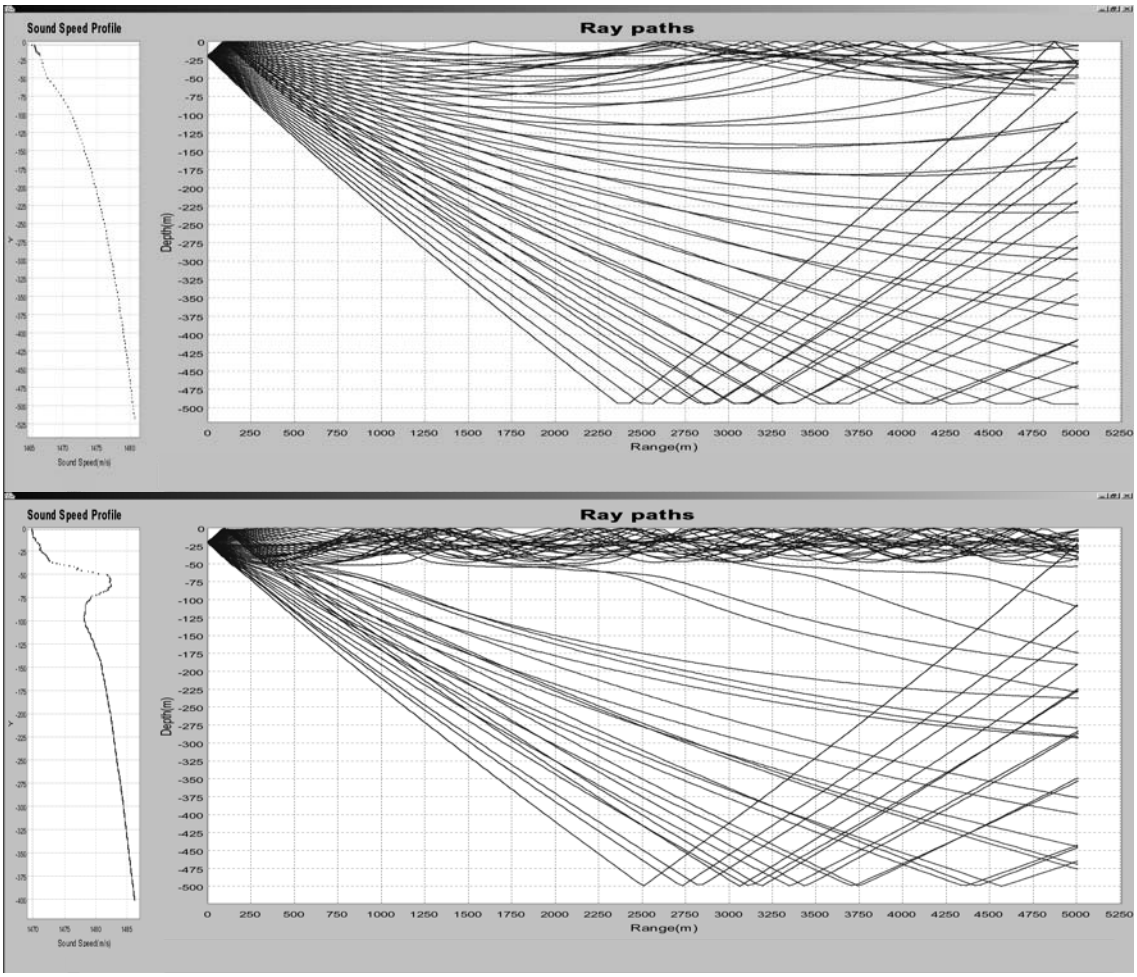

Figure 5. Sound propagation for two typical sound speed profiles during the over wintering period of herring in the Ofotfjorden.

Observatory technology gives excellent temporal resolution. This enables us to do detailed studies and observations of biological possesses in the ocean not possible from a moving RV. During the over-wintering phase of herring they typically separate into two layers (Paper 6). Figure 6 shows fish transportation that occurred between the two layers. By showing that the transportation appears around the same time for the inner and outer transducer, one can conclude that this process, at a minimum, ranges over the distance between the transducers which is around 400 m. As similar movements go both ways between the two layers the phenomenon is supposed to represent a natural biological process but can also be triggered by predators or vessels passing nearby.

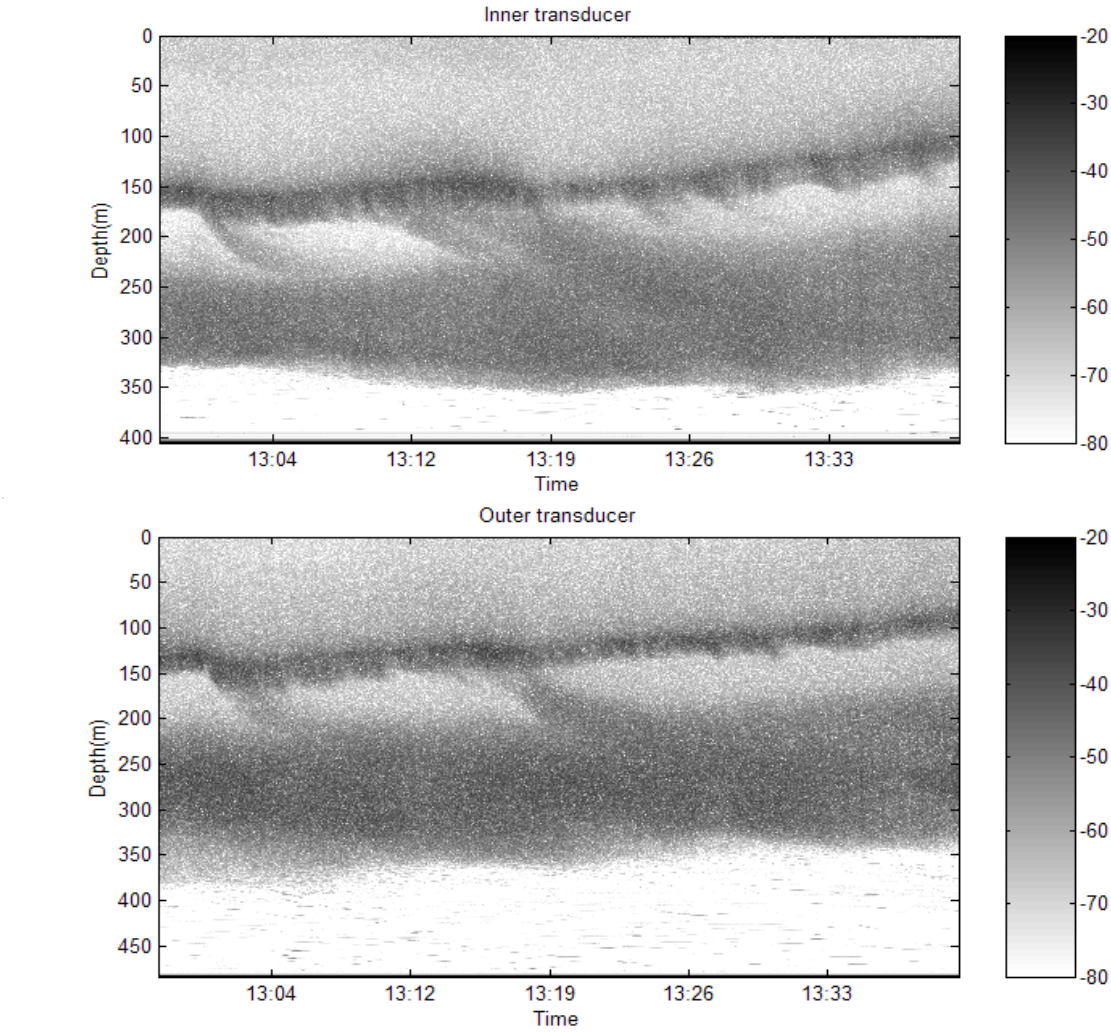

Figure 6. Transport of biomass between herring layers. Upper panel shows data from inner transducer while lower panel shows data from outer transducer. Gray scale values indicate volume backscattering in dB as indicated by the side bar.

The bottom mounting enables undisturbed observation of the upper water layers including the sea surface. This is unavailable to RVs due to the depth of their transducers. The dense aggregation of herring draws killer whales into the Ofoten where visual observation of whales is common during the wintertime. Figure 7 shows

an echogram of what, most likely, is a pack of killer whales crossing the inner transducer. This can be deduced from the swimming characteristics.

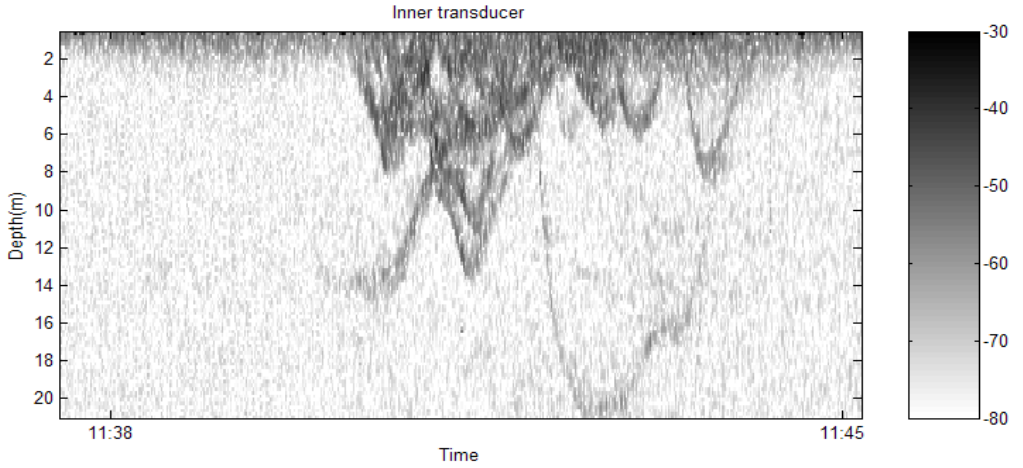

Figure 7. Pack of killer whales crossing the inner transducer. Gray scale values indicate volume backscattering in dB as indicated by the side bar.

Detailed interaction dynamics of herring and predators can be studied by observatory technology. This is demonstrated in Figure 8. At around 60 m a denser herring layer appears. From this layer it is apparent there is an ascent of herring to the surface, probably to gulp air (Thorne and Thomas, 1990). From the same layer descending herring can be seen. In between the herring, predators appear as the stronger individual echoes.

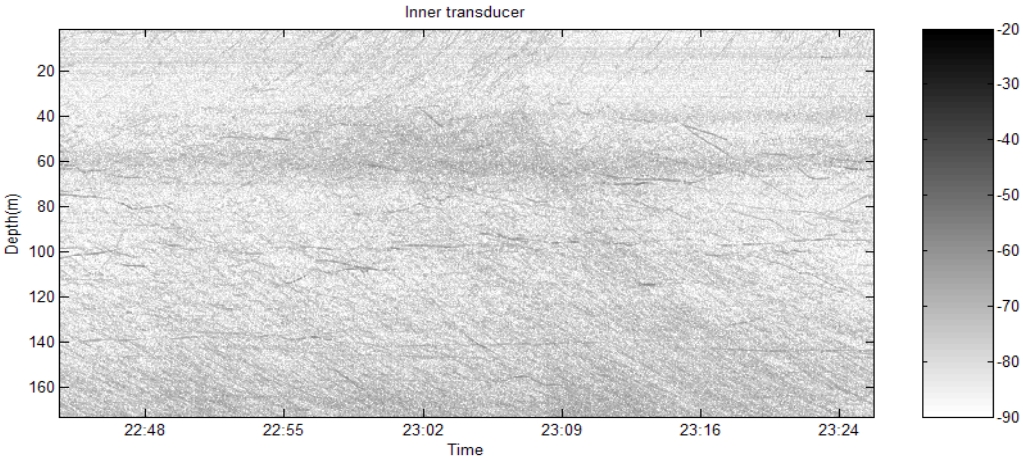

Figure 8. Herring taking in air (upper 20 m) and sinking down (below 60 m). At 60 m a herring layer is seen, it looks like the ascent and descent of herring starts from here. Predators can be seen as more dispersed single echoes inside the herring aggregation. Gray scale values indicate volume backscattering in dB as indicated by the side bar.

Outside the observatory towards Vestfjorden there is a sill. This topographic feature may produce internal waves (Osborne and Burch, 1980; Farmer and Armi, 1999). We consider the characteristic movement of the individual fish in Figure 9 may be caused by internal waves.

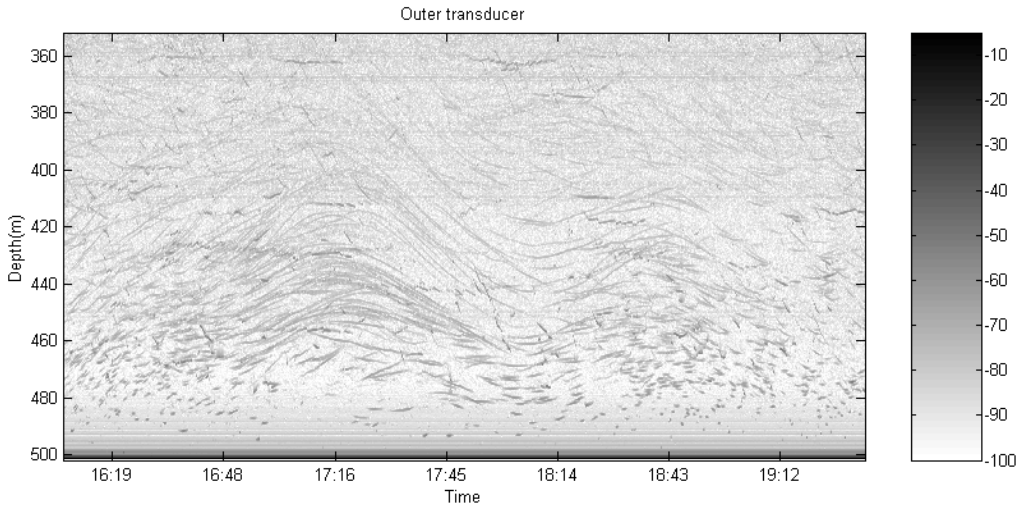

Figure 9. Internal waves influencing fish in the water mass. Gray scale values indicate volume backscattering in dB as indicated by the side bar.

The observation in Figure 9 was found by randomly examining a small subset of data. This shows the potential for detailed investigation using stationary-mounted transducers and indicates that there is yet more to be discovered in data already collected. There is a need for algorithms that can automatically examine data and pinpoint important and interesting characteristics.

Paper 4 describes in-situ calibration of a bottom-mounted transducer using a ROV. Two different measurement techniques were used. First, RV “G.O. Sars” measured the echo backscattering from the water column close to the two bottom mounted transducers, this was then compared with the echo reflections from the calibration sphere. Results show that the difference in backscattering was -0.13 dB for the inner transducer and 0.15 dB for the outer transducer. The small difference between the two measurement methods is a good indication of correct observations. Successive detections of the sphere were also used to reconstruct the 3D beam pattern of the transducer. This was done to find out if there had been any changes during and after the deployment.

Due to the lack of spatial information in data from the two bottom-mounted transducers an ADCP was deployed to study herring movements over the observatory site. This is described in paper 5. The result shows that the herring mainly float with the current in the upper 150 m. Vertical speed shows that the fish schools have a downward component compared to the water. This corresponds to sinking and was also observed by Ona (2003). In Paper 6 it is speculated that sinking is taking place in the deeper areas and the ascent along the walls of the fjord in a vertical circular movement.

The calibration results from Paper 4 were used to correct the backscattering values when comparing data with that obtained from the RV in Paper 6. In this paper data from the bottom-mounted EK60 units is used to determine timing of vertical migration; depth of fish layers and is compared to data collected from a moving RV. Timing of the vertical migration was found and defined as night from 15:50 to 07:10 and day from 09:50-12:50 during the measuring period. The depth of the layers was

estimated to be 20-70 m for the top layer at night, 160-190 m for the top layer at daytime, 110-195 m for the bottom layer at night and 290-400 m for the bottom layer during daytime. Comparison between ship data and stationary data shows that there is less difference between day and night for the stationary system compared to the ship observations. This might be due to vessel avoidance behaviour (Vabø, 1999).

3. Towards routinely usage of AUVs and stationary observatories in marine research.

This thesis demonstrates the applications of AUV and observatory in marine research application. Although an implementation (Paper 1,2,3 and 4) and usage (Paper 3,5 and 6) is demonstrated, an effort is needed to get it into routinely operations and integrate with to days monitoring strategies.

3.1 Implementation and further development of AUV

To be able to use AUVs on a routine basis tighter cooperation between research and industry has to be established. An example of important discoveries due to such cooperation is evident in Church and Warren (2002) where the HUGIN 3000 AUV discovered the German submarine U-166. Also, there is a need for a long-term national program, as carried out in the UK (Fernandes and Brierley, 2002), to get the technology into routine use and show the advantages of AUVs for Norwegian marine research.

Autonomous operations are perfectly suited, end even better than RVs due do less avoidance (Paper 3), for collecting standardised information about the environment as well as fish stocks. Over time such operation could possibly take over some of the RV tasks. The operation distance is determined by battery capacity and the possibility of taking over future marine monitoring tasks will strongly depend on improvement of this capacity.

For vessel related operations, one is interested to use the AUV to gather data supplementing or verifying that from the research vessel. Common tasks would be inspection, fish avoidance investigations (Vabø, 1999; Handegard, 2004: Paper 3) and dead zone measurements (Ona and Mitson, 1996). These operations are typical near-vessel short-term operations spanning from an hour to one day. In the inspection mode the AUV will be sent to do close-up measurements. Typically a fish school will be approached at high speed for species identification and collecting acoustic target strength data. In vessel avoidance investigations one wants to map the avoidance signature around the mother vessel. This demands that the AUV is able to move and navigate above survey speed of the RV. Acoustic dead zone studies imply running the AUV as close to the bottom as possible and to follow the bottom topography to identify and quantify organisms that are acoustically hidden from the mother vessel.

In pursuit experiments one wants to study individual moving targets over time. This can be fish schools or whales. Such a task demands a silent AUV that can track and

follow a defined target over an extensive time span without getting too close; losing it, or getting confused by another target. Such approaches might become important for understanding and quantifying behavioural dynamics, for example in relation to predator prey interaction.

The development in sonar technology and multi-frequency acoustics, enabling species discrimination (Korneliussen and Ona, 2002), will enhance the utilization of AUVs as self- sustained research platforms for detection, identification and quantification of marine life.

At this time the most critical points in the AUV development are battery capacity and AUV speed. Solar driven AUVs have been developed and tested for experimental purposes (Ageev, 1999). Their problem is the low utilization of the potential power from the sun. When solar cell technology has been developed further and enhanced to be able to meet the power needs from sensors and propulsion systems the primary limitation of AUVs will be overcome. This will bring solar driven AUVs to full autonomous capability for, with its unlimited power source, it can theoretically stay at sea for years. Unfortunately, this is more relevant for lower latitudes than in Norwegian waters where the access of light is often reduced by clouds or winter darkness.

3.2 Implementation and further development of stationary system.

Based on the experience from the Ofoten observatory we see a large potential for improvement of methodology for monitoring marine resources and the environment. The following elements are given special attention:

1) Development of specialised sensor and infrastructure technologies

2) Establishment of innovative solutions that allow marine observatories to be combined with oil industry infrastructure

3) Development of data handling and analysis systems that efficiently manage the expanding amount of data.

Development of specialised sensor and infrastructure technologies are needed to reduce instrument size, power consumption and enhance robustness. Miniaturization of instruments makes them easier to handle, more suited for underwater usage and in many cases reduces power consumption. Observatories are usually expensive to establish and have a lower cost associated with running and maintenance. Robustness is important for long-term deployment, this increases the stability and reduces the running cost of the observatory. A developed infrastructure helps coordinate and synchronize data storage, it also eases making data available to other scientists. Due to the vastness of the ocean it is unrealistic to obtain a sufficient coverage based on cabled systems. Therefore, self-sustained autonomous systems needs particular attention. An important issue is also to establish subsurface instrument platforms resistant to underwater activity like commercial fishing.

Norwegian offshore industries are world leading with respect to underwater operations, underwater infrastructure and underwater installations. There is a unique

opportunity to combine this competence and experience with the needs of the marine research community to deploy offshore sensors for long-term surveillance. The establishment of new oil and gas fields in Norwegian sub Arctic areas, with its corresponding infrastructure to land, gives a unique opportunity to deploy underwater junction boxes connected to the cable gates going to land. Due to the strong requirements of operational stability of oil infrastructure there is a need to develop solutions that prevent the potential conflicts between monitoring demands and operational stability. The newly established Expert centre of Underwater Technology (www.eut.no), a conglomerate of businesses and competence institutions in the Bergen region, has taken this onboard as a "lighthouse" project.

The need for bigger joint projects like the NEPTUNE (Neptune, 2004) observatory with its piloting test beds VENUS (Dewey and Tunnicliffe, 2003) and MARS (McNutt et al., 2003) is apparent to develop the technology and experience with equipment, interdisciplinary and international cooperation over decades. One of the ultimate goals for observatories is to minimize the cost of data sampling while maximizing the information content that can be extracted from the system. In the big picture an observatory is just a basic building block for a larger global survey system which involves real-time data from RVs, commercial vessels, and satellites. One step in the correct direction is the European EZONET project (Pride and Solan, 2003) whose goal is to link different observatories along the coasts in Europe.

Observatories can gather large amounts of data continuously, far beyond the surveys of today. This represents several challenges that need attention within data sampling, storage, reduction, compression and information extraction. For long-term observatories data storage space is critical. Intelligent sampling and data reduction are necessary to reduce the amount of data in a controlled manner, preserving the important information contents and ignoring data with no information regarding the scientific goals. Non-destructive compression will further reduce the storage space needed. Finally, efficient information extraction algorithms are needed so as to be able to utilize the data in a scientific context.

Around half a century has passed since one of the first observatories was established based on fixed stations sampled from passing ships. The development has moved toward fully automatic observatories delivering real-time data. As more and more observatories are established, the next step is to connect these in a global network and thus establish a global surveillance system. This will create further new challenges in operational modelling, parallel to those experienced earlier by meteorologists and physical oceanographers. In addition it will be necessary to go one step further by coupling physical and biological models. This is due to the fact that fish are mobile relative to the physical currents and the behaviour of the organisms has to be considered (Giske et al., 2001).

3.3 Combining AUV and stationary systems

Stationary systems and AUVs should be combined at two levels, the physical level and the data level. At the physical level one wants to utilize the infrastructure of the stationary system to prolong deployment of AUVs. This can be done by implementing underwater modems, underwater GPS and underwater docking stations (Sing et al., 2001; Stokey et al., 2001). Underwater modems is used for real-time communication between AUV and user, underwater GPS gives the AUV more precise underwater navigation abilities while the underwater docking station provide infrastructure for download collected data, upload new mission plan, report AUV status and recharge batteries.

At the data level one wants to combine the spatial data from AUV and the temporal data from stationary system. A goal is to link observations from the stationary system with the observation from AUV. To gain forecasting abilities in data models, there is a need for appropriate continuous observation systems, which can provide models with the required data. The data from AUVs gives spatial corrections to the models while the data from stationary observatories gives continuously corrections at discrete geographic locations.

4. Concluding remarks

This thesis focuses on some of the basic technological building blocks needed for global surveillance systems. So far the experience is that AUVs are still in their infancy and full utilization in standard operation demands further development in robustness, user friendliness and flexibility. Running costs are high and are a major obstacle to development by the research community. AUVs are more technologically advanced than observatories and it is clear that this technology needs maturation to become a suitable operational tool for the research community. The development of a national user forum is suggested as a vehicle to speed up development. Observatory technology has been utilized in marine research for decades. We have here demonstrated that the approach is suitable for biological research and might become important in the ecosystem approach to fisheries management by uncovering and quantifying biological processes. Simple systems are already easy and cheap to use. The potential of such systems is limited by our imagination. A full utilization demands further development of infrastructure technology as well as smaller, more robust and low-powered sensors. The development of AUV and observatory technology and utilization of these in marine research calls for an extensive interdisciplinary cooperation for establishing the technology. Just as crucial is the development of routines for operation and also models that fully utilize the information. With a focused research effort within these areas such systems can be operational for management within few years.

References

Ageev, M. D., Blidberg, D. R., Jalbert, J., Melchin, C. J., and Troop, D. P. 1999. Results of the Evaluation and Testing of the Solar Powered AUV and its Subsystems. In Proceedings from 11th International Symposium on Unmanned Untethered Submersible Technology, Durham, New Hampshire, 19–22 September 1999, 9 pp.

Austin, T., Edson, J., McGillis, W., von Alt, C., Purcell, M., Petitt, R., McElroy, M., Ware, J., and Stokey, R. 2000. The Martha's Vineyard Coastal Observatory: a long term facility formonitoring air-sea processes. Proceedings from OCEANS 2000 MTS/IEEE Conference and Exhibition, Providence, RI, USA, 11- 14 September 2000, Vol 3, pp. 1937-1941.

Axenrot, T., Didrikas, T., Danielsson, C., and Hansson, S. 2004. Diel patterns in pelagic fish behaviour and distribution observed from a stationary, bottom-mounted, and upward-facing transducer. ICES Journal of Marine Science, 61:1100-1104.

Brierley, A. S., and Thomas, D. N. 2002. Ecology of southern Ocean Pack Ice. In Advances in Marine Biology. Ed. Southward, A. J., Tyler, P. A., Young, C. M., Fuiman, L. A. Academic Press. London. 337 pp.

Chance, T. S., and Northcutt, J. G. 2000. The Hugin 3000 AUV, Sea Technology, 41(12):10-14.

Church, R., and Warren, D. 2002. Autonomous Underwater Vehicles: The Latest Tool for Archaeological Investigations. Marine Technology Society Journal, 36(3):45-50.

Committee on the Implementation of a Seafloor Observatory Network for Oceanographic Research. 2004. Lessons from Existing Ocean Observatories in Enabling Ocean Research in the 21st Century. National Research Council, pp. 28-36.

Dalen, J., Nedreaas, K., and Pedersen, R. 2003. A comparative acoustic abundance estimation of pelagic redfish (Sebastes mentella) from hull-mounted and deep-towed acoustic systems. ICES Journal of Marine Science, 60:472-479.

Dewey, R., and Tunnicliffe, V. 2003. VENUS: Future Science on a Coastal Mid-Depth Observatory. Proceedings from 3rd International Workshop on Scientific Use of Submarine Cables and Related Technologies, Tokyo, Japan, pp. 232-233.

Doubleday, W. G., and Rivard, D. 1981. Bottom trawl surveys. Canadian Special Publication of Fisheries and Aquatic Sciences, 273 pp.

Farmer, D. M., and Trevorrow, M. V. 1999. Intermediate range fish detection with a 12-kHz sidescan sonar. The Journal of the Acoustical Society of America, 106(5):2481-2490.

Farmer, D., and Armi, L. 1999. The Generation and Trapping of Internal Solitary Waves over Topography. Science, 283(5398):188-190.

Fernandes, P. G., and Brierley, A. S. 1999. Using an autonomous underwater vehicle as a platform for mesoscale acoustic sampling in marine environments. ICES Journal of Marine Science, CM 1999/M:01.

Fernandes, P. G., Brierley, A. S., Simmonds, E. J., Millard, N. W., Mcphail, S. D., Armstrong, F., Stevenson, P., and Squires, M. 2002. Fish do not avoid survey vessels. Nature, 404:35-36.

Fernandes, P. G., Stevenson, P., Brierley, A. S., Armstrong, F., and Simmonds, E. J. 2003. Autonomous underwater vehicles: future platforms for fisheries acoustics. ICES Journal of Marine Science, 60:684-691.

Foote, K. G., Knudsen, H. P., Vestnes, G., MacLennan, D. N., and Simmonds, E. J. 1987. Calibration of acoustic instruments for fish densety estimation: A practical guide. ICES Cooperative Research Report, 144:69 pp.

Foote, K. G., Ostrowski, M., Røttingen, I., and Slotte, A. 1997. Abundance estimation of Norwegian spring spawning Herring wintering in the Vestfjord system, December 1996. ICES, FF:13:1-23.

Fox, C. G., Radford, W. E., Dziak, R. P., Lau, T.-K., Matsumoto, H., and Schreiner, A. 1995. Acoustic detection of a seafloor spreading episode on the Juna de Fuca Ridge using military hydrophones arrays. Geophysical research letters, 22(2):131-134.

Fréon, P., Gerlotto, F., and Soria, M. 1992. Changes in school structure according to external stimuli: description and influence on acoustic assessment. Fisheries Research , 15(1-2):45-66 .

Fréon, P., Gerlotto,. F and Soria, M. 1996. Diel variability of school structure with special reference to transition periods. ICES Journal of Marine Science, 53(2):459-464.

Giske, J., Huse, G., and Berntsen, J. 2001. Spatial modelling for marine resource management, with a focus on fish. SARSIA, 86:405-410.

Godø, O. R., and Wespestad, V. G. 1993. Monitoring changes in abundance of gadoids with varying availability to trawl and acoustic surveys. ICES Journal of Marine Science, 50:39-51.

Godø, O.R., Patel, R. Torkelsen, T., and Vagle, S. 2005. Observatory Technology In Fish Resources Monitoring. Proceedings of the International Conference "Underwater Acoustic Measurements: Technologies & Results" Heraklion, Crete, Greece, 28th June - 1st July 2005.

Griffiths, G., McPhail, S. D., Rogers, R., and Meldrum, D. T. 1998. Leaving and

returning to harbour with an Autonomous Underwater Vehicle. Proceedings of Oceanology International 98, Brighton, UK, 14 pp.

Handegard, N.O. 2004. Cod reaction to an approacing bottom trawling vessel investigated using acoustic split-beam tracking. University of Bergen, PhD Thesis, 149 pp.

Handegard, N.O., Patel, R., and Hjellvik, V. 2005. Tracking individual fish from a moving platform using a split-beam transducer. The Journal of the Acoustical Society of America, 118(4):2210-2223.

Huse, I., Korneliussen R. 2000. Diel variation in acoustic density measurements of overwintering herring (Clupea harengus L.). ICES Journal of Marine Science. 57:903-910.

International Ocean Systems. 2000. Getting Autosub back, International Ocean Systems, 4(5):43-45.

International Ocean Systems. 2001. Now Marlin goes missing, International Ocean Systems, 5(1):48-50.

Iwakami, H., Ura, T., Asakawa, K., Fujii, T., Nose, Y., Kojima, J., Shirasaki, Y., Asai, T., Uchida, S., Higashi, N., and Fukuchi, T. 2002. Approaching Whales by Autonomous Underwater Vehicle. Marine Technology Society Journal , 36(1):80-85.

Korneliussen, R. J., and Ona, E. 2002. An operational system for processing and visualizing multi-frequency acoustic data. ICES Journal of Marine Science, 59:293-313.

Lashkari, K., and Lowder, S. 1996, MBARI Ocean Acoustic Observatory, Sea Technology, 37(6):61-66.

Laval, B., Bird, J., and Helland, P. 2000. An Autonomous Underwater Vehicle for the Study of Small Lakes. Journal of Atmospheric and Oceanic Technology , 17(1):69-76.

McNutt, M., Massion, G., Raybould, K., Bellingham, J., and Paull, C. 2003. MARS: a cabled observatory testbed in Monterey Bay. EGS - AGU - EUG Joint Assembly, Abstracts from the meeting held in Nice, France, 6 - 11 April 2003, 1 pp

MacLennan, D. N., and Simmonds, E. J .1992. Fish and Fisheries in Fisheries Acoustics, Calibration. Chapman & Hall, London, 325 pp.

Michaels, A. F., Knap, A. H. 1996. Overview of the U.S. JGOFS Bermuda Atlantic Time-series Study and the Hydrostation S program. Deep Sea Research Part II: Topical Studies in Oceanography, 43:157-198.

Millard, N. W., Griffiths, G., Finegan, G., McPhail, S. D., Meldrum D T, Pebody, M., Perrett, J. R., Stevenson, P., and Webb, A. T. 1998. Versatile Autonomous

Submersibles the realising and testing of a practical vehicle. Journal of the society for Underwater Technology, 23(1):7-17.

Neptune. 2004. Science Planning for the NEPTUNE Regional Cabled Observatory in the Northeast Pacific Ocean. Report of the NEPTUNE Pacific Northwest Workshop, Portland, pp 78.

Nortek AS. 2001. Continental Current Profiler User manual, pp 54.

Olsen, K. 1971 .Influence of vessel noise on the behaviour of herring In Modern Fishing Gear of the World. 3 ed. London: Fishing News (Books) Ltd., pp. 291-294.

Olsen, K., Angell, J., Pettersen, F., and Løvik, A. 1983. Observed fish reactions to a surveying vessel with special reference to herring, cod, capelin and polar cod. (FAO fisheries reports).

Olsen, K. 1990. Fish behaviour and acoustic sampling. Rapp. P.-v. Réun. Cons. Int. Explor. Mer., 189:147-158.

Ona, E. 2003. An expanded target-strength relationship for herring. ICES journal of Marine Science, 60:493-499.

Ona, E., and Mitson, R. B. 1996. Acoustic sampling and signal processing near the seabed: the deadzone revisited. ICES Journal of Marine Science, 53:677-690.

Ona, E., and Hansen, D. 1991. Software for target tracking of single fish with split beam echo-sounders. Institute of Marine Research, Bergen, Norway, Oct. 1991.

Ona, E., and Vestnes, G. 1985. Direct meashurement of equivalent beam angle on hull-mounted transducers. ICES. C.M. 1985/B:43.1-10.

Osborne, A. R., and Burch, T. L. 1980. Internal solitons in the Andaman Sea. Science, 208(4443):457-460.

Pietrek, M. 2001. Inside the Windows Messaging System. Dr. Dobb's Journal, Juli 2001, pp 14-20.

Priede, M., and Solan, M. 2003. The European Seafloor Observatory Network. Hydro International, 7(7):6-9.

Roe, H., and Griffiths, G. 1993. Biological information from an Acoustic Doppler Current Profiler. Marine biology, 115(2):339-346.

Røttingen, I., and Slotte, A. 2001. The relevance of a former important spawning area in the present life history and management of Norwegian spring-spawning herring. Lowell Wakefield Fisheries Symposium Series. Issue 18, 297-313 pp.

Røttingen , I., and Tjelmeland, S. 2003. Evaluation of the absolute levels of acoustic estimates of the 1983 year class of Norwegian spring-spawning herring. ICES Journal of Marine Science, 60(3):480-485.

Schofield, O., and Glenn, S. 2004. Introduction to special section: Costal Ocean

Observatories. Journal of Geophysical research, 109, C12S01, doi:10.1029/2004JC002577.

Simmonds, E. J., and MacLennan, D. N. 2005. Survey design. In Fisheries Acoustics Ed. 6, Chapman & Hall, London, pp 437.

Simrad. 2001. Simrad EK60 Scientific echo sounder. Norway. 857-164204/AA000

Singh, H., Bellingham, J., Hover, F., Lerner, S., Moran, B., von der Heydt, K., and Yoerger, D. 2001. Docking for an Autonomous Ocean Sampling Network. IEEE Journal of Oceanic Engineering, 26(4):498-513.

Singh, H., Pizarro, O., Duester, A., and Howland, C. J. 2000. Optical Imaging From the ABE AUV, Sea Technology, 41(4):39-43.

Smith, S., An, P., Holappa, K., Whitney, J., Burns, A., Nelson, K., Heatzig, E., Kempfe, O., Kronen, D., Pantelakis, T., Henderson, E., Font, G., Dunn, R., and Dunn, S. 2001. The Morpheus Ultramodular Autonomous Underwater Vehicle. IEEE Journal of Oceanic Engineering, 26(4):453-465.

Sonnier, C. 2004. 'Outside the Box': Survey by AUV. Hydro International, 8(1):56-57.

Soria, M., Freon, P. and Gerlotto, F. 1996. Analysis of vessel influence on spatial behaviour of fish schools using a multi-beam sonar and consequences for biomass estimates by echo-sounder. ICES Journal of Marine Science, 53(2):453-458.

Stokey, R., Allen, B., Austin, T., Goldsborough, R., Forrester, N., Purcell, M., and von Alt, C. 2001. Enabling Technologies for REMUS Docking: An Integral Component of an Autonomous Ocean-Sampling Network. IEEE Journal of Oceanic Engineering, 26(4):487-497.

Thorne, R. E., and Thomas, G. L. 1990. Acoustic Observations of Gas Bubble Release by Pacific Herring (Clupea harengus pallasi). Canadian journal of fisheries and aquatic sciences, 47:1920-1928.

Trimble, M. G. 1999. EOD Robotic Work Package, Cetus AUV Family, Sea Technology, 40(12):37-41.

Ura, T., and Obara, T. 2000. R-One Robot, Sea Technology, 41(7):30-34.

Vabø, R. 1999. Measurements and correction models of behavorial induced biases in acoustic estimates of wintering herring (Clupea harengus L.). University of Bergen, PhD Thesis, Bergen. 161 pp.

Yu, S.-C., and Ura, T. 2004. A System of Multi-AUV Interlinked with a Smart Cable for Autonomous Inspection of Underwater Structures. International Journal of Offshore and Polar engineering, 14(4):265-273.

Zedel, L., Knutsen, T., and Patro, R. 2003. Acoustic Doppler current profiler observations of herring movement. ICES Journal of Marine Science, 60:846–859.

Papers

Patel, R., Jalving, B., Godø,O. R. 2001.**The Hugin concept, Hugin as a multi platform for marine research**. I Congreso International de Ciencia y Tecnologia Marina, Pontevedra, abril, 2001, 8 pp. (Published)

Patel, R. 2004. **Remote Controlling Windows Applications.** Dr. Dobb's journal, June 2004, pp 12-20. (Published)

Patel, R., Handegard, N. O., Godø, O. R. 2004. **Behaviour of herring (*Clupea harengus* L.) toward an approaching autonomous underwater vehicle.** ICES Journal of Marine Science. 61: 1044-1049. (Published)

Patel, R., Ona, E. 2005. **Calibration and data correction on stationary bottom mounted transducers.** Manuscript, 18 pp. (Manuscript, not submitted)

Patel, R., Godø, O. R. 2005. **Diel variation in acoustic density of overwintering Norwegian spring spawning herring (*Clupea harengus* L.*)* as observed from a moving vessel and stationary bottom mounted platform.** Manuscript, 19 pp. (Manuscript, not submitted)

Patel, R., Godø, O. R. 2005. **Observing behaviour of overwintering herring (*Clupea harengus* L.) in Ofoten with Acoustic Doppler Current Profiler.** Manuscript, 18 pp. (Manuscript, not submitted)

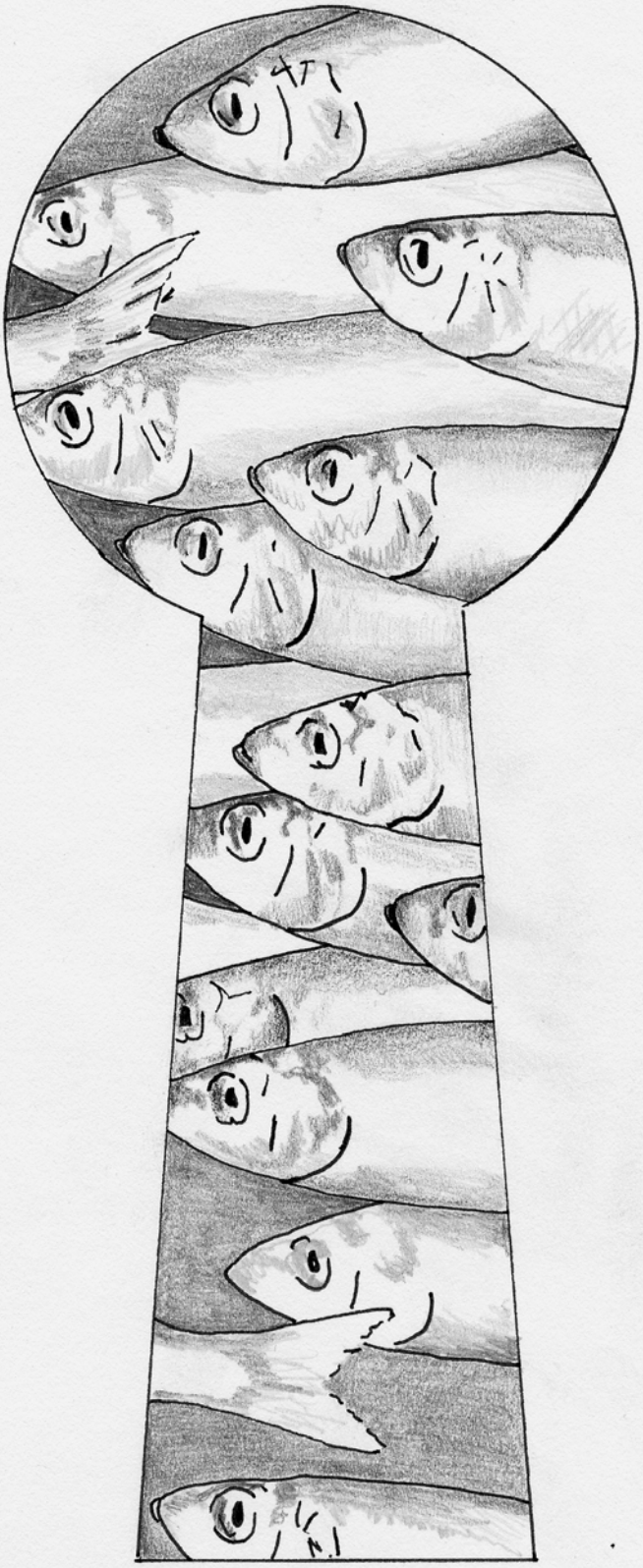

The HUGIN concept, HUGIN as a multi purpose platform for Marine Research.

R. Patel*
Institute of Marine Research, P. O. Box 1870 Nordnes
N-5817 Bergen, Norway.
e-mail: ruben@imr.no
B. Jalving
FFI – Norwegian Defence Research Establishment, P.Box 25
2027 Kjeller, Norway
e-mail: Bjorn.Jalving@FFI.NO
O.Godø
Institute of Marine Research, P. O. Box 1870 Nordnes
N-5817 Bergen, Norway.
e-mail: olavrune@imr.no

Abstract

HUGIN is a series of autonomous underwater vehicles (AUV) originally intended for detailed bathymetric seabed surveying. First a traditional HUGIN operation and the most important vehicle systems are presented. The paper presents how the HUGIN vehicles have been turned into flexible multi-sensor platforms for marine research, military research and versatile deep-water seabed mapping operations. The paper focuses on software design and the strategy for easy integration of new payload sensors.

Introduction.

Reliable monitoring of marine resources is an imperative to sustainable management of marine resources. Such monitoring has traditionally been done through scientific survey with research vessels using bottom trawl and acoustic assessment methodologies, see e.g. Gunderson (1993), and MacLennan and Simmonds (1991). Fish behaviour, either as an effect of ship disturbance or due to variable natural behaviour has in later years been shown to seriously affects survey results (Aglen, 1994;Godø, 1994). To solve these problems more sophisticated instrumentation and platforms are needed that can cope with the demands documented in the more recent studies.

During later years the development of AUVs has come to the level of commercial application. It is expected that AUV will become an important tool for marine monitoring and mapping due to their depth tolerance, autonomous capabilities, stabile and noiseless operation. Till now very few operations using AUVs for studying marine living resources has been carried out (Fernandes et al., 2000).

The HUGIN project was started in 1995 as a co-operation between Statoil, The Norwegian Defence Research Establishment (FFI), Norwegian Underwater Invention (NUI) and Kongsberg Simrad AS (KS). The object was to design an untethered vehicle for high-resolution seabed mapping down to about 2000m (Vestgård and Kristensen 1998).

Two prototypes, HUGIN I and HUGIN II has been built and tested. These are both rated to 600m. One vehicle, the HUGIN 3000, sustaining 3000 m depth, is sold for commercial usage to C&C Technologies Inc.

The Institute of Marine Research (IMR) in Norway aims at establishing survey methodology for absolute abundance estimation of marine resources within Norwegian jurisdiction within

the next 5 years. This challenge is not unique to Norway. By developing an AUV carrying the appropriate instrumentation we believe that our ability to study many of the problems related to behavioural aspects will be highly improved through close and silent observation from this platform. Some typical examples of problems in current methodologies are listed below. Fish close to surface that are unavailable from the bottom mounted transducer of the research vessel can be studied from an AUV with an upward looking transducer. Running the AUV close to the bottom can minimize the effect of bottom acoustic dead zone. Detailed information on the acoustic properties of single fish can be obtained through running the AUV close to the individuals of interest. Using towed bodies can in some cases solve the problems, but towing speed and cable length restrict this approach (Dalen and Bodholt., 1998). Further, noise from the cable can also affect the fish and make this an inappropriate approach to reliable studies of mobile organisms.

In this paper the development of HUGIN as a multipurpose platform with particular emphasis observing marine life, will be described. Concepts and solutions that demonstrate HUGIN's abilities to run a survey with a range of sensors simultaneously will be presented. This paper will also focus on the software designed to meet these challenges.

We will first give an overview of how the HUGIN vehicle is operated on a survey and a more technical overview of the HUGIN internals [KB00] [KJKV98]. This is followed by a detailed technical description of the plugin and multi platform concept in HUGIN. The Navigation and Control processor is then overviewed. Finally we describe how the EK60MK1 is connected to the HUGIN system.

HUGIN Operation.

Launch and recovery

The AUV is deployed from a launch/recovery system located at the stern of the mother ship. The vehicle executes the survey according to a programmed mission plan. When initiated by the mission plan or commanded by the operator, the vehicle ascends to the surface using its propulsion system. Upon reaching the surface, the vehicle drops its nose cone and releases a retrieval line. This line is used to pull the vehicle onto the launch/recovery ramp system projecting into the water from the stern of the mother ship. Se Figure 1.

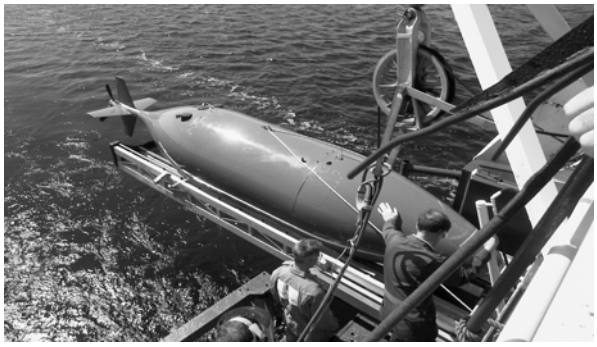

Figure 1. Launch of HUGIN 3000 on R/V Simrad Echo

UUV mode

In UUV (untethered underwater vehicle) mode HUGIN is operated close to the mother ship. The acoustic links function as an "acoustic tether", which enables the operator to supervise operation and control the vehicle in general. Operator interaction could for instance be optimisation of the survey sensor parameters or reprogramming of the mission plan. For example, should hazards be located along a pipeline route, the mission can be altered for closer inspection. The mission plan is a set of waypoints and altitude, depth and propeller speed references as well as commands for controlling mission modes, payload sensors etc.

In the mother ship, the AUV position is tracked by combining Differential Global Positioning System (DGPS) and Super Short Baseline system (SSBL) data. Combined DGPS-SSBL position data is transmitted to the AUV navigation system to bind the position drift.

During the survey, subsets of the payload and the vehicle data is compressed and transmitted to the surface and displayed as real-time plots and status windows, providing on-line quality control of the collected data. The HUGIN Operator Station also includes a chart view, displaying the "mission plan", mother ship position and vehicle position and heading.

AUV mode

In AUV mode HUGIN operates independently of the mother ship. In this mode the operator does not have real-time supervision or control of the vehicle. The navigation system position drift is bounded by DGPS fixes at the surface at regular intervals or operation within a pre-calibrated transponder array (LBL) navigation system.

For surveying of a limited area (for example a site survey), the Aided Inertial Navigation System (AINS) can maintain good position accuracy with only Doppler Velocity Log (DVL) aiding. A prerequisite is that the dive phase is limited (when the DVL has no bottom track) and that the vehicle mission geometry is optimised to cancel out most of the systematic error growth. A favourable geometry is the "lawnmower" pattern.

Basically, the difference between UUV mode and autonomous mode is the presence of a mother ship transmitting position updates.

Noise measurements.

The HUGIN vehicle was noise measured at a military acoustic measuring station lying at Hegreneset in Norway. The facility has locations for dynamic and static measuring. The dynamic measurement is used for moving vessels. This location has two buoys, each with two hydrophones attached. The hydrophones and buoys can be individual regulated in depth. The target position is tracked during the measurement. Centre depth is 380 meters. There is some background noise from ship traffic and two fish farms nearby. Figure 2 shows the set up for the dynamic noise measurement.

In our experiment we positioned the survey vessel J.Hjort about 2 nautical miles away from the station. HUGIN was run trough the dynamic measurement location 13 times holding a speed of 3-4 knots.

Data from all the run shows that noise from J.Hjort is totally dominating at a distance of two nautical miles. We did not get the measurements we wanted and will try to repeat this

experiments under better conditions, to get a complete noise image of HUGIN. This is important for further research on how HUGIN affect fish during a survey.

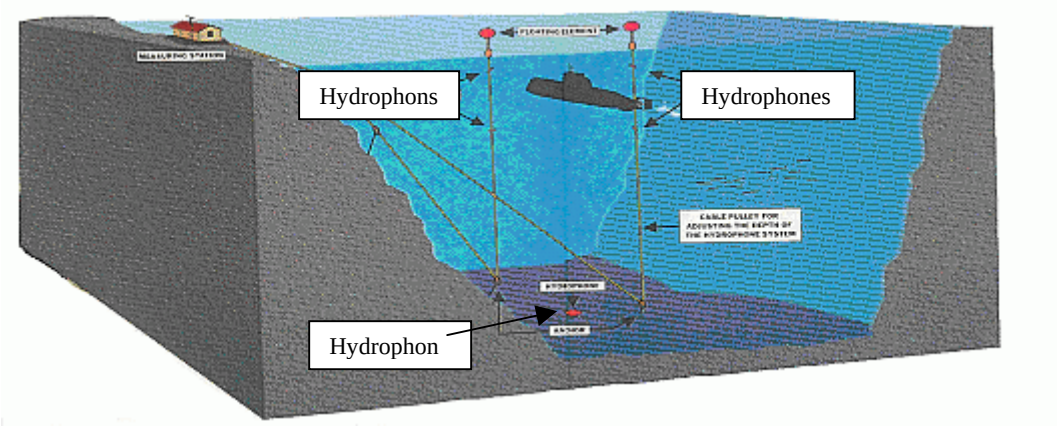

Figure 2 Dynamic range in Herdlefjord

HUGIN system overview.

The bottom side consists of tree computers together with payload and HUGIN basic sensors. These tree computers makes the core in HUGIN and is linked together on a LAN, they are called Control Processor (CP), Navigation Processor (NavP) and Payload Processor (PP).

When HUGIN is submerged all communication with topside has to go through the CP. CP also has responsibility to rout the messages to PP,NavP or CP itself. Some basic sensors is also connected CP.

NavP has the navigation responsibility; it will give the other processors access to navigation data and handle tasks as auto-heading, auto-depth and auto-height as well as detecting critically operation condition for emergency accent.

PP is used to handle additional user payloads; the PP will be the communication gate between the payloads and the rest of the system.

The topside system consists of the HUGIN Operation Station (HUGINOS) and the different payload OS'es. Upper half of Figure 3 shows the topside. When the vehicle is submerged all communication from topside has to go trough the HUGINOS. This is why the payload OS'es is connected to HUGINOS as shown in Figure 3.

It is important to get a module-based design; this makes it easier for error detection and upgrading the system. As we can se form Figure 3 the design of the AUV is reflected at topside, where each payload has its own payloadOS. This yields also for the core computers, but is less clear in the figure.

Figure 3 shows an overview of the HUGIN system. The upper left half shows the topside and the rest is bottom side. Stippled lines show the communication paths when HUGIN is on deck. This communication is done using physical connection and TCP/IP protocol. In this

way we can get access to all tree processor and all the payloads. This makes it easy to download data and upgrade software.

The pointed lines show the radio and acoustic links. The radio link (RFL) is used when HUGIN is emerged and lying in the sea. We have tree acoustic links; Acoustic command link (ACL), Acoustic data link (ADL) and Acoustic emergency link (AEL). The ACL is used to send commands down to HUGIN, it operates on a speed of 55 b/s. ADL carries the data from HUGIN to topside, and the link operates on a speed of 2000 b/s. The transponder telemetry capabilities of the acoustic position system (HiPAP) are also used for AEL. The AEL link can be used to send emergency ascend messages to HUGIN.

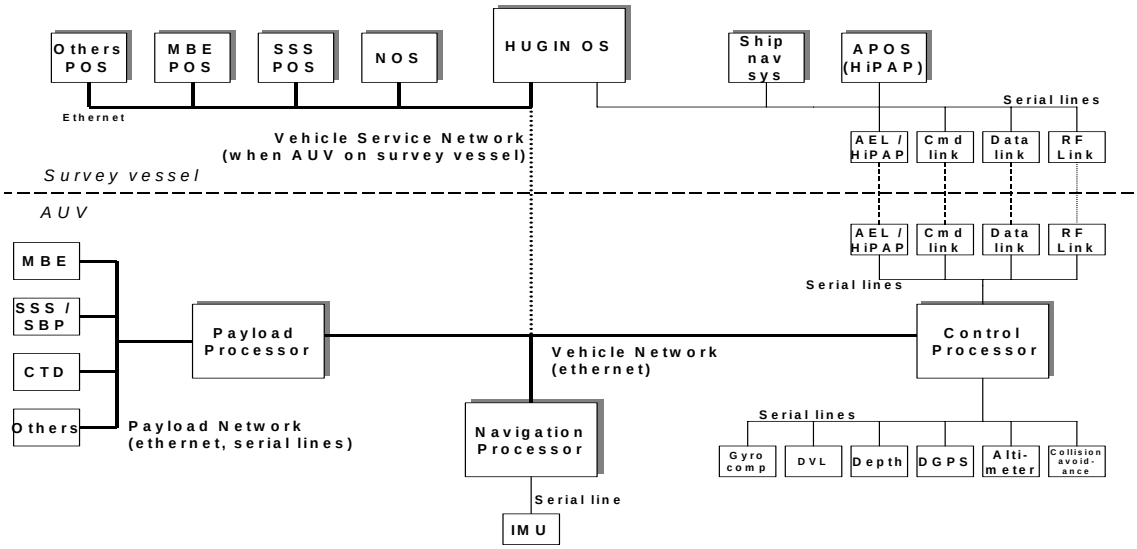

Figure 3. HUGIN overview.

The multi platform concept.

HUGIN being a multi platform means that it can be equipped with many sensors at once and installation of new sensors will be easy. Physically adding a new sensor induces connecting it to the payload network shown in Figure 3. This requires the sensor to be able to communicate using the TCP/IP protocol.

The sensors are connected to HUGIN in software using a plugin philosophy. This means that for every new payload we connect, there has to be written a plugin module at bottom side. The plugin is an interface between the payload and the rest of the HUGIN system and all plugins are managed by PP. In each plugin there is defined a set of plugin functions. These functions can be called from PP, and will in our case constitute the interface between PP and plugin.

In many cases it is important to be able to monitor and control the payload from topside. This is done by the payloadOS. The payloadOS's communicate with HUGINOS using a pos-server. The pos-server is written as a plugin module for HUGINOS. Due to the limited data transfer rate on the acoustic links, most of the payload OS's has to be special designed to work with the HUGIN system.

Using this design gives us some advantages. Each new payload introduces new separated hardware and software. This implies that we do not have to alter any of the software or hardware components in the HUGIN system; this means no recompiling and no new bugs will be introduced in the core system.

HUGIN Top side.

HUGINOS is the key point of communication with HUGIN. When HUGIN is submerged all communication between top and bottom side has to go trough HUGINOS. HUGINOS is also used to send commands to CP. Navigation are done from the NavP and is running on the same machine as HUGINOS. POS-handler is responsible to act as a server for the different POS'es, and as an operation station for PP. The server part of POS-handler communicates using CORBA. Each POS has to connect to the POS-handler server to communicate with its corresponding payload in HUGIN. In cases where the POS do not support CORBA there has to be written a protocol converter.

Payload Processor.

PP is the link between the plugins and the rest of HUGIN. When PP starts up it connects to the respective plugins. Only PP can communicate with the plugins, which signify that all communication with the payload goes trough PP. To mange this, PP has to route messages to the correct plugin and decide which plugin is to send its data. The part of PP doing all this is called Plugin Manager in Figure 4. The figure shows how plugins are connected to the plugin manager inside PP. Dotted lines shows the data flow between payload network and HUGIN network. As we can see all data from and to plugins has to go trough the payload manager.

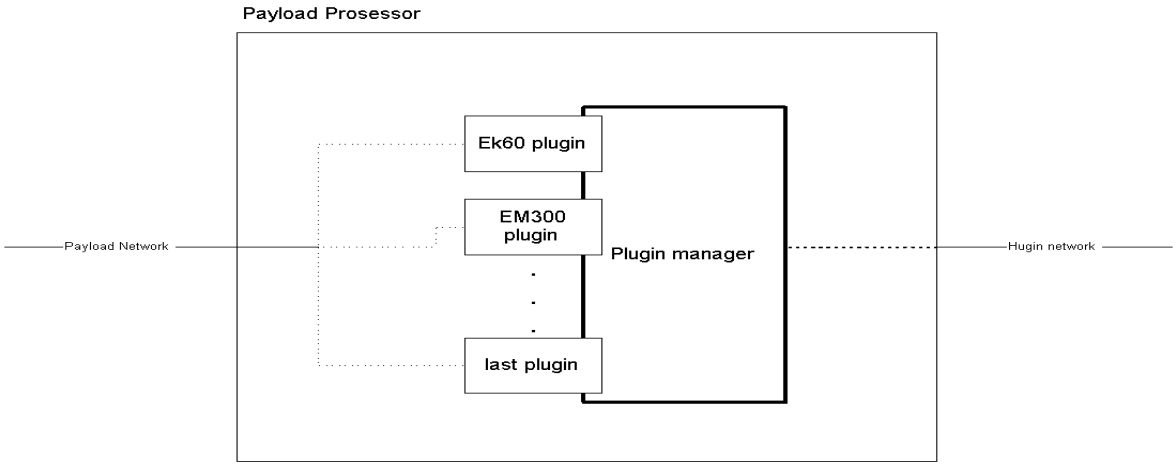

Figure 4 PP plugin system.

Navigation Processor.

In UUV mode the survey vessel tracks HUGIN with a super short baseline acoustic position system (SSBL). The survey vessel is equipped with the following navigation instrumentation:

- SSBL (Super Short Baseline system)
- DGPS (combining Differential Global Positioning System)
- Heading/roll/pitch attitude sensor
- Acoustic communication links

By combining DGPS with SSBL data compensated for attitude, an AUV position estimate in global coordinates is obtained. This position estimate is sent to the AUV on the acoustic communication link.

HUGIN 3000 is equipped with an aided inertial navigation system (AINS). The inertial navigation system (INS) calculates position, velocity and attitude of the vehicle using high frequency data from an Inertial Measurement Unit (IMU). An IMU consists of three accelerometers measuring specific force and three gyros measuring angular rate. A Kalman Filter utilizes in a mathematical optimal manner a wide variety of navigation sensors for aiding the INS.

Control Processor.

CP contains all the functionality to make the HUGIN system run. In fact HUGIN can run with only the aid of CP. CP is the only processor who can communicate with the survey vessel using the acoustic links. This means that all data transmitted are received acoustically and has to go trough CP. Hence making it a vital piece of the HUGIN system.

The vehicle control system architecture is based on a hierarchical structure. A mission plan constitutes the highest level, containing the sequence of reference values and operation mode settings required to perform a complete mission step at any point during the operation through the acoustic command link. HUGIN operates and navigates to its preprogrammed mission plan, and a certain degree of built-in autonomy allows the vehicle to operate for certain periods without operation intervention. The operator has full access to the vehicle status, and can modify operational and mission status as required during a survey.

CP also has the responsibility for running the Autopilot and can be programmed to hold a specific heading, altitude and speed. The data from the Autopilot is used to control the propulsion and steering system, which also is CP's responsability. HUGIN is programmed to handle certain conditions and errors that can put the AUV in danger. If there is no immediate danger, CP interprets this as a warning, more serious situations will be interpreted as emergency and CP will initiate an emergency accent.

EK60MK1.

When using the EK60MK1 echo sounder in HUGIN, we will be able to monitor and control it. This is done using the acoustic links. It is important for us to be able to se a real-time image of the water column HUGIN covers. And to adjust the EK60MK1 to optimise the quality of the data collected. The real time image will also help us decide where to steer the vehicle.

To monitor and adjust the EK60MK1 we have developed an application on topside. From this application we can send commands to the EK60MK1 in HUGIN and monitor some of the echogram data. The application connects to the HUGINOS pos server.

The EK60MK1 application is not developed for remote controlling. Since it is a Win32 application we can send event messages to it simulating Graphical User Interface (GUI) calls like button clicks and menu selections. Use of Inter Process Communication (IPC) in Win32 can only be done if the applications are on the same machine. And this is not the case for the HUGIN system. In fact the communication has to go trough tree different machines running two different OS'es. To solve this problem we use an IPC/TCP bridge. This application resides on the same machine as the EK60MK1 SW. The bridge listens on a TCP/IP port for incoming commands, if the command is to the EK60MK1 it is translated to corresponding IPC call and sent to the EK60MK1 application.

Conclusion.

The first HUGIN AUV system was developed for a very specific purpose, bathymetric mapping for offshore oil and gas applications. Based on this concept and the HUGIN 3000, HUGIN 2000 will serve as a multi platform for instruments. HUGIN 2000 is under development and is scheduled for its first sea trial in June 2001. HUGIN will then be equipped with an EK60MK1 echo sounder. We expect that HUGIN 2000 will be an important scientific tool in the future; giving a better window in to the ocean depths, improve the quality of routine observation, which in turn will give more accurate stock assessment. In the long term we also expect savings in the form of money and time, using HUGIN. As the data sampling instruments is getting smaller, using less power and sampling more data. AUV's surely will play an important role in the future.

References.

Aglen, A. 1994. Sources of Error in Acoustic Estimation of Fish Abundance. In Fernø, A. and Olsen, S: Marine Fish Behaviour in Capture and Abundance Estimation , 107-133. Oxford, Fishing News Books, Blackwell Science Ltd.

Dalen, J., Bodholt, H. 1991. Deep towed vehicle for fish abundance estimation, concept and testing. Norway, Bergen.

Fernandes, P. G., Brierley, A. S., Simmonds, E. J., Millard, N. W., McPhail, S. D, Armstrong, F., Stenenson, P., and Squires, M. 2000. Fish do not avoid survey vessels. NATURE 404, 35-36.

Godø, O. R. 1994. Factors Affecting the Reliability of Groundfish Abundance Estimates from Bottom Trawl Surweys. In Fernø, A. and Olsen, S. Marine Fish Behaviour in Capture and Abundance Estimation , 166-199. Oxford, Fishing News Books, Blackwell Science Ltd.

Gunderson, D.R: Surveys of Fish Resources. John Wiley & Sons, New York. 1993.

MacLennan, D.N., Simmonds, E.J. 1993. Fisheries Acoustics. Chapman & Hall, Lonon.

Ona, E. and Svellingen, I. 1999. High-resolution target strength measurements in deep water. The Journal of the Acoustical Society of America, 105(2):1049.

Vestgård, K., Kristensen, J. 1998. Hugin – An untethered underwater vehicle for seabed surveying. Proceeding from Oceans 1998, Nice,France, pp.118-123.

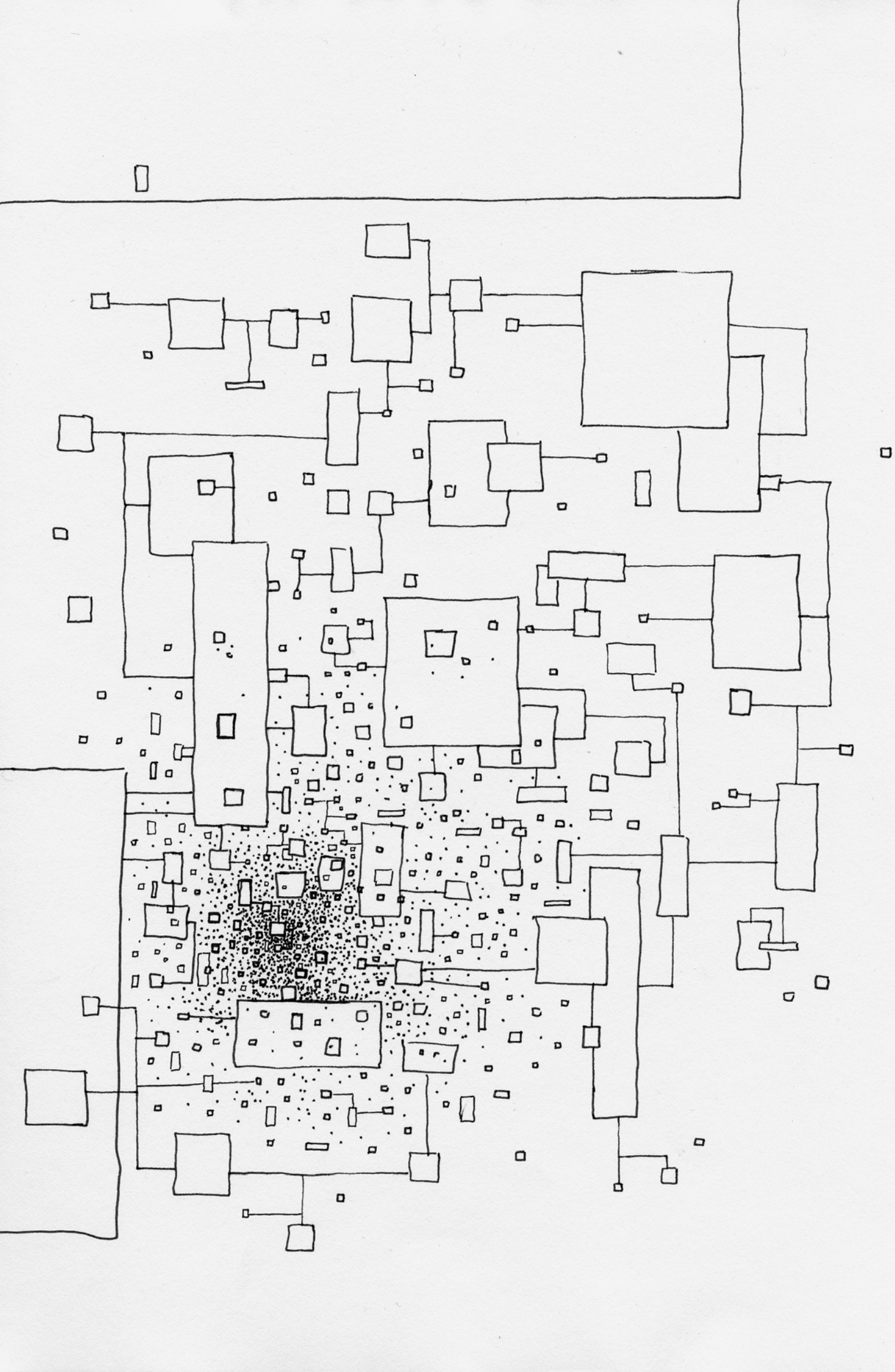

Remotely Controlling Windows Applications

Autonomous vehicles still need a driver

Ruben Patel

A common way of collecting scientific data involves the use of electronic sampling equipment. Typical scenarios for collecting biological data include long-time surveillance, surveillance near specific biomasses, and surveillance using autonomous platforms. In this article, I describe how I communicate with an EK60 SIMRAD echo sounder embedded in the High-precision Underwater Geosurvey and Inspection System (HUGIN) Autonomous Underwater Vehicle (AUV). Although this autonomous vehicle was originally designed for seabed mapping, its software can accommodate any sensor that can connect to the AUV.

As it turns out, the Institute of Marine Research in Norway uses scientific echo sounders for biomass measurements. While the echo sounders work well for remote sensing, they are unfortunately attached to a very large mother ship, which fish tend to react to because of engine and propeller noise. Consequently, the behavior of the fish is altered, introducing bias into the measurements. However, due to its low noise level, the AUV can get closer to schools of fish without introducing fish reaction. Because of this, we decided to embed our sensor in the AUV, thereby letting us move sensors closer to the biomass and collect detailed information and less biased data.

AUV Operation and Communication

The AUV has the ability to run in autonomous or controlled mode.

- In autonomous mode, the AUV conducts a preprogrammed survey with no communication with the mother vessel. This lets us use the mother ship for other activities. When the AUV survey is finished, it is recovered at a predefined time and location.
- In controlled mode, the AUV is remotely controlled from the mother ship using acoustic communication links. The pilot controls the trajectory of the AUV using a 55 bps link. Data from the AUV and its onboard sensors is transmitted over a data link running at 2000 bps. Critical data from the AUV is prioritized and occupy 1000 bps, meaning there is 1000 bps remaining to share among all the payload sensors. Since the acoustic communication links have a limited range of 2000 meters vertical, the mother ship has to follow the AUV to maintain communication.

Ruben is currently working on his Ph.D. at the Institute Of Marine Research in Norway, focusing on autonomous and stationary remote sensing of marine resources. He can be contacted at ruben.patel@imr.no.

The High Precision Acoustic Positioning system (HiPAP) tracks the position of the AUV. When running the AUV in the beam of the mother ship's echo sounder, we get detailed information of the biomass location relative to the AUV. This helps us steer the AUV close to the biomass of interest. Figure 1 shows the trajectory of the AUV while approaching and penetrating an enormous school of herring. This biological aggregation is common in some of the fjords in Norway during the herring's wintering phase. Since no cables are attached between the AUV and mother ship, the AUV can maintain a speed of 4 knots at its maximum depth of 2000 meters. In Figure 1, data was collected by running the mother ship directly above the AUV. The sea bottom is the thick red line and the herring school the biggest red aggregation. Two smaller schools of fish can be seen in the beginning of the image, and one small school directly above the biggest. The AUV trajectory can bee seen as a red line enhanced by blue. Dispersed fish (blue dots) can be seen distributed in the image. The image is contaminated due to acoustic interference form the AUVs sensor and communication system. The depth range is 550 meters and the distance from the start of the image to the end is around 3 kilometers. Initially, the stepwise AUV trajectory was to approach the school gradually. This was not successful as the school turned downward and disappeared. Still, this is an excellent performance compared to towed bodies.

The communication protocol between the sensor in the AUV and the control program on the mother vessel is complex. Figure 2 is an overview of the top side and bottom side of the HUGIN system. The horizontal dashed line indicates physical separation of the top side and bottom side. The vertical dashed line is the network connection when the AUV is connected directly to the topside system, this is done only when the AUV is onboard the mother ship. All commands and data sent to or received from the AUV go through the HUGIN Operator Station (HUGIN OS). This computer is also used for navigation, mission

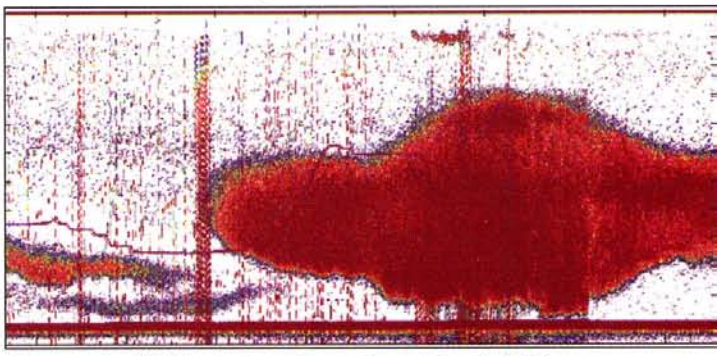

Figure 1: *AUV trajectory through a school of fish.*

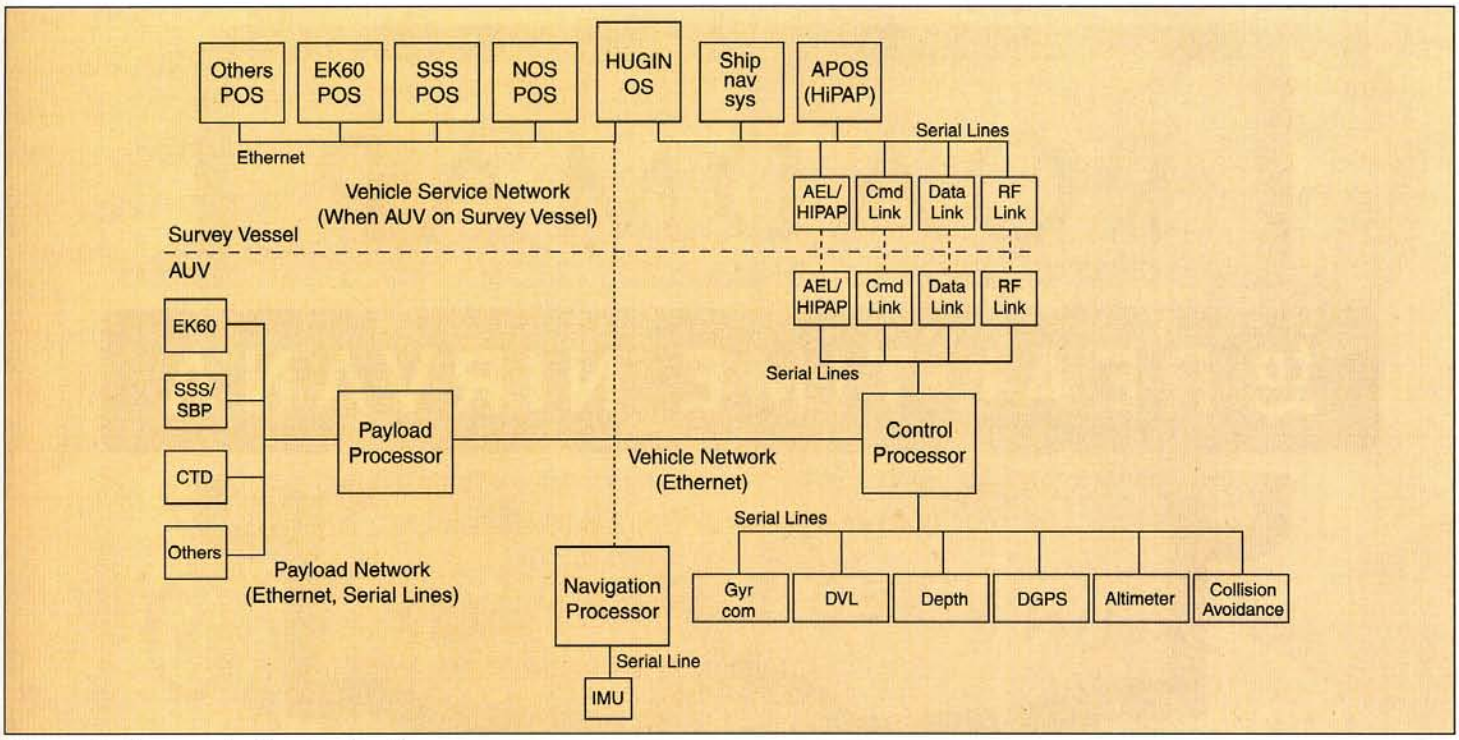

Figure 2: *Communication protocol.*

planning, and monitoring AUV performance. Sensors are controlled from Payload Operator Stations (POS); if a POS wants to send a command to its corresponding sensor, it has to first send it to the HUGIN OS. In turn, the command is sent over the acoustic data link to be received by the control processor. The control processor sends the command to the payload processor, which addresses it to the correct sensor plugin. All sensor plugins rely on the payload processor and are implemented as Dynamic Link Libraries (DLLs). From this point on, it is up to the programmer of the DLL to forward the message to its sensor. In our case, we send the command using TCP/IP to a bridge program. This design abstracts much of the complexity of the infrastructure in the AUV, and sensors can be added in a systematic manner.

Controlling the Application

The Windows-based applications we run for these studies remotely control the EK60 sensor in the AUV from the mother ship. You have several options when remotely controlling Windows applications. Commercial software packages that let you do this include PcAnywhere and Citrix. While these products give total control over the PC, they don't meet the AUV's communication speed and protocol needs. Consequently, I developed an alternative approach that, as a side benefit, can be used over any protocol.

The basic idea behind the approach I present here is to send events from one application to another using interprocess communication (IPC) based on Windows messages. This lets me send commands to applications from programs on the same machine for opening dialog boxes, pressing buttons, and reading and setting the states of different controls. In other words, I can send commands to applications just as if I were using a keyboard and mouse. This concept opens the possibility to remotely controlling many Windows applications. You can implement complex timers for sampling data at different hours. Sensors can be connected to other sensors and programs. In our case, we wrote a bridge program that translates messages between two communication protocols, letting us communicate with the sensor from different machines.

Figure 3 shows the three abstraction layers of the remote-control system. The first layer defines the fundamental functions for finding Windows handlers and performing simple commands

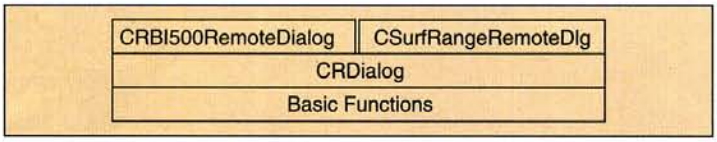

Figure 3: *Abstraction layers in the bridge design.*

on controls (Listing One). The next layer is a generic dialog box class, which encapsulates some of the fundamental functions (Listing Two). The last classes are dialog box classes that reflect the dialog boxes in our application. In this example, we need to access the BI500 Dialog and Surface Range Dialog dialog boxes (see Listings Three and Four, respectively).

Spying on Applications

Before writing the bridge program, I had to decide what commands to send to the application and what data to retrieve. Typical steps for executing a command are to open the correct dialog box, alter one or more of the controls in it, then press the OK button on the opened dialog boxes. This means that I have to map all the necessary events that are generated during the command execution. Since the control of the application lies in different windows, I have to map the events to open the corresponding dialog boxes, then I have to identify events for executing different commands, and finally the event for pressing the OK button. I did this using Microsoft's Spy++ program to spy on the message loop in the application we want to remotely control while executing the commands manually.

Remote Dialog Boxes

The Set Surface Range command controls the vertical depth range across the echogram. All the other commands are implemented in a similar manner. To set the surface range to 200 meters, for instance, I have to:

1. Open the BI500 dialog box.
2. Press the Surface Range button to open the Surface Range Dialog Box.
3. Enter the number 200 into the Range text box.
4. Press OK in the Surface Range Dialog Box.
5. Press OK in the BI500 dialog box.

(continued on page 18)

```
//handle GPT transceiver not found dialog box.
CGPTTransceiverNotFoundDlg *gptNotFound =
     new CGPTTransceiverNotFoundDlg("SIMRAD EK60",
      "GPT Transceiver Not Found");
// Check if GPTTransceiverNotFound dialog is open
// if so press the retry button until ok
while(gptNotFound->isOpen())
{
   gptNotFound->PressButtonRetry();
   Sleep(2000);
}
```

Example 1: *Sending events to press the Retry button.*

```
For(;;)
{
  nBytes=-1;
  If(test) nBytes=getCmdLineCommand(cmd);
     // Manually sending commands from cmd line
  Else if(remote) nBytes=getRemoteCommand(cmd);
     // Receiving commands over TCP/IP
  If(nBytes>0)   translateCmdToEventAndSen...(cmd)
  if(lostConnectionWithClien()) waitForClient()
    sleep(400);
}
```

Example 2: *Pseudocode for the bridge program.*

(continued from page 15)

Using Spy++, I map the events that have to be sent to the application to perform each of the steps mentioned. The events are collected in a header file in Listing Five.

Using the defined classes, I can set the range to 200 meters using Listing Six. Line 3 starts the application if it is not started. We then control the range value to see if it is within the valid range using the macro in line 1. A new instance of the Surface Range Dialog box is created in lines 8 and 9. The parent and child window names are set. These names are used to find the windows handler in the window tree. In line 10, the command for setting the range is executed; see Listing Four. Line 41 shows the start of the method for setting the range. This method calls the *SetText* method in line 33. In line 35 the BI500 dialog is first opened, then the Surface Range Dialog box is opened by pressing the Surface Range button in the BI500 dialog box. Line 36 inserts the range value and closes the dialog boxes by pressing the OK button in each of them. As you see from the code, the *PostMessage* and *SendMessage* functions are the core of the communication. These functions send specified messages to a window and call the window procedure of the specified window. *SendMessage* does not return until the window procedure has processed its message. In contrast, *PostMessage* returns immediately without waiting for the window procedure to process the message.

Error Handling

The example works only if no errors are cast by the application. If an error is thrown, a dialog box appears, notifying users of the error. In most cases, the error box blocks the application for further input. We use two methods of dealing with this. Before any command is executed, we search for error or warning boxes and close them. The other method to avoid errors is by checking the commands that are sent to the application. One problem I had with our sensor was that our application sometimes lost connection to the general-purpose transceiver (GPT). This is the piece of hardware that does the actual sampling and signal processing of the raw data collected from the transducer. This caused an error box to appear. After pressing Retry three or four times, it worked fine and data was collected. I solved this problem by sending events to press the Retry button as long as the error dialog box was open; see Example 1.

Controls in dialog boxes often have a range limit and, if you try to set some value out of range, an error box appears. I avoided these types of errors by testing the range of each control and checking the range of the value before it was sent to the control, as in Listing Six, line 4.

The Bridge

The bridge program was made for running in two modes. F testing purposes, a command-line interface gives me the abi ty to send commands to the application. In remote mode, t bridge programs listen on a TCP/IP port. Received messages a translated to events and sent to the application. Example 2 pseudocode for the bridge program.

Between every command translation, I test for potential GI error boxes. These rarely occur, but would halt the applicatic for further input if not closed. I then test if we are in test or r mote mode. These modes receive commands differently an therefore, we have two different functions for each mode. If valid command is received, the *nBytes* variable contains th number of bytes the command occupies. If the command co tains a valid command number of bytes, it is translated to even and sent to the application. If the client has lost connection wi the bridge, we wait for the client to reconnect.

Conclusion

You need to be careful when remotely controlling application It is important to map all the potential errors that can appe during application use. One unknown error can halt the whc communication. Dialog boxes can use some time before the appear or close. It is therefore important to halt any commanc before we are sure that the dialog box is open or closed. In m case, I poll the window tree to see if we can find the dialc box. Some programs are unstable and occasionally shut dow or halt. A good rule is to check whether the sensor program running before sending any commands. If it is not running, the start it before the command is sent. It was necessary to impl ment commands for stopping the sensor, restarting the cor puter, and shutting down the computer. I needed to stop th sensor and shutdown the computer before the AUV was launche and recovered. This was to reduce the risk for damaging th transducer and hard disk. There is always the danger of gettir a total machine halt, like the blue screen in Windows. To r cover from this, the control processor can recycle power on a the sensors at command from the HUGIN OS.

I tested the system during a cruise period over two week My experience during this cruise is that this way of remote co trolling and reading data from an application can indeed be use for remote sensors. The method is easy to implement and ca be used in many ways. If the application behavior is well in vestigated a robust communication protocol can be developec

DDJ

Listing One

```
1   // Header
2   #ifndef __GLOBAL_HH__
3   #define __GLOBAL_HH__
4   #include <windows.h>
5
6   typedef struct
7   {
8       HWND    hwnd;
9       const char *title;
10  } FindWnd;
11
12  CALLBACK CheckWindowTitle( HWND hwnd, LPARAM lParam );
13  HWND FindWinTitle(const char *title);
14  HWND FindWndByTitle(const char *parent,const char *child);
15  HWND WaitForDialogToOpen(char *parent,int timeout);
16  HWND WaitForDialogToClose(char *parent);
17  HWND OnShotOpenDialog(char *parent);
18  HWND LeftClickInAt(const char *parent,const char *child,int x,int y);
19
20  #endif

1   // Cpp file
2   #include "Global.h"
3
4   // Se if the specified window has a specified title
5   CALLBACK CheckWindowTitle( HWND hwnd, LPARAM lParam )
```

```
{
    char    buffer[MAX_PATH];
    // Get the window title form window
    GetWindowText( hwnd, buffer, sizeof( buffer ) );
    FindWnd * fw = (FindWnd *)lParam;
    // Compare window tile with title to be checked.
    if(strcmp( buffer, fw->title ) == 0 )
    {
        fw->hwnd = hwnd;
        return FALSE;
    }
    return TRUE;
}
// Find a parent window by it window title
HWND FindWinTitle(const char *title)
{
   FindWnd fw;
    fw.hwnd = 0;
    fw.title = title;
    EnumWindows( (WNDENUMPROC) CheckWindowTitle, (LPARAM) &fw );
    return fw.hwnd;
}
// Find a child window by it window title
HWND FindWndByTitle(const char *parent,const char *child)
{
    FindWnd fw;
    fw.hwnd = 0;
    fw.title = child;
    HWND hWnd = FindWinTitle(parent);
    if(child==NULL) return hWnd;
    else
    {
   ::EnumChildWindows(hWnd, (WNDENUMPROC) CheckWindowTitle, (LPARAM) &fw);
        return fw.hwnd;
    }

}
// Halt until a dialog is opened
HWND WaitForDialogToOpen(char *dlgName,int timeout)
{
    HWND    hWndDlg;
    hWndDlg = NULL;
    // Loop until the window is opened
    do
    {
        hWndDlg= FindWndByTitle(dlgName,NULL);
    } while(!hWndDlg);
    return hWndDlg;
}
// Halt until a dialog is closed
HWND WaitForDialogToClose(char *dlgName)
{
    HWND    hWndDlg;
    hWndDlg = NULL;
    // Loop until the window is opened
    do
    {
        hWndDlg= FindWndByTitle(dlgName,NULL);
    } while(hWndDlg);
    return hWndDlg;
}
// Open dialog
HWND OnShotOpenDialog(char *dlgName)
{
    HWND    hWndDlg;
    hWndDlg = NULL;
    // Get the handler
    hWndDlg= FindWndByTitle(dlgName,NULL);
    return hWndDlg;
}
// Left click in a child window at position x,y
HWND LeftClickInAt(const char *parent,const char *child,int x,int y)
{
    // Get window handler
    HWND    hWnd = FindWndByTitle(parent,child);
    WPARAM wParam = MK_RBUTTON;
    LPARAM lParam = MAKELPARAM(x,y);
    // simulating left mouse click in window
    if(!::PostMessage(hWnd, WM_RBUTTONDOWN ,wParam,lParam))
        return NULL;
    return hWnd;
}
```

Listing Two

```
// RDialog.h: interface for the CRDialog class.
#ifndef __CRDialog_H
#define __CRDialog_H

#include <windows.h>

class CRDialog
{
public:
    CRDialog(char *parent,char *child);
    ~CRDialog();

    HWND    IsDialogOpen(char *dlgName); // Check if the dialog
                                         // with name in dlgName is open
    long    SetText(int nIDDlgItem,char *text);  // Set text in a control
    DWORD   SetCheck(int nIDDlgItem,BOOL checked);  // Check or
                                                    // uncheck a check
box
    HWND    CloseDialog(void);              // Close this dialog box
    BOOL    PressButton(int nIDDlgItem);   // Press a button

    char *m_sParent;                        // String to parent window
    char *m_sChild;                         // String to this dialog box

};
#endif
```

```
// CRDialog class implementation
#include <stdio.h>
#include "CRDialog.h"
#include "Global.h"
#include "EK60MK1ID.h"

// Set string of parent and child window
CRDialog::CRDialog(char *parent,char *child)
{
    int len1=strlen(parent)+1;
    int len2=strlen(child)+1;
```

(continued on page 20)

(continued from page 19)

```
12      m_sParent = new char[len1];
13      m_sChild = new char[len2];
14      sprintf(m_sParent,"%s",parent);
15      sprintf(m_sChild,"%s",child);
16  }
17  CRDialog::~CRDialog()
18  {
19      delete[] m_sParent;
20      delete[] m_sChild;
21  }
22  // Close dialog box
23  HWND CRDialog::CloseDialog(void)
24  {
25      // Find handler of dialog box form string
26      HWND    hWndDlg = FindWinTitle(m_sChild);
27      // Close dialog by pressing the OK button
28      ::SendDlgItemMessage(hWndDlg,RIDC_BUTTON_OK,BM_CLICK,0,0);
29      // wait for dialog to close
30      return WaitForDialogToClose(m_sChild);
31  }
32  // Return handler of dialog specified by window name
33  HWND CRDialog::IsDialogOpen(char *dlgName)
34  {
35      return FindWndByTitle(dlgName,NULL);
36  }
37  // Set text in control in dialog box
38  long CRDialog::SetText(int nIDDlgItem,char *text)
39  {
40  return::SendDlgItemMessage(FindWndByTitle(m_sChild,NULL),
                          nIDDlgItem,WM_SETTEXT,0,(LPARAM)text);
41  }
42  // Check or uncheck a check control
43  DWORD CRDialog::SetCheck(int nIDDlgItem,BOOL checked)
44  {
45      // manipulate control in dialog
46      DWORD   wParam ;
47      // Check it
48      wParam = (WPARAM) (checked)?(BST_CHECKED):(BST_UNCHECKED);
49  ::SendDlgItemMessage(FindWndByTitle(m_sChild,NULL),nIDDlgItem,
                                                  BM_SETCHECK,wParam,0);
50      // Check if success
51      return::SendDlgItemMessage(FindWndByTitle(m_sChild,NULL),
                    nIDDlgItem,BM_GETSTATE,0,0);
52  }
53  // Press a button
54  BOOL CRDialog::PressButton(int nIDDlgItem)
55  {
56      HWND hWndDlg;
57      // Check if the dialog is open
58      hWndDlg = IsDialogOpen(m_sChild);
59      // get handler of button to press
60      HWND hWndCont = ::GetDlgItem(hWndDlg,nIDDlgItem);
61      // Press it
62      ::PostMessage(hWndCont,BM_CLICK,0,0);
63      return TRUE;
64  }
```

Listing Three

```
1   // BI500RemoteDlg.h: interface for the BI500RemoteDlg class.
2   #ifndef __BI500RemoteDialog_H
3   #define __BI500RemoteDialog_H
4
5   #include "EK60MK1ID.h"
6   #include "CRDialog.h"
7
8   class CBI500RemoteDlg:public CRDialog
9   {
10  public:
11      CBI500RemoteDlg(char *parent,char *child);
12      virtual ~CBI500RemoteDlg();
13
14      BOOL PressButtonSurfaceRange();
15      BOOL PressButtonOK();
16  private:
17      HWND OpenDialog(void);
18      BOOL SetText(int nIDDlgItem,char *text);
19      BOOL PressButton(int nIDDlgItem);
20
21  };
22
23  #endif
```

```
1   // BI500RemoteDlg.cpp: implementation of the BI500RemoteDlg class.
2
3   #include "CBI500RemoteDlg.h"
4   #include "global.h"
5
6
7   CBI500RemoteDlg::CBI500RemoteDlg(char *parent,char *child)
8       :CRDialog(parent,child)
9   {}
10  CBI500RemoteDlg::~CBI500RemoteDlg()
11  {}
12  HWND CBI500RemoteDlg::OpenDialog(void)
13  {
14      HWND    hWndDlg;
15      // Check if dialog is already open
16      hWndDlg = IsDialogOpen(m_sChild);
17      if(hWndDlg) return hWndDlg;
18      // Open the dialog
19      if(!::PostMessage(FindWinTitle(m_sParent), WM_COMMAND,
                                  RID_INSTALL_BI500,0 )) return NULL;
20      // get dialog handler
21      hWndDlg = WaitForDialogToOpen(m_sChild,1000);
22      return hWndDlg;
23  }
24  BOOL CBI500RemoteDlg::SetText(int nIDDlgItem,char *text)
25  {
26      OpenDialog();
27      CRDialog::SetText(nIDDlgItem,text);
28      CloseDialog();
29      return TRUE;
30  }
31  BOOL CBI500RemoteDlg::SetSurfVals(char *Surf)
32  {
33      SetText(RIDC_LIST_NOSURFVALS,Surf);
34      return TRUE;
35  }
36
37
38  BOOL CBI500RemoteDlg::PressButton(int nIDDlgItem)
39  {
40      HWND hWndDlg;
41      hWndDlg = IsDialogOpen(m_sChild);
42      if(!hWndDlg) hWndDlg=OpenDialog();
43      HWND hWndCont = ::GetDlgItem(hWndDlg,nIDDlgItem);
44      ::PostMessage(hWndCont,BM_CLICK,0,0);
45      return TRUE;
46  }
47
48  BOOL CBI500RemoteDlg::PressButtonSurfaceRange()
49  {
50      return PressButton(RIDC_BUTTON_SURFRANGE);
51  }
52  BOOL CBI500RemoteDlg::PressButtonOK()
53  {
54      return PressButton(RIDC_BUTTON_OK);
55  }
```

Listing Four

```
1   // CSurfRangeRemoteDlg: interface.
2   #ifndef _SURFRANGEREMOTEDLG_H
3   #define _SURFRANGEREMOTEDLG_H
4
5   #include "EK60MK1ID.h"
6   #include "CRDialog.h"
7   #include "CBI500RemoteDlg.h"
8   #include "Global.h"
9
10  class CSurfRangeRemoteDlg :public CRDialog
11  {
12  public:
13      CSurfRangeRemoteDlg(char *parent,char *child);
14      virtual ~CSurfRangeRemoteDlg();
15
16      BOOL SetRange(char *range);
17      BOOL SetStart(char *start);
18
19  private:
20      HWND OpenDialog(void);
21      HWND CloseDialog(void);
22      BOOL SetText(int nIDDlgItem,char *text);
23  };
24
25  #endif
```

```
1   // CSurfRangeRemoteDlg: implementation.
2   #include "SurfRangeRemoteDlg.h"
3
4   CSurfRangeRemoteDlg::CSurfRangeRemoteDlg(char *parent,char *child)
5   :CRDialog(parent,child)
6   {}
7   CSurfRangeRemoteDlg::~CSurfRangeRemoteDlg()
8   {}
9   HWND CSurfRangeRemoteDlg::OpenDialog(void)
10  {
11      HWND    hWndDlg;
12      // Open BI500 dialog
13      CBI500RemoteDlg BI500RDlg(m_sParent,"BI500 Dialog");
14      // Press the Surface Range button in the BI500 dialog
15      BI500RDlg.PressButtonSurfaceRange();
16      hWndDlg = WaitForDialogToOpen(m_sChild,1000);
17      return hWndDlg;
18  }
19  HWND CSurfRangeRemoteDlg::CloseDialog(void)
20  {
21      HWND    hWndDlg = FindWinTitle(m_sChild);
22      // Close dialog
23      ::SendDlgItemMessage(hWndDlg,RIDC_BUTTON_OK,BM_CLICK,0,0);
24      // wait for dialog to close
25          WaitForDialogToClose(m_sChild);
26      //CRDialog::CloseDialog();
27      CBI500RemoteDlg BI500RDlg(m_sParent,"BI500 Dialog");
28      BI500RDlg.PressButtonOK();
29      return NULL;
30  }
31
32
33  BOOL CSurfRangeRemoteDlg::SetText(int nIDDlgItem,char *text)
34  {
35      OpenDialog();
36      CRDialog::SetText(nIDDlgItem,text);
37      CloseDialog();
38      return TRUE;
39  }
40
41  BOOL CSurfRangeRemoteDlg::SetRange(char *range)
42  {
43      SetText(RIDC_LIST_SRANGE,range) ;
44      return TRUE;
45  }
46
47  BOOL CSurfRangeRemoteDlg::SetStart(char *start)
48  {
49      SetText(RIDC_LIST_STARTSURF,start);
50      return TRUE;
51  };
```

Listing Five

```
1   #define RID_INSTALL_BI500       32878   // ID to activate BI500 dialog
2   #define RIDC_BUTTON_SURFRANGE   0x510   // Button to push for activating
                                               // Surface Range Dialog box.
3   #define RIDC_LIST_SRANGE        0x3ec   // ID for surface range text box
4   #define RIDC_BUTTON_OK          0x01    // Ok button id
```

Listing Six

```
1   #define IsInRange(val,min,max) if(val>=min && val<=max)
2   nRang=200;
3  startEK60MK1App();// Start sensor program if not started
4   IsInRange(nRange,0,15000)    // Check range
5   {
6       char val[5];
7       itoa(nRange,val,10);
8       CsurfRangeRemoteDlg *surfRangeDlg
9       = new CSurfRangeRemoteDlg("SIMRADEK60","SurfaceRange Dialog");
10      surfRangeDlg->SetRange(val); // Set range
11      delete surfRangeDlg;
12  }
```

DDJ

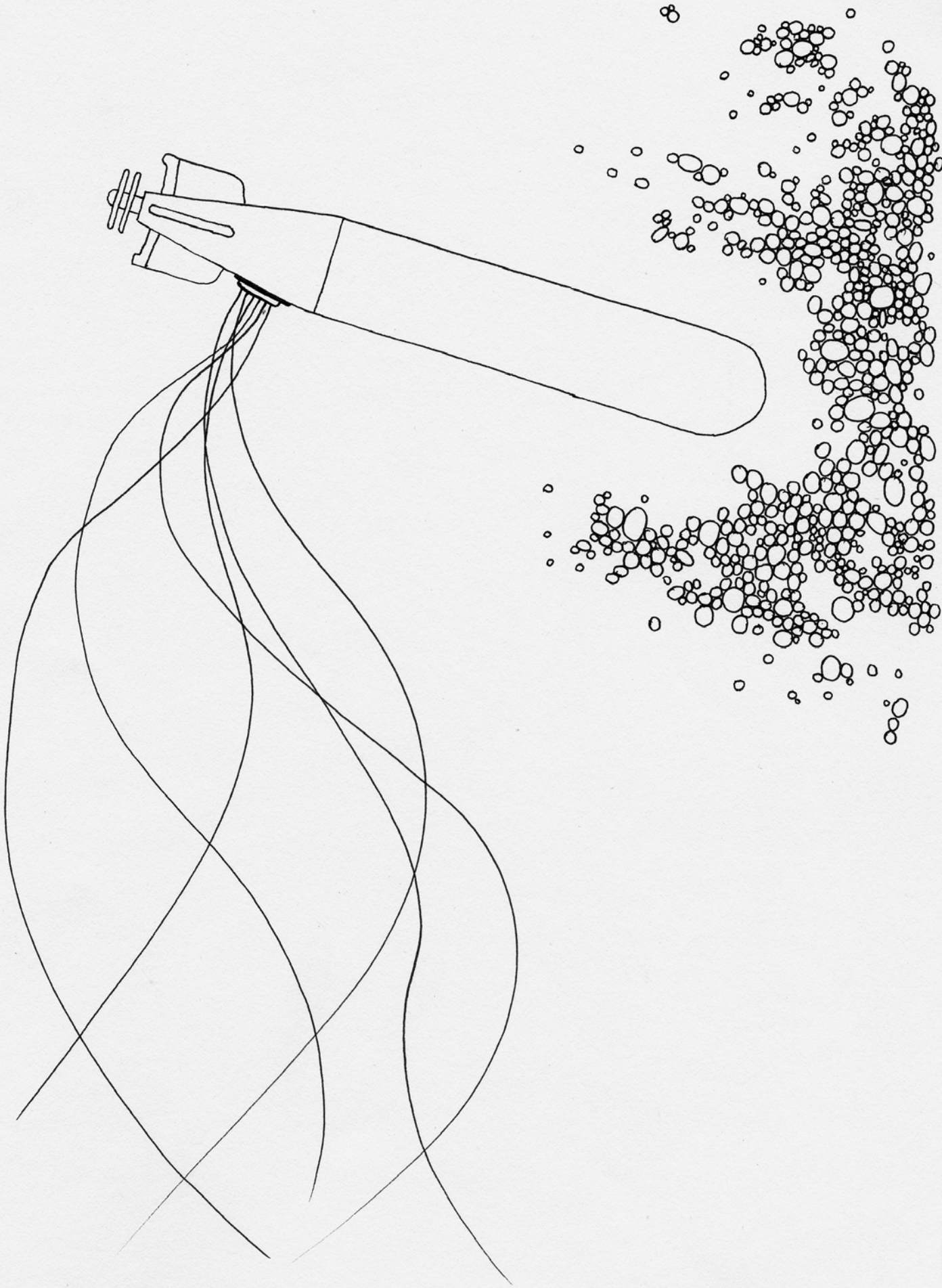

ICES Journal of Marine Science, 61: 1044–1049 (2004)
doi:10.1016/j.icesjms.2004.07.002

Behaviour of herring (*Clupea harengus* L.) towards an approaching autonomous underwater vehicle

Ruben Patel, Nils Olav Handegard, and Olav Rune Godø

Patel, R., Handegard, N. O., and Godø, O. R. 2004. Behaviour of herring (*Clupea harrengus* L.) towards an approaching autonomous underwater vehicle. – ICES Journal of Marine Science, 61: 1044–1049.

The reaction of schooling wintering herring (*Clupea harengus* L.) in Ofotfjord in northern Norway is studied when approached by an autonomous underwater vehicle (AUV) with electrical propulsion. The reaction of herring is recorded running the AUV in the beam of the mother vessel's 38-kHz echosounder and in more detail with an onboard 120-kHz echosounder. The results indicate an insignificant reaction of herring to the approaching AUV, although some variations were observed depending on the experimental set-up. Technical uncertainty in the recordings close to the AUV transducer creates some ambiguity in the results. No reaction could be identified from the ship's sounder when the AUV passed under the vessel. Processing of the onboard echosounder data suggests a mean avoidance distance of 8.0 m in these experiments. In a realistic autonomous survey situation it is assumed that the AUV can approach as closely as 5–10 m to herring schools without affecting the acoustic observation, which makes it a potentially useful platform for hydroacoustic research and survey. More systematic studies are needed to precisely define the threshold reaction distance to the AUV, and the work should be conducted with transducers on a more silent platform than RV "Johan Hjort", which was used in this study.

Keywords: acoustic sampling, autonomous underwater vehicle, AUV, avoidance distance, over-wintering herring.

Received 21 March 2003; accepted 3 May 2004.

R. Patel, N. O. Handegard, and O. R. Godø: Institute of Marine Research, PO Box 1870, NO-5817 Bergen, Norway. Correspondence to R. Patel: fax: +47 55 23 68 30; e-mail: ruben@imr.no.

Introduction

Acoustic measurement methods have frequency-dependent limitations in range. The low frequencies and long pulse duration used for long-range observations reduce resolution, resulting in a loss of detail and a reduction in target position accuracy. Near-bottom observations are affected by the acoustic "dead zone" (Ona and Mitson, 1996). To minimize the effects of these limitations, the sampling instruments can be brought closer to the objects of interest, thus allowing detailed studies to be carried out on high-resolution behaviour, target strength, and tilt angle distributions. In this paper, we use the Hugin Autonomous Underwater Vehicle (AUV) to bring our sensor, a 120-kHz echosounder, closer to the fish targets. The echosounder has a range of 200 m. The Hugin AUV is used primarily for bottom mapping (Kristensen and Vestgård, 1998) and not for bioacoustic surveillance.

Fish avoidance from a research vessel has been reported in acoustic surveys (Olsen, 1971, 1990; Olsen *et al.*, 1983; Soria *et al.*, 1996), in combined acoustic and visual surveys (Fréon *et al.*, 1992), and in trawl surveys (Ona, 1988; Ona and Godø, 1990; Nunnallee, 1991). In contrast, Fernandes *et al.* (2002) observed no avoidance of North Sea herring (*Clupea harengus* L.) from a silent research vessel when using an AUV to describe fish behaviour. The problem of avoidance from AUVs has never been addressed previously. Before introducing the AUV as a standard platform in fisheries research, the avoidance effect needs clarification. Here, we investigate herring avoidance from an approaching AUV.

The experiments were conducted in Ofotfjord in north Norway during the period 23–26 November 2002, when the herring is in a non-feeding state (Slotte, 1999) and energy minimization is important. This period can thus be looked upon as an exercise in predation avoidance and energy conservation (Huse and Ona, 1996). We expect the herring schools to be in a vigilant state, since killer whales (*Orcinus orca* L.) feed on herring in this area during the study period (Nøttestad and Axelsen, 1999).

Material and methods

The noise level of the AUV was measured at a military acoustic measuring station located at Hegreneset in

1054-3139/$30.00

Norway. During the measurements, RV "Johan Hjort", the mother vessel for all our experiments, was positioned about 1000 m away from the station with engines running. The AUV was run through the dynamic measurement location 13 times maintaining a speed of 3−4 knots. Data from all the runs show that noise from RV "Johan Hjort" totally dominated the sound spectra (H. P. Knudsen, pers. comm.).

The AUV was painted red-orange. Shaped like a torpedo, it is 6-m long, the diameter at its thickest point 0.7 m. Tests were conducted during both *autonomous* and *steered* runs. During steered runs, the AUV and its sensors can be operated remotely through an acoustic link. We could also view real-time data from the 120-kHz echosounder through the acoustic link.

Operation

When the AUV is running horizontally, the 120-kHz beam points down. The transducer fixed to the hull tilts and rolls with the AUV. Some of the acoustic links used by the AUV interfered with the 38-kHz and 120-kHz sounder. During the steered surveys, the trajectory of the AUV could be altered so that the herring schools could be approached at different angles. To ensure that the school was approached as planned, we tried to keep the AUV in the beam of the mother vessel's 38-kHz echosounder. This gave us a real-time overview over the AUV's position in relation to the herring school. We also continually observed the position of the AUV relative to the mother vessel using a High Precision Acoustic Positioning system (HiPAP). This enabled us to maintain the AUV within a horizontal distance of 50 m from the mother vessel. Data were collected during three separate experiments. AUV trajectories for all experiments are shown in Figure 1.

In the analysis, we used data from the 38-kHz and 120-kHz sounders. Data from the AUV have a vertical resolution of 0.048 m for experiment 1, and 0.19 m for experiments 2 and 3. The reduction in vertical resolution was done to reduce the bandwidth and hence reduce the amount of noise in our data from the RV "Johan Hjort" in the steered experiments. Data from the RV "Johan Hjort" have a vertical resolution of 1.0 m. For the AUV, the horizontal resolution is determined by the vessel speed (1.9 m s^{-1}) and echosounder pulse repetition rate (1 s^{-1}). On RV "Johan Hjort", we used log-based pinging with one ping per 9.3 m. For experiments 1 and 2 we kept the AUV below 150 m to minimize avoidance associated with RV "Johan Hjort" by herring (Vabø *et al.*, 2001).

Autonomous operations

Experiment 1 was an autonomous survey. A zigzag path was programmed into the AUV. RV "Johan Hjort" monitored the survey by remaining stationary at the pre-programmed corner points of each zigzag line. The AUV position could then be updated each time it was within communication range. Since the AUV was outside the echo beam of the research vessel, we had no overview of the school extension and therefore had to rely on the AUV echosounder data to determine when it was inside the schools.

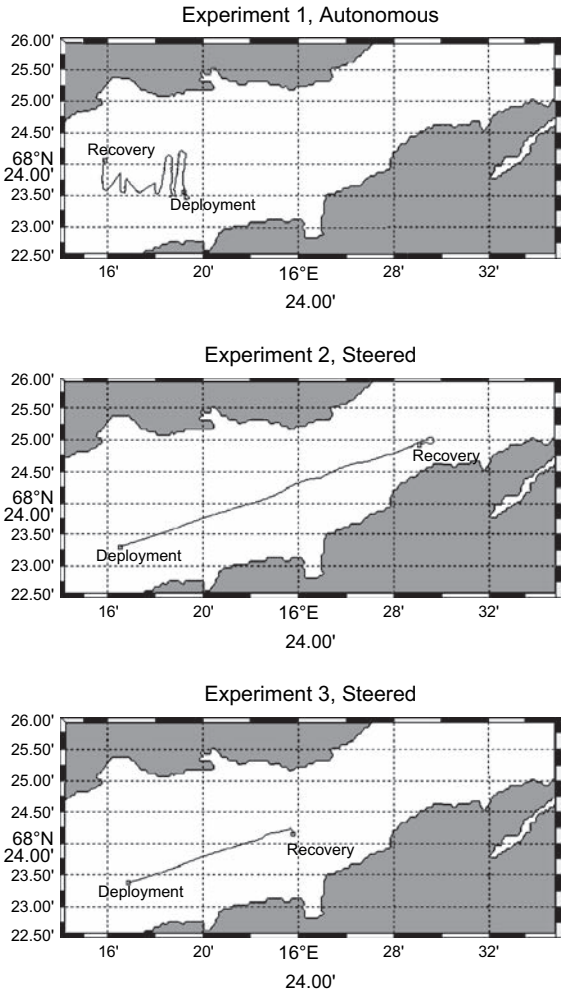

Figure 1. AUV path for each experiment.

Steered operation

Experiments 2 and 3 were run in this mode. The AUV was run in straight lines along the fjord. In both cases, we positioned RV "Johan Hjort" directly above the AUV, except when course change was needed due to commercial fishing activities, mainly small vessels, fishing saithe (*Pollachius virens* L.), with handlines. As a result, we lost the AUV's echo from the mother vessel's echo beam for short periods. This did not interfere with the data acquisition, as we could use the HiPAP system to determine the position of the AUV. Figure 2a, b shows echosounder data from the mother vessel and the corresponding data from the AUV.

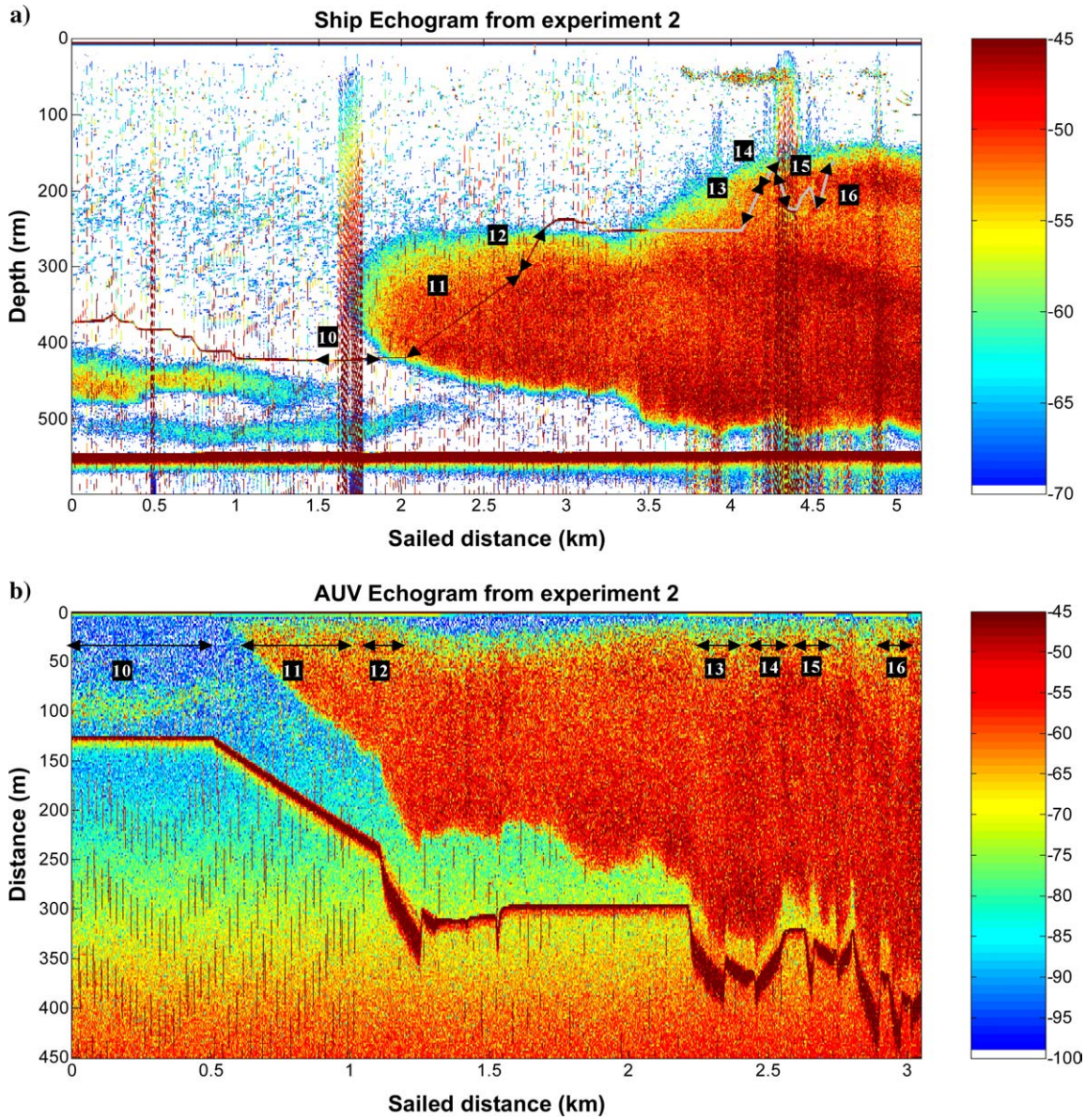

Figure 2. Data from experiment 2. The arrows on the AUV path correspond to the AUV echosounder data sets used in our analysis (Table 1). The colour bar gives volume backscattering strength (dB rel 1 m^{-1}) (a). AUV as observed from the ship's echosounder during the experiment. The backscattering from the AUV can be seen from 0 to 3.5 km sailed distance in the echogram. From 3.5 to 4.6 km the AUV could not be seen in the ship's echogram and a line draws the path. The slope of the path reflects the AUV's tilt angle, as measured by sensors in the AUV (b). Data collected from the AUV during the experiment. Note that the y-axis is the distance from the AUV's transducer.

Analyses

Analyses were done after segmenting the data, each segment corresponding to a continuous path and a constant tilt angle of the AUV. Some of the data sets indicated varying school density caused by navigation in the periphery of the schools and not as a result of avoidance. These data sets were discarded. An exception is the potential inclusion of such data in autonomous operation (experiment 1), as the mother vessel did not monitor the vertical extent of the herring schools. Avoidance was expected to appear as a reduction in density close to the AUV. Because the data considered in this study are close to the transducer, where the signal-to-noise ratio is high, acoustic interference was considered to be negligible.

A background signal was extracted by using areas where there was little evidence of the presence of fish and was

subtracted from the data to suppress the effect of ringing. To determine avoidance distance from the AUV, we fitted a sigmoid function to the average density profiles from the 120-kHz echosounder as a function of distance from the body. This type of function has a maximum and minimum marginal value, the maximum value representing normal school density and therefore reflecting a situation without avoidance. The minimum value corresponds to the point nearest the AUV, where avoidance is maximal. The avoidance distance, d95, was defined as the distance where the sigmoid function reached 95% of its maximum value. The 95% of maximum point was chosen to avoid numerical artefacts associated with estimating the asymptote of the relationship. The distance where the sigmoid function reached 5% of its maximum value is denoted d05 and represents the distance from the AUV where few fish occurred. The avoidance span is defined as the distance between d05 and d95 (Figure 3). Data sets greater or equal to 200 pings were split into intervals of 90−100 pings. We calculated the d05 and d95 values for each interval and used these to calculate the standard deviation for the data set. We also carried out a visual inspection of the AUV echogram to look for single fishes closer to the d05 distance.

Earlier avoidance experiments from this area show that herring can react strongly to vessel stimuli at this time of the year (Vabø, 1999). No significant avoidance from the research vessel is expected below 150 m (Vabø *et al.*, 2001). Diurnal time variations for over-wintering herring have been reported. Herring aggregations are deeper and denser during daytime (07:00 to 16:00) and more disperse and higher in the water column during night-time (16:00 to 07:00) (Huse and Ona, 1996; Huse and Korneliussen, 2000). However, because of the limited data in this study, we do not discriminate between daytime and night-time runs.

The data from the mother ship were investigated to see if we could observe any avoidance was contaminated by acoustic interference. Subsections free from acoustic contamination were used to investigate any AUV avoidance. We plotted density profiles as a function of depth around the position of the AUV. Any avoidance would appear as density reduction close to the AUV echo.

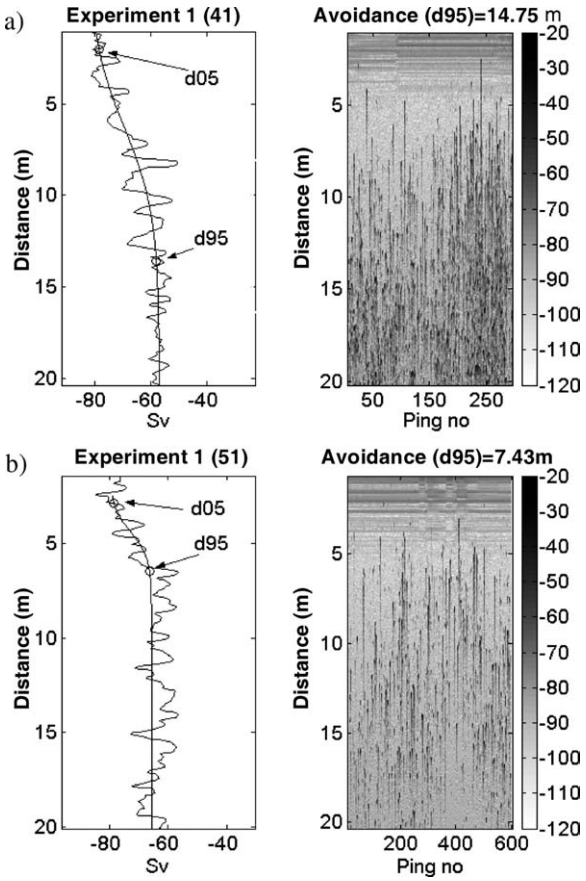

Figure 3. Echogram and density gradient with fitted sigmoid function from data sets 41 (a) and 51 (b) from experiment 1. The colour bar gives volume backscattering strength (dB rel. 1 m^{-1}). Numbers above echogram correspond to data sets in Table 1. The estimates of d95 and d05 are marked with circles. Note that ping scale differs between data sets 41 and 51.

Results

Data from experiment 1 (41, 51, 71, and 61 in Table 1) showed a mean avoidance distance of 13.7 m, and a mean avoidance span of 10.6 m. There was a noticeable drop in standard deviation for the smallest d05 distances, while values for d95 were more stable. Figure 3 shows the corresponding echograms and density profile for data sets 41 and 51. The high variances in data sets 41 and 71 may be an artefact caused by running the AUV on the outer edges of a school. For example, data set 41 gives a high variance because of the upward-sloping school boundary (Figure 3).

We encountered the densest schools during experiment 2 (data sets 1−8, Table 1). The mean avoidance distance was 4.6 m and the mean avoidance span 2.1 m, with relatively low overall variances.

Data from experiment 3 (data sets 11, 13, 15, 16 in Table 1) gave a mean avoidance distance of 8.9 m and a mean avoidance span of 5.27 m. Visual inspection of the AUV echograms showed individual fish closer than the minimum d05 value in Table 1.

The echogram data from the mother ship did not reveal any density reduction around the echo from the AUV. This lack of density reduction can be explained by the acoustic beam coverage at the AUV depth and the sampling interval of 1 m. In Figure 2a, b the data are segmented into seven corresponding intervals numbered from 10 to 16. Intervals 11 to 16 contain data where the AUV is inside the school. Close examination of the data (Figure 2b) 0−10 m from the

Table 1. Results of the analyses from the three experiments. The d95 and d05 values give the distance to the AUV in metres, with their corresponding standard deviations; Svd95 and Svd05 are the volume backscattering corresponding to the d95 and d05 distances; the angle column gives the AUV tilt angle; time represents the start time when the first ping in the data set was obtained along with its duration. The missing standard deviation in data sets 1, 8, 12−16 is due to lack of data.

Data set	No. of pings	d95 (m)	S.d. d95 (m)	Svd95 (dB rel 1 m^{-1})	d05 (m)	S.d. d05 (m)	Svd05 (dB rel 1 m^{-1})	Angle (deg)	Time (hh:mm)	Duration (min)
Experiment 1										
41	295	14.72	2.66	−57.7	3.86	2.65	−76.3	0	13:52	5
71	160	27.06	3.30	−57.0	2.81	2.22	−77.7	0	15:52	2.5
51	600	7.43	2.38	−62.8	3.14	1.28	−77.4	0	18:05	10
61	180	5.48	2.06	−69.6	2.47	1.38	−83.4	0	18:42	3
Experiment 2										
1	113	4.38	–	−59.5	3.24	–	−75.8	−20.0	19:34	1.8
2	280	3.05	2.43	−54.2	1.72	0.50	−69.1	0	19:40	4.7
3	450	4.57	1.44	−54.1	2.29	0.62	−65.8	12	19:45	7.5
4	480	3.24	1.28	−54.5	1.90	0.22	−73.0	0	19:52	8
5	92	4.38	2.3	−54.8	1.91	0.30	−67.6	−19.3	20:01	1.5
6	860	3.24	1.90	−55.6	1.72	0.39	−77.9	0	20:03	14.3
7	480	8.39	1.07	−55.5	2.48	1.44	−73.7	12.0	20:24	8
8	120	5.15	–	−58.7	4.76	–	−69.8	27	20:32	2
Experiment 3										
11	466	4.19	2.12	−58.1	2.47	1.14	−76.5	12.4	16:30	5.44
12	100	21.44	–	−56.0	2.67	–	−79.8	29	16:36	5.4
13	113	2.85	–	−64.8	1.71	–	−85.2	25.0	16:50	1.4
14	96	7.81	–	−60.0	6.86	–	−73.7	13.5	16:51	1.1
15	86	7.24	–	−56.5	2.29	–	−78.1	−19.0	16:52	1.0
16	77	10.10	–	−61.1	3.62	–	−78.4	29.5	16:57	0.9

AUV's transducer shows weaker backscattering than for greater distances. If avoidance can be detected from the mother ship's echogram it should appear as regions of weaker echo above and under the AUV echo.

Discussion

No avoidance reaction around the AUV was seen on the mother vessel's echosounder. This means that avoidance, if it exists, is too small to be detected with the ship's echosounder resolution. However, a limited avoidance was inferred from the AUV's data at a mean distance of 8.0 m. This is seen as low intensity areas in front of the AUV transducer. We discovered during the analysis that sampling problems and acoustic effects might have biased our conclusion.

The acoustic beam, in our case a circular cone of 7°, is very narrow within the threshold distance. Detection probability close to the transducer is therefore low, but few and strong signals are assumed to give an unbiased mean with higher variance. The interpretation of the density profiles with decreasing density and distance was complicated because of the increase in variance, which resulted in oscillating profiles. Background radiation and side lobes give positive bias, while saturation gives a negative bias. The effect of ringing was observed when examining the background signal. For each data set we calculated the background noise and subtracted it from the data set. Echoes at close range to the transducer may drive the signal to saturation; this will give a negative bias to the signal, and appear as density reduction and apparent avoidance reaction. Samples closer than the far field range (1 m) are discarded. Similar considerations should also be done for ranges shorter than far field of herring. In our analysis, we assume that this far field is shorter or equal to that of our instrument. The AUV's echosounder transmitted at 1000 W, and therefore underestimation caused by non-linear acoustic effects may occur (Baker and Lunde, 2002). These effects can still result in uncertainties in our estimates of avoidance distances, but they are more related to estimation of the near-field distance (d05) than to the distance where avoidance is difficult to detect (d95), which we consider relatively robust. As a result, we feel that our interpretation of avoidance distances of the AUV is not strongly influenced by acoustic effects.

Avoidance may be defined as fish escaping out of the echo beam, or as biased tilt angles leading to reduced backscattering. Both effects will lead to underestimation and similar reaction range profiles. Since the fish's behaviour is affected in both cases, we have not discriminated between these two effects. The observation

of single fish closer than the minimum d05 distance can give the impression that some of the herring are not driven by an anti-predator alertness. These events were rare and can be considered as abnormal behaviour.

Our study indicates that the AUV is a gentle intruder, its presence seemingly being ignored beyond an average distance of 8.0 m. This form of intrusion can be viewed as a car moving at very slow speed through a dense crowd of people. The gradients close to the AUV from this kind of behaviour would most likely look like the one obtained from experiments 2 and 3. Fernandes *et al.* (2002) observed an avoidance of 7 m from the Autosub AUV, which is generally consistent with our estimates. By comparison, RV "Johan Hjort" is expected to have an avoidance distance of 150 m (Vabø *et al.*, 2001).

For more detailed investigation of avoidance reaction to the AUV a sonar approach as used in studies of predator–prey interaction may be useful (Nøttestad and Axelsen, 1999; Nøttestad *et al.*, 2002a, b). To gain more accurate avoidance distance measurements one could also apply cameras or Doppler profiler integrated within the AUV to observe tilt angles and swimming speeds relative to the AUV. Similar studies should be repeated to record the potential avoidance reaction threshold for different species. Some noise measurements have been done for the AUV, but more detailed studies, such as those described by Mitson (1995) and Mitson and Knudsen (2003) and performed by Griffiths *et al.* (2001) on the Autosub AUV, should be carried out.

Acknowledgements

This work was funded by the Norwegian Research Council, grant number 130889/122. We are grateful to the crew of RV "Johan Hjort" for their professionalism and for helping with deployment and recovering of the AUV. We thank the Norwegian Underwater Intervention (NUI) for installing the EK60 and letting us experiment with the AUV, Kongsberg SIMRAD (KS), and the Norwegian Defence Research Establishment (FFI) for supporting us in connecting the EK60 to the rest of Hugin's software system.

References

Baker, A. C., and Lunde, P. 2002. Nonlinear effects in sound propagation from echo sounders used in fish abundance. Technical Note. Bergen. CMR-TN02–F10008. 26 pp.

Fernandes, P. G., Brierley, A. S., Simmonds, E. J., Millard, N. W., McPhail, S. D., Armstrong, F., Stevenson, P., and Squires, M. 2002. Fish do not avoid survey vessels. Nature, 404: 35–36.

Fréon, P., Gerlotto, F., and Soria, M. 1992. Changes in school structure according to external stimuli: description and influence on acoustic assessment. Fisheries Research, 15: 45–66.

Griffiths, G., Enoch, P., and Millard, N. W. 2001. On the radiated noise of the Autosub autonomous underwater vehicle. ICES Journal of Marine Science, 58: 1195–1200.

Huse, I., and Korneliussen, R. 2000. Diel variation in acoustic density measurements of overwintering herring (*Clupea harengus* L.). ICES Journal of Marine Science, 57: 903–910.

Huse, I., and Ona, E. 1996. Tilt angle distribution and swimming speed of overwintering Norwegian spring spawning herring. ICES Journal of Marine Science, 53: 863–873.

Kristensen, J., and Vestgård, K. 1998. Hugin: an untethered underwater vehicle for seabed surveying. Proceedings from Oceans 1998, Nice, France, pp. 118–123.

Mitson, R. B. 1995. Underwater noise of research vessels. ICES Cooperative Research Report, No. 209. 61 pp.

Mitson, R. B., and Knudsen, H. P. 2003. Causes and effects of underwater noise on fish abundance estimation. Aquatic Living Resources, 16: 255–263.

Nøttestad, L., and Axelsen, B. E. 1999. Herring schooling manoeuvres in response to killer whale attacks. Canadian Journal of Zoology, 77: 1540–1546.

Nøttestad, L., Fernö, A., and Axelsen, B. E. 2002a. Digging in the deep: killer whales' advanced hunting tactic. Polar Biology, 25: 939–941.

Nøttestad, L., Fernö, A., Mackinson, S., Pitcher, T., and Misund, O. A. 2002b. How whales influence herring school dynamics in a cold-front area of the Norwegian Sea. ICES Journal of Marine Science, 59: 393–400.

Nunnallee, E.1991. An investigation of the avoidance reactions of Pacific whiting to demersal and midwater trawl gear. ICES CM 1991/B: 5. 19 pp.

Olsen, K. 1971. Influence of vessel noise on the behaviour of herring. *In* Modern Fishing Gear of the World, 3rd ed., pp. 291–294. Ed. by H. Kristjonsson. Fishing News (Books) Ltd, London. 537 pp.

Olsen, K. 1990. Fish behaviour and acoustic sampling. Rapports et Procès-Verbaux des Réunions du Conseil International pour l'Exploration de la Mer, 189: 147–158.

Olsen, K., Angell, J., Pettersen, F., and Løvik, A. 1983. Observed fish reactions to a surveying vessel with special reference to herring, cod, capelin and polar cod. FAO Fisheries Report, 300: 131–138.

Ona, E. 1988. Trawling noise and fish avoidance, related to near-surface trawl sampling. Proceedings from Workshop on Year Class Variations as Determined from Pre-recruit Investigations. Bergen, Norway, 1: 169–180.

Ona, E., and Godø, O. R. 1990. Fish reaction to trawling noise: the significance for trawl sampling. Rapports et Procès-Verbaux des Réunions du Conseil International pour l'Exploration de la Mer, 189: 159–166.

Ona, E., and Mitson, R. B. 1996. Acoustic sampling and signal processing near the seabed: the deadzone revisited. ICES Journal of Marine Science, 53: 677–690.

Slotte, A. 1999. Differential utilization of energy during wintering and spawning migration in Norwegian spring-spawning herring. Journal of Fish Biology, 54: 338–355.

Soria, M., Fréon, P., and Gerlotto, F. 1996. Analysis of vessel influence on spatial behaviour of fish schools using a multi-beam sonar and consequences for biomass estimates by echo-sounder. ICES Journal of Marine Science, 53: 453–458.

Vabø, R. 1999. Measurements and Correction Models of Behavorial Induced Biases in Acoustic Estimates of Wintering Herring (*Clupea harengus* L.). University of Bergen, Bergen. 161 pp.

Vabø, R., Olsen, K., and Huse, I. 2001. The effect of vessel avoidance of wintering Norwegian spring spawning herring. Fisheries Research, 58: 59–77.

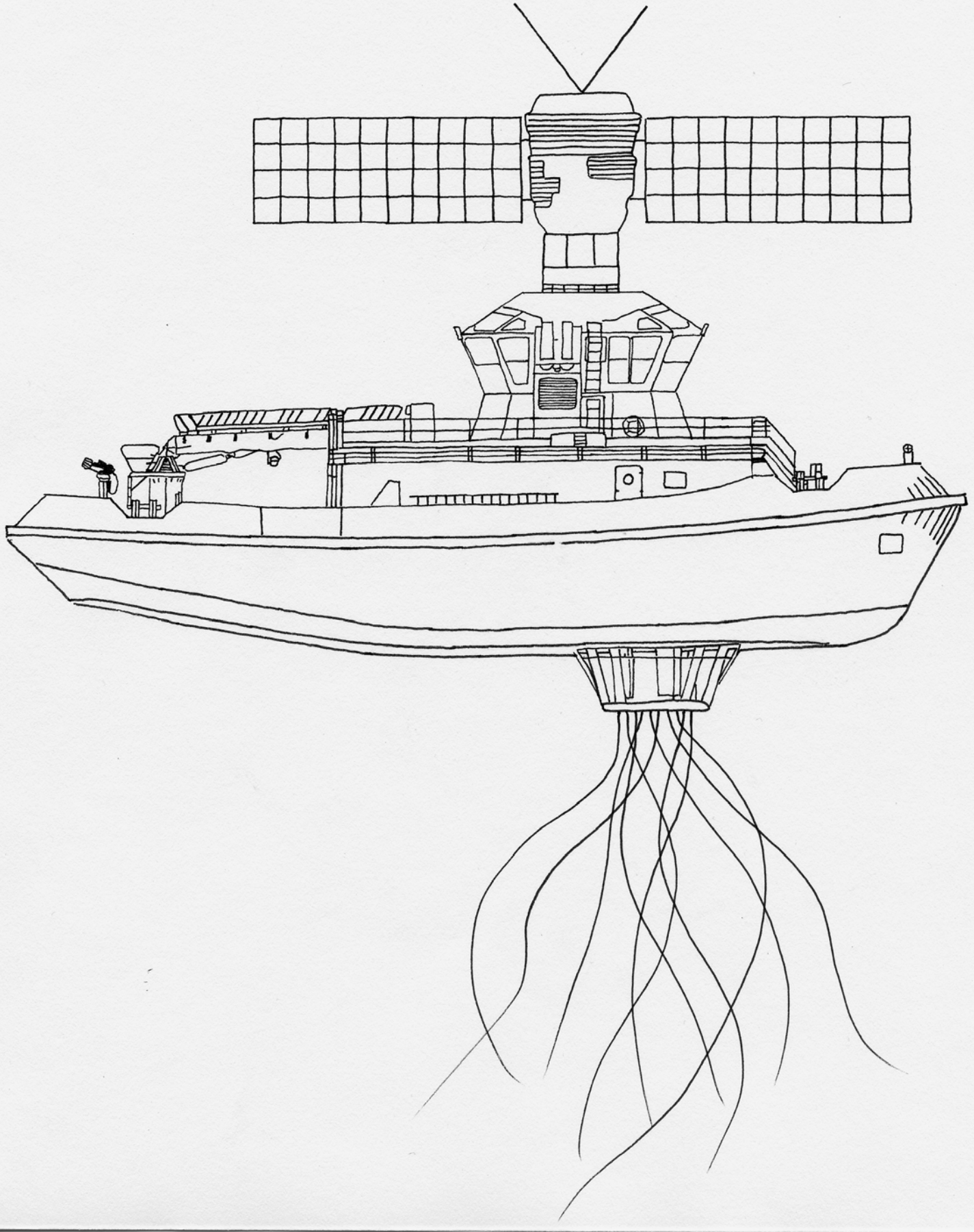

Manuscript

In-situ calibration of deep bottom mounted echo sounder systems.

Ruben Patel and Egil Ona

Abstract

A calibration procedure for bottom mounted split beam echo sounders are presented, using a research vessel and Remote Operated Underwater vehicle. A procedure for correction of un-calibrated raw echo sounder data is also presented and discussed. The examples given are from a calibration in the Ofotfjord, Narvik, Norway on two bottom-mounted transducers at 400 meter and 500 meters depths. The calibration was controlled by comparing data collected from the vessel with data collected from the bottom-mounted system. A calibration accuracy of about ± 0.2 dB was achieved on non-ideal elliptical beams of specialized ES38DD split beam transducers. Comparable fish densities were recorded in the same depth layers from a research vessel and the bottom mounted system. Deviations may be accounted for differences in dorsal and ventral target strength of herring.

Introduction

Acoustic echo sounder systems used for biomass measurements needs to be calibrated in order to compare data trough time, between instruments and for absolute biomass estimation. Calibration of the Simrad EK60 scientific echo sounder is done regularly on all the research vessels of the Institute of Marine Research in Norway (IMR). Using a scientific split beam system, this involves a guiding of a calibration sphere at approximately fixed depth through different locations in the acoustic beam (Ona, 1999). This is now a standardized procedure when conducted from a research vessel, but in some occasions, like here, it requires imagination, skill and advanced equipment due to the psychical placement and configuration of the transducers.

Different approaches are used depending on the measurement set-up and platform holding the echo sounder. Standard procedure for transducers mounted in the keel of vessels is suggested by Foote et al. (1987), using a three-winch setup for controlling the positioning of the reference target. The sphere is moved systematically so it covers the main lobe of the acoustic beam.

Ona and Vestnes (1985) used brute force procedure in order to measure the equivalent beam angle on a hull-mounted single beam transducer on RV Eldjarn. A diver fastened a single 20 meter long nylon line of the calibration sphere close to the transducer. The vessel was then slowly trimmed down to 10˚ both to starboard and port by pumping oil into different compartment in the RV. The integrated energy of the sphere, and alongship and athwartship angles of the vessel was manually recorded using two spirit level-meters with an accuracy of 0.05 degrees.

Dalen et al. (2003) calibrated a transducer mounted on a towed body by suspending a calibration sphere some meters underneath the transducer surface. The vehicle was deployed and calibration data was gathered at different depths. In order to cover the acoustic beam with the sphere, the vehicle was maneuvered so that the sphere swung randomly until the whole beam was covered.

A more advanced calibration procedures for towed body is described in MacLennan and Simmonds (1992). This procedure holds the target steady while the body is rotated on a motorized gimbal table. The tilt angle of the body is retrieved from angle encoders.

The Hugin Autonomous underwater vehicle (AUV) was fitted with a 120 kHz downward looking scientific split beam echo sounder. A calibration sphere was suspended in the water column at proper distance. The sphere was attached to a line anchored to the sea bottom and stretched by a small float. This made the sphere stationary and the AUV was tilted, rolled and moved in order to cover all the quadrants of the transducer surface with measurement data (Patel et al. 2004)

In this paper we present a new calibration method and corrections to previously recorded data where only nominal echo sounder performance have been entered. The calibration was conducted in Ofotjord on two bottom-mounted transducers t 400 meter and 500 meters depths Afterwards, the calibration results were controlled by comparing data on herring densities recorded on the research vessel with data collected from the bottom-mounted system.

Material and Methods

The transducers to be calibrated are part of an observatory located at the border between Vestfjord and Ofotfjord. The bottom-mounted units consist of 38 kHz pressure compensated transducers (Simrad ES38DD) and corresponding EK60 General Purpose Transceivers (GPT) connected on gimbal suspension systems. This makes the transducers face align horizontal to the sea surface independent of the sea bottom slope on the mounting location. The system was deployed from a military mine hunting vessel (KNM Tyr, 42.5 m) using a winch. From the same vessel a remote controlled underwater vehicle (ROV) was used to monitor the deployment and adjust the orientation according to the onboard compass.

A cable connects the bottom units to a cabin at land where data is collected on a standard PC. The cable consists of optical fibre for data transmission and a metal core for power. The cabin resides on a remote location and the nearest town is located 5 km on the other side of the fjord. We use a wireless Ethernet connection between the town and the cabin to be able to remote control the system and for data transmission.

Before deployment, the manufacturer, Simrad A/S, measured the directivity patterns of the transducers in the standard tank for such measurements. Since to the pressure effect on the transducers (Figure 3) and the fact that the baffle, witch in our case is the suspension frame and sea bottom, can affect the equivalent beam angle of the transducer as much as 15% (MacLennan and Simmonds, 1992) the transducer had to be calibrated in-situ, after deployment. The standard split beam calibration method (Foot et al. 1987) was used as basis. The calibration was done using RV GO. Sars and ROV Aglanta. The ship was set in dynamic position mode (DP) and the ROV was deployed to determine the exact position of the bottom units, using video and an acoustic transponder system (HiPAP) from positioning the ROV relative to the vessel. A calibration sphere was attached 4.7 meters under the ROV. The sphere was then piloted down to the bottom units to a suitable distance from the transducer face (37 m on inner transducer and 24 m on outer transducer). The pilot manoeuvred the ROV within an ellipse of radius 2.3 m x 7.0 m over the inner transducer and within an ellipse of radius 1.44 m x 4.4 m over the outer transducer. Despite the small geometrical area the pilots managed to move the sphere within the transducer beam covering all the four quadrants of the split beam system. In several instances, nosy fish, mainly Saithe (*Pollachius virens)* close to the ROV and sphere was observed from the ROV cameras. The time used for calibrating two

transducers was about three hours. An Ocean mapping/navigation system was used to monitor the position of the bottom units, ROV and research vessel. The ships position from the Global Positioning System (GPS) and ROV's HiPAP system position was fed to the map system, giving a 3D real-time overview of the operation. In order to cover all the transducer quadrants with the sphere, the ROV pilot needed a real time view of the spheres position in the acoustic beam of the bottom-mounted echo sounder. For this, a PC was connected to the ships Ethernet. Using the ships satellite link and a therminal emulator program it was possible to control and monitor the EK60 PC on land, simultaneously showing the echo sounder display and sphere position as detected by the echo sounder. Figure 1 shows a conceptual diagram over the calibration situation.

Prior to the calibration, operational control data had been collected from the ship and the bottom mounted transducers, the ship was manoeuvred over the two transducers. The ping repetition rate was set to 5 seconds to reduce the ship and bottom echo sounder interference. The orientation of the transducers, separation distance and the different beam shapes (circular on vessel transducer and elliptical on bottom mounted transducers) necessitated focus on a common depth range where the transducer sampling volume is nearly identical. Data focused around this depth is used to compare the backscattering data from herring as recorded by the two systems.

This is done by calculating the sampling volume as function of distance and finding the comparable depth ranges. The sampled volume for the ship transducer is given in equation (1).

$$V_s = (d+r)^2 \pi \tan(\alpha)\tan(\alpha) c \frac{\tau}{2}, \quad (1)$$

where d is the depth of the transducer, r is the range from the surface, α opening angle, c sound speed, τ pulse duration length. The sampling volume for the bottom-mounted transducer is given in equation (2)

$$V_h = (B-r)^2 \pi \tan(\alpha)\tan(\beta) c \frac{\tau}{2}, \quad (2)$$

where B is the depth of the upward looking transducer, r is the range from the surface, α is the along ship opening angle, β is the athwart ship opening angle, c sound speed and τ pulse duration length.

The common range at which both sampling volumes is equal is derived by solving V_s=V_h for r. The equal volume range is called r_0. In order to compare ship data and data from the stationary system a depth interval based on r_0 is calculated. The calculated interval ensures that the total difference between ship sampling volume and the sampling volume from the bottom-mounted system is equal on both sides of r_0. The volume difference is given in equation (3)

$$dV(r) = \left| V_h(r) - V_s(r) \right| \qquad r = [10, B], \quad (3)$$

where $dV(r)$ is the absolute value of the volume difference, $V_h(r)$ is the sampling volume for the bottom mounted system, $V_s(r)$ is the sampling volume for the ship transducer, r is the range from the surface, r_0 is the range to where both system has the same amount of sampling

volume and *B* is the depth of the bottom mounted system. The comparable volume interval (CVI) is expressed by equation (4).

$$(4) \qquad \int_{x_1}^{r_0} dV(r)dr = \int_{r_0}^{r_0+d} dV(r)dr,$$

and is solved for x_1. The CVI is then $[x_1, r_0+d]$, where d is an user chosen range, see Figure 5 for illustration. CVI is then used to select depth interval of volume backscattering data from the two systems. The average volume backscattering is estimated for both data sets and the difference is calculated. This difference must correspond to the correction formulas obtained from the calibration operation.

The data from the calibration operation was downloaded to the ship to calculate correction formulas for the two bottom mounted transducers. The Simrad BI60 post-processing system was used to isolate sphere echoes form fish echoes. However, the normal beam fitting procedure for split beam systems, using the "lobe" routines could not be applied for this particular transducer directivity patterns. The beam pattern was measured and simulated by SIMRAD before deployment. Figure 2 shows the measured beam pattern. Since the beam pattern not only is elliptical, but also contain a local minimum at acoustic axis in the widest direction, conventional estimation of centre gain, beam opening angles and angular offsets could not be done directly. Here, we instead, selected detections within one degree of the top point as the reference point for gain estimation, i.e $b^2(\alpha,\beta) = 1$. From this point, the measured target strength (TS) was calculated by averaging the detections within the one-degree intervals. New gain was calculated from equation (5).

$$(5) \qquad G_{new} = \frac{(TS_m - TS_t)}{2} + G_{old},$$

where G_{new} is the new transducer gain, TS_m is the target strength of sphere during calibration, TS_t theoretical target strength of sphere and G_{old} is the old transducer gain. The correction formula is derived from the volume backscattering. In linear domain this is given in equation (6).

$$(6) \qquad s_v = p_r \cdot TVG \cdot C,$$

where s_v is the volume backscattering, p_r is the receive power, *TVG* is the time varying gain and *C* is an frequency dependent constant. *TVG* is given in Equation (7).

$$(7) \qquad TVG = r^2 \cdot 10^{\frac{2\alpha r}{10}},$$

where *r* is the range and α the absorption constant. *C* is given in Equation (8).

$$(8) \qquad C = 10^{-\frac{2G+\Psi}{10}} \cdot \frac{32\pi^2}{p_t \lambda^2 c \tau},$$

where G is the gain, Ψ is the two way beam pattern, p_t is the transmit power, λ is the wave length and τ is the pulse length in seconds. Equation (5),Equation (6), Equation (7) and Equation (8) is taken from (SIMRAD,1997). In order to simplify the calculation Equation (6), Equation (7) and Equation (8) is expressed in dB. This gives Equation (9), Equation (10) and Equation (11).

(9) $$s_v = 10\log_{10}(p_r) + 10\log_{10}(TVG) + 10\log_{10}(C)$$

(10) $$10\log_{10}(TVG) = 20\log_{10}(r) + 2\alpha r$$

(11) $$10\log_{10}(C) = -2G - \Psi + 20\log_{10}(32\pi) - 10\log_{10}(p_t) - 20\log_{10}(\lambda) - 10\log_{10}(c) - 10\log_{10}(\tau)$$

Putting Equation (10) and Equation (11) into Equation (9) and rearranging gives Equation (12).

(12) $$\begin{aligned} S_v = {} & 10\log_{10}(p_r) + 20\log_{10}(32\pi) - 10\log_{10}(p_t) \\ & - 20\log_{10}(\lambda) - 10\log_{10}(\tau) + 20\log_{10}(r) \\ & \underbrace{+ 2\alpha r - 2G - \Psi - 10\log_{10}(c)}_{M} \end{aligned}$$

In this case we need to correct for G, c and α. The term in Equation (12) effected by these variables is called M. This means that the correction formula can be expressed as in Equation (13).

(13) $$S_{vnew} = S_{vold} - M_{old} + M_{new}$$

where S_{vnew} is the corrected volume backscattering, S_{vold} is the old uncorrected volume backscattering, M_{old} is the M used in S_{vold} and M_{new} is the M as it would appear in S_{vnew}. M is given in Equation (14).

(14) $$M = 2\alpha r - 2G - \Psi - 10\log_{10}(c)$$

Results

The deployment of the bottom-mounted system resulted in the outer transducer athwart direction to point 110° and the inner transducer athwart direction pointing 130°. The monitoring system has been in regular operation since November 2002. Harsh weather condition, hardware and software failure has occurred and resulted in a few system halts. The system has gradually been improved to increase stability, and the data is now available over Internet in real time. The area where the bottom-mounted transducer is located is a popular fishing ground, resulting in one instance of cable damage, most likely due to trawling activities.

During the ROV inspection, accumulation of marine snow on the transducer head was observed, but the transducers are too deep for problems with respect to bio fouling. Figure 7 shows 2D and 3D overview of the operation. The snapshot is taken after calibration of the inner transducer. In the Figure 7, the research vessel and ROV are on its way to outer

transducer. The ships auto position system is set to use the ROV as reference point, which in practical sense means that the ROV pilot has control over both the research vessel and the ROV at the same time. Figure 8 shows echogram from the calibration of the outer transducer. The sphere detections had to be selected manually by post processing whenever disturbing fish echoes came close to the sphere echo.

During data collection for comparisons between densities recorded by vessel and bottom mounted systems, the horizontal distance between ship GPS and bottom mounted transducer were 12 m for the inner transducer and 15 m from the outer transducer (Figure 4). The calculated difference in sampling volume, from the ship transducers at 10 m depth and bottom-mounted transducer at 500 m depth, is plotted in
Figure 5. The depth interval for comparative data is calculated using the parameters in Table 1. For the inner transducer the equal volume range is calculated to r_0=257 m, using d = 25 m and solving for x_1 in equation (4) gives the equal volume interval [232 m, 282 m]. For the outer transducer the equal volume range is calculated to r_0=322 m, using d = 25 m and solving for x_1 in equation (4) gives the equal volume interval [297 m, 347 m].
Figure 6 shows the average volume backscattering (S_v) taken over the CVI depth interval. The average volume backscattering difference (ΔS_v) is 2.1 dB for the inner transducer and 4.8 dB for the outer transducer.

Data from the inner transducer showed 894 sphere detections and 38 within one degree of the highest peak. For the outer transducer there were 569 sphere detections and 17 within one degree of the highest peak (Figure 9). Theoretical target strength for the calibration sphere is TS_t=-33.60 dB, averaged measured target strength for the inner transducer is TS_m= -35.75 dB and for the outer transducer TS_m=-38.17 dB. Using equation (5) the new gain for the inner transducer is G_{new}=20.23 dB and for the outer transducer G_{new}=19.02 dB. Inserting parameters from Table 2 into Equation (13) gives the correction formula for the inner transducer in equation (15)

(15) $$S_{vnew} = S_{vold} + 0.0012r + 2.22\,,$$

and for the outer transducer in equation (16)

(16) $$S_{vnew} = S_{vold} + 0.0012r + 4.64\,,$$

where S_{vnew} is the corrected volume backscattering, S_{vold} is the old volume backscattering and r is the range. Equation (14) corresponds to ΔS_v. Ignoring the small range dependency shows that the difference between the two methods is 2.09-2.22 = -0.13 dB for the inner transducer and 4.79-4.64=0.15 dB for the outer transducer, corresponding to an error of about 3% in the density estimates. These results are also summarized in Table 3.

Discussion

Experience during the deployment period shows that it is important with a redundant system for remote observation stations. For some systems, the sequence in which each component is started will have effect on its functionality. In order to perform a controlled power recycling it is possible to install devices that switch power on and off trough mobile phone short messages format (SMS). This can be installed as a complete isolated system. Equipment deployed in areas with heavy fisheries activity should be trawl proof. In this case the equipment was not trawl proof due to the cost involved. Despite this weak point, the system has only been harmed once by fishing activity over four years of operation. Some instances of power failure have occurred, due to weakness and failures in the system from the power company. It seems

that this remotely, low populated area is more exposed to failure in the power supply than more urban areas on the coast. This can be due to small or no redundancy in the power delivery system. It is thus necessary to have some alternative backup system that can provide the instrumentation power for at least a couple of days.

The ROV camera revealed accumulation of marine snow on the transducers. This made it impossible to observe potential bio fouling. However, at these depth bio fouling usually does not occur and the accumulation of marine snow should have minimal effect on the acoustic characteristics of the transducer.

Manually isolation of sphere targets was conducted for removing fish targets in the calibration data set. Even with careful removals, there is a small probability that some of the accepted data contain erroneously accepted multiple targets, a mix between the sphere echo and a fish echo, but both the pulse duration filter and the phase stability filter implemented in the echo sounder will remove most of these. However, the use of light on the ROV attracts fish, but was needed during navigation of the ROV. If a few mixed echoes were to be accepted, this will usually result in higher target strength of the sphere, and the correction factor will be underestimated. There might also be some bias due to the elliptical form of the acoustic beam, as computation of the correct equivalent beam is more complicated for this beam than for a conventional, circular beam. The calibration accuracy may therefore be somewhat less than the usual ±0.1 dB, as claimed for the research vessel systems, and ±0.2 dB seem to be more appropriate here.

Comparing the difference between ship data and data from the bottom mounted system with the correction formula shows that there is only a small (< 0.2 dB) difference between the two methods. We therefore conclude that the correction procedure suggested does a good job in correcting for the data sampled with the un-calibrated bottom mounted system.

An alternative option would be to plan the attachment of a calibration sphere permanently above both transducers. In this way, continuous monitoring of system changes and performance that may affect the observations could be part of the data collection. However, bio-fouling or air bubbles trapped on the sphere might also affect the reference target.

References

Dalen, J., Nedreaas, K., Pedersen, R. 2003. A comparative acoustic-abundance estimation of pelagic redfish (Sebastes mentella) from hull-mounted and deep-towed acoustic systems. ICES Journal of Marine Science, 60:472-479.

Foote, K. G., Knudsen, H. P., Vestnes, G., MacLennan, D. N., Simmonds, E. J. 1987. Calibration of acoustic instruments for fish densety estimation: A practical guide. ICES cooperative research report. No. 144, 69 pp.

MacLennan, D. N., Simmonds, E. J .1992. Fish and Fisheriesin Fisheries Acoustics,Calibration.Chapman & Hall,London

Ona, E.(Ed.) 1999. Methodology for target strength Measurements. ICES Cooperative Research Report. No. 235, 59 pp.

Ona, E., Vestnes, G.1985.Direct measurement of equivalent beam angle on hull-mounted transducers. ICES. C.M. 1985/B:43, pp. 1-10.

Patel, R., Handegard, N. O., Godø, O. R. 2004. Behaviour of herring (Clupea harengus L.) towards an approaching autonomous underwater vehicle. ICES Journal of Marine Science, 61:1044-1049.

SIMRAD. 1997. SIMRAD EK500 Fisheries research echo sounder. Operator manual.

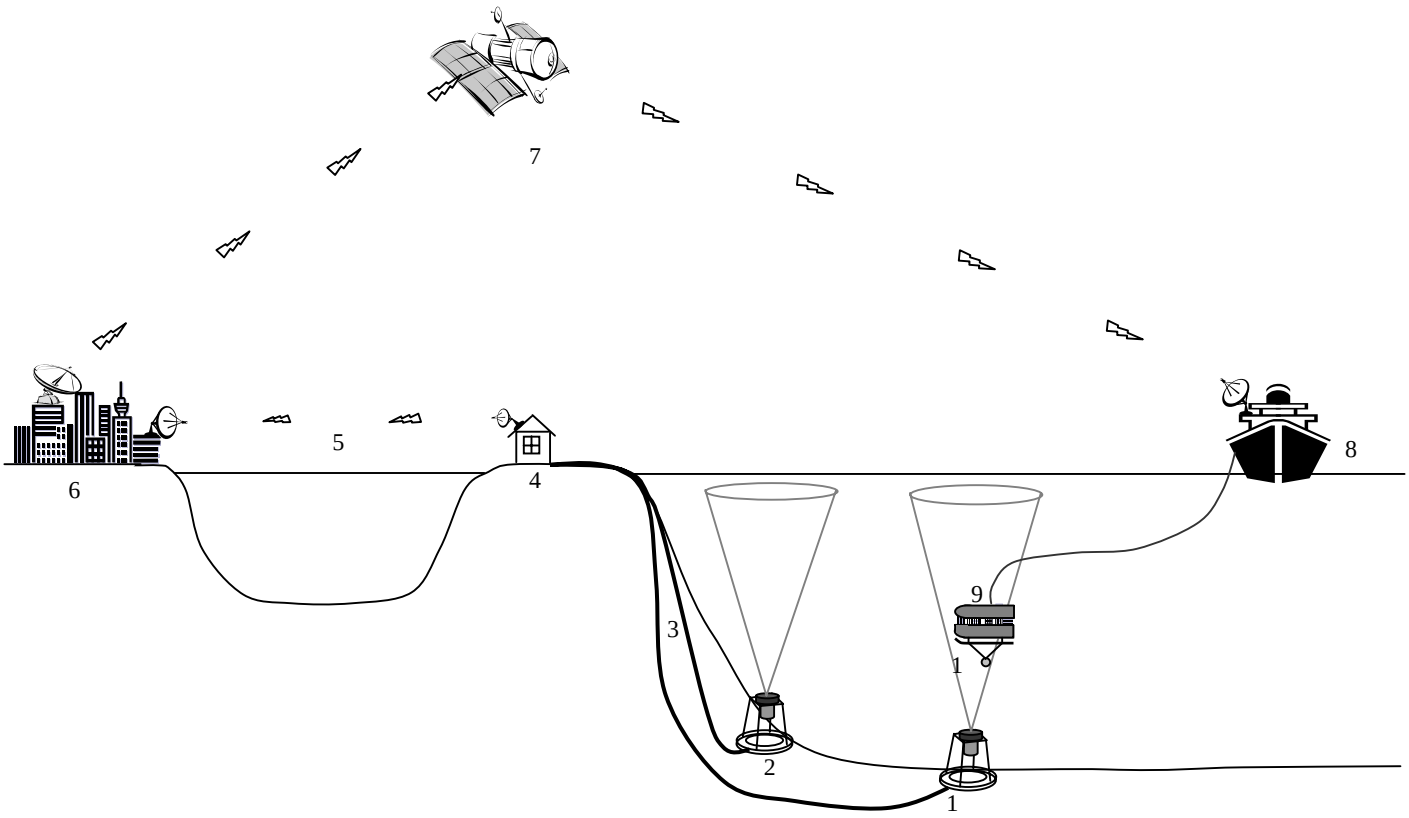

Figure 1. Calibration setup for the bottom-mounted transducers. 1 and 2 shows the bottom-mounted transducers. Cables from transducers to land station (3).Cabin on land for data collection (4). Wireless data link (5). Løddingen town (6) where the data is distributed to Ethernet. Sattelite link (7). RV ”G. O. Sars.” (8). ROV ”Aglanta” (9) with Calibration sphere (10).

a)

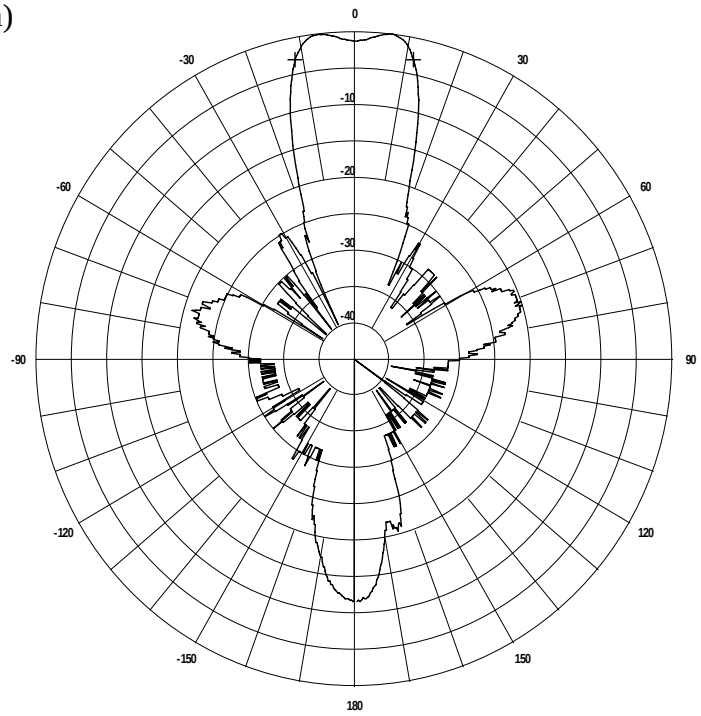

b)

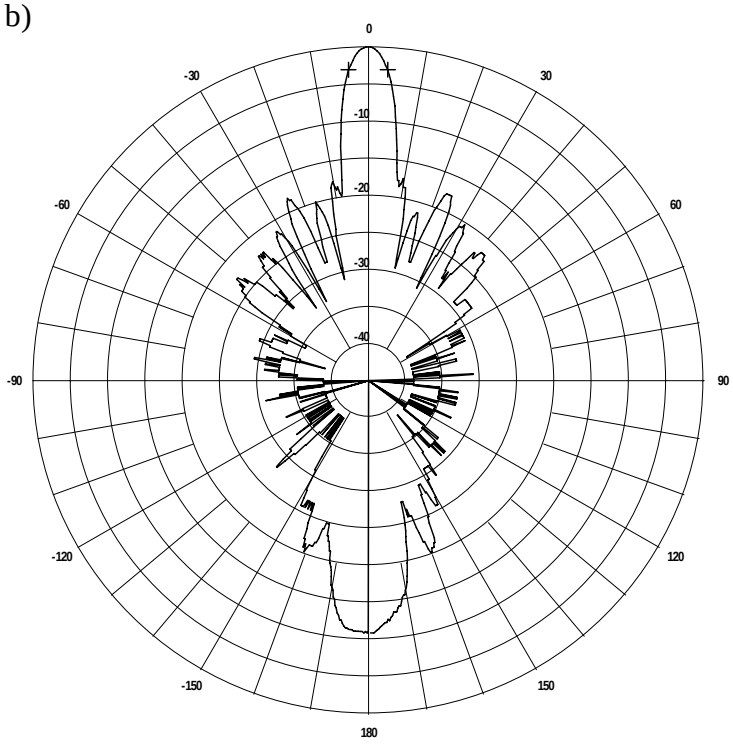

Figure 2. Polar plot of beam pattern as measured by SIMRAD in water tank. The lobe is asymmetrical in the athwart and along ship direction. a) Athwart ship angle measurements. Note the bimodal peak b) Along ship angle measurements. Range show target strength TS in dB rel. $1m^{-1}$. Theta shows the measured angle.

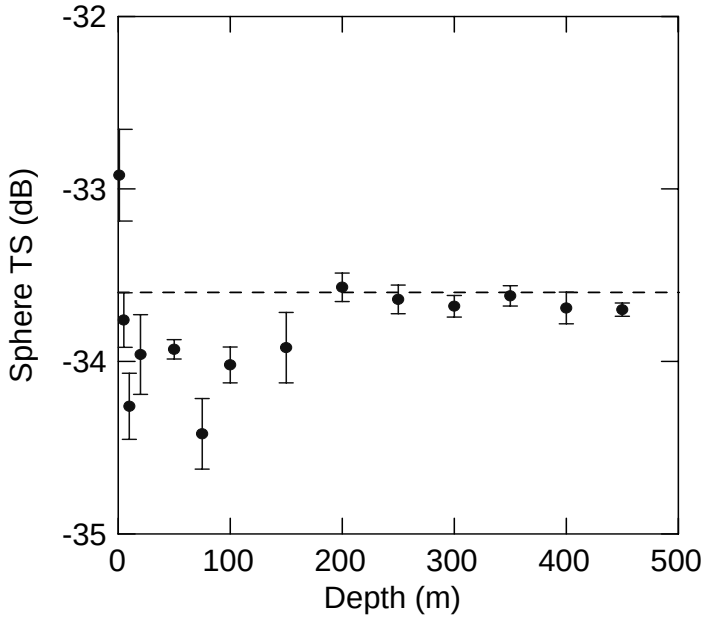

Figure 3. Shows the depth effect on a depth compensated 38 kHz transducer, ES38DD. The target strength of a calibration sphere changes as function of depth. The signature may differ among different transducers. (Reference: Ona & Svellingen 1999)

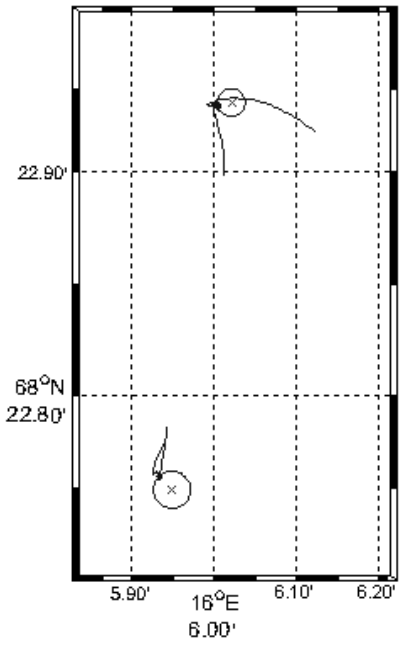

Figure 4. Position of bottom mounted transducers and ship during data collection for comparative measurements of density. Track lines indicate ship position and cross shows bottom mounted transducer position. The upper and lower rang ring is 12 m and 15 m in radius.

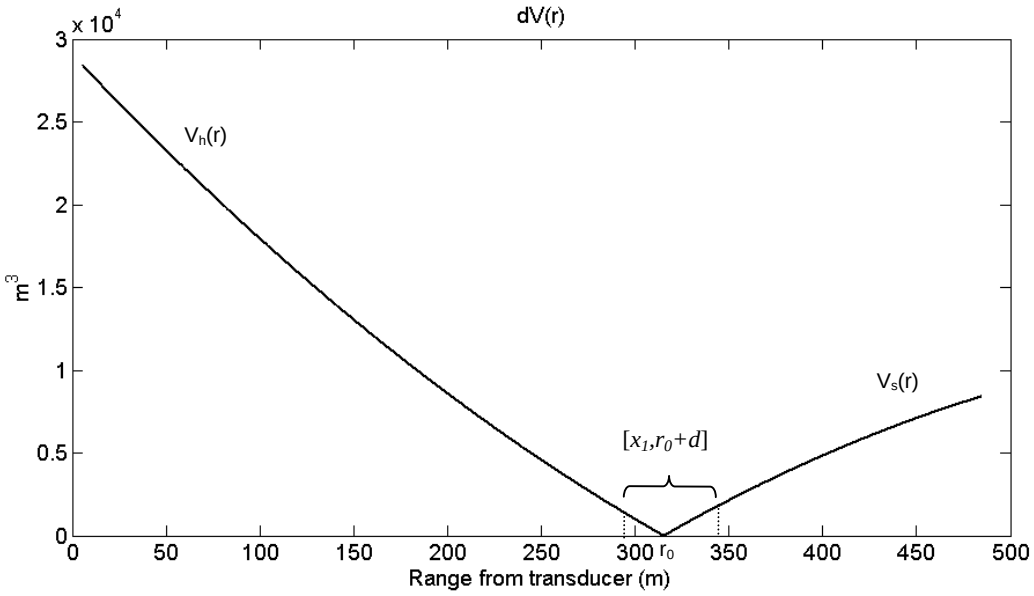

Figure 5. Difference in sampling volume from the deepest bottom mounted transducer and ship transducer.

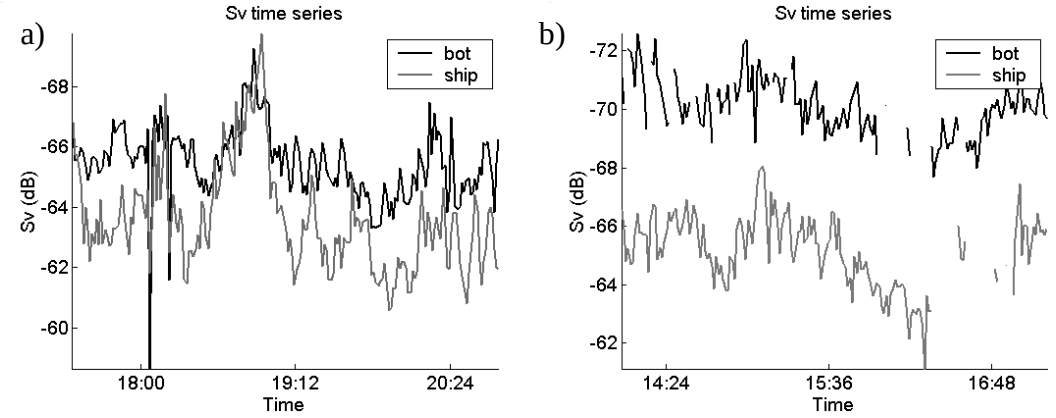

Figure 6. Time series of volume backscattering in dB from bottom-mounted transducer (bot) and ship transducer (ship). a) Data for the inner transducer and b) data from the outer transducer, both before calibration.

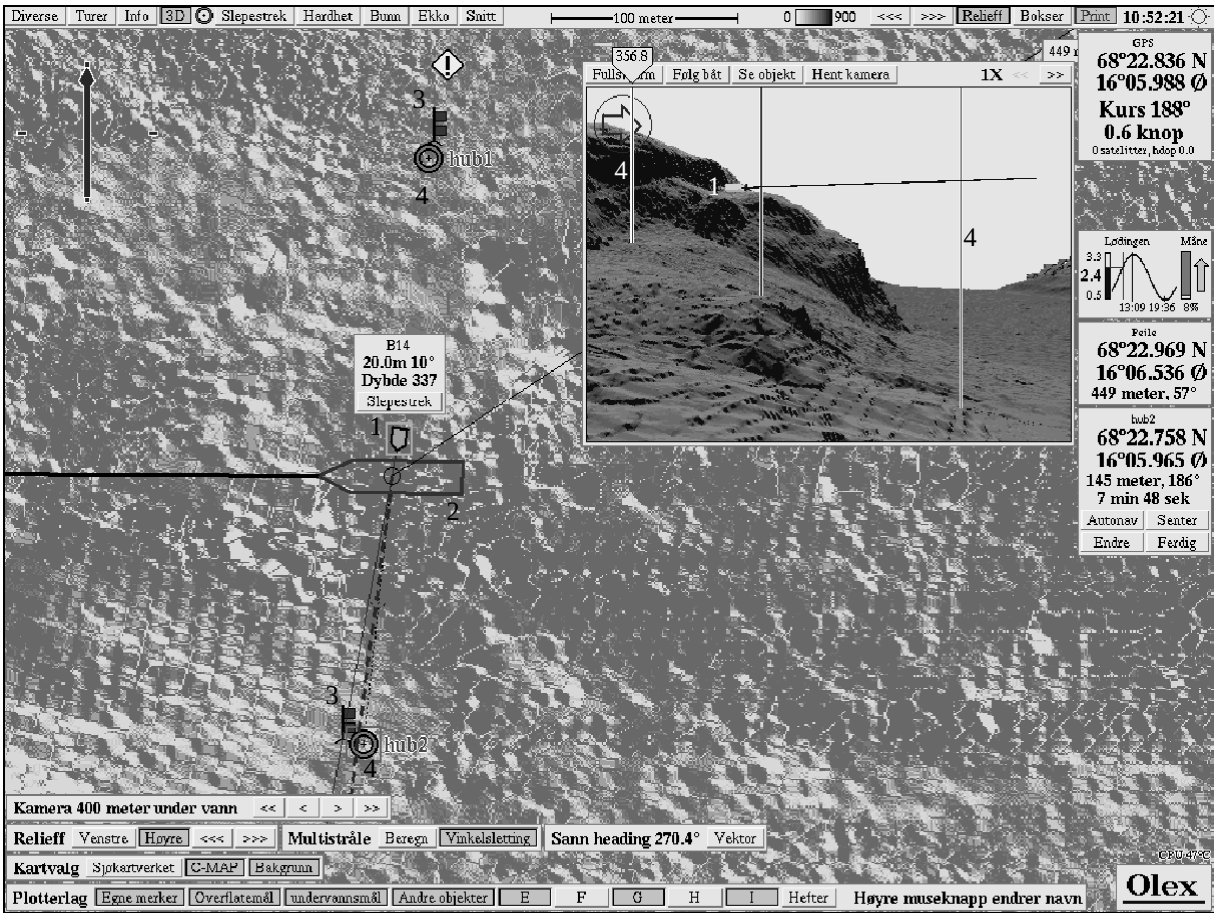

Figure 7. 2D and 3D view of the calibration operation. 2D view: (1) ROV and (2) RV between the two bottom mounted transducers. Flag (3) shows position taken under deployment of the system. (4) Shows new positions obtained during relocation for calibration. 3D view: Camera is positioned 400 m under water west for the outer transducer or hub2 in figure. Camera heading is east. (1) Indicates ROV, RV cannot be seen due to camera depth, but middle (5) bar shows RV's horizontal position. Two outer (4) bars show position of transducers.

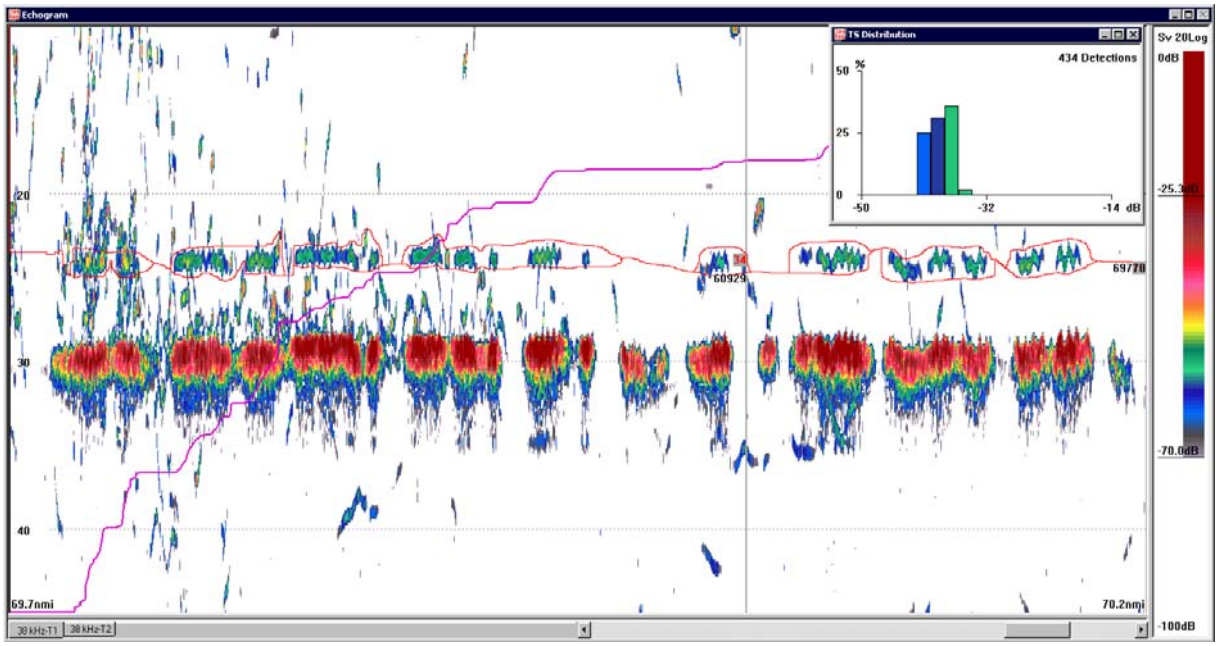

Figure 8. Echogram from calibration of outer transducer and the TS distribution of calibration sphere detections. The Echogram is upside down due to the upward looking orientation of the transducer. The strong large echo signal at 30 m is the ROV. The calibration sphere is the weaker shorter echo at 24 meters. The line around the sphere echo shows manually selected targets for isolating the calibration sphere. Individual tracks around the ROV and vertically across the echogram are echoes of individual Saithe.

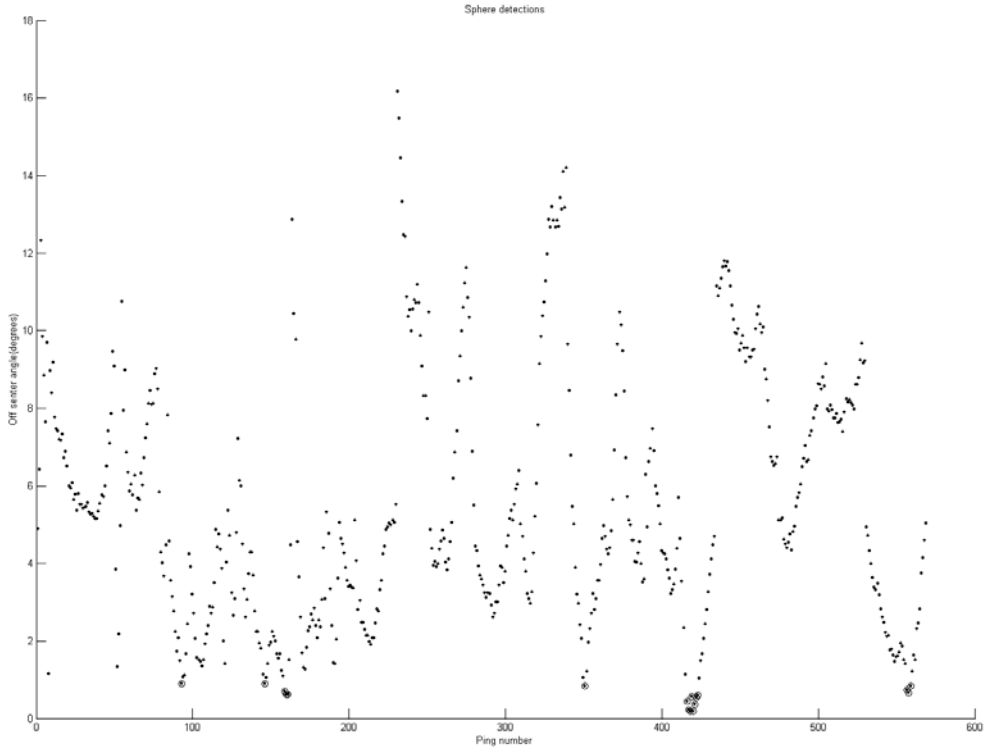

Figure 9. Sphere detection plotted against off centre angle. Black dots indicate detections. Circled black dots indicate detections within one degree of acoustic axis.

Table 1. Parameters used in calculating comparison interval for ship data and data from the bottom mounted system. B is the depth of the bottom mounted transducer, c is sound speed in water, τ pulse duration length, α along ship opening angle, β athwart ship opening angle, d user chosen offset from r_0 , r_0 range at which sampling volume form ship and bottom mounted system is same magnitude and depth and CVI is the depth interval where data is to be compared.

Parameters	Inner Transducer	Outer Transducer
B (m)	400	500
c (m/s)	1475	1475
τ (s)	1.024/1000	1.024/1000
α (degrees)	7	7
β (degrees)	23	23
d (m)	25	25
r_0 (m)	257	322
CVI (m)	[232, 282]	[297, 347]
ΔS_v (dB)	2.09	4.79

Table 2. Old and new transducer parameters influencing the volume backscattering.

Transducer	α (db/km)	G (dB)	10log(Ψ) (dB)	c (m/s)
Old inner, outer	9.75	21.30	-15.30	1500
New inner	10.36	20.23	-15.30	1475
New outer	10.36	19.02	-15.30	1475

Table 3. Comparison of correction factors obtained from volume backscattering measurements (ΔS_v) from ship and bottom mounted system and the calibration operation (Sphere).

	ΔS_v(dB)	Sphere(dB)	Diff(dB)
Inner transducer	2.09	2.22	-0.13
Outer transducer	4.79	4.64	0.15

Manuscript

Diel variation in acoustic density of overwintering Norwegian spring spawning herring (*Clupea harengus* L.*)* as observed from a moving vessel and stationary bottom mounted platform.

Ruben Patel and Olav Rune Godø.

Abstract
Norwegian Spring Spawning Herring (*Clupea harengus* L.) is studied in the Ofotfjord in northern Norway. The diel variation in acoustic density is studied as observed from a stationary system and from a moving research vessel (RV). The stationary system has a greater temporal resolution then the data from the moving RV. The layer depth and thickness, biological diurnal periods and duration is therefore studied from this system. Analysis shows that there exist small-scale spatial variations between the stationary transducer locations. The comparisation between the ship data and stationary data reveal different diurnal backscattering profiles and indicate that the ship affects the acoustic backscattering top layer.

Key words: stationary bottom mounted transducers, upward looking transducers, vertical migration, diurnal migration, acoustic survey.

Patel, R., and Godø, O. R: Institute of Marine Research,P.O. Box 1870, N-5817 Bergen, Norway. Correspondence to Ruben Patel Fax: +47 55-23-68-30. E-mail: ruben@imr.no

Introduction

The Norwegian Spring Spawning Herring (NSSH) (*Clupea harengus* L.) is a large oceanic stock with spawning area, and in periods wintering areas, located along the Norwegian coast (Misund et al 1998;Toresen and Østvedt 2000). The Norwegian fjord system; Tysfjorden, Ofotfjorden and Vestfjorden have been the over wintering ground for the Norwegian Spring Spawning Herring in recent years. The herring enters the area in the beginning of October and start the migration to the spawning grounds in January (Røttingen et al.,1994). Herring do not feed during the over wintering (Slotte ,1999).

The huge aggregation of herring (several million tonnes) confined in a relative small geographic area has routinely been surveyed by research vessels for acoustic abundance estimation. Further, in conjunction with these investigations, survey methodological studies including in-situ acoustic target strength (TS) measurements from a stationary platform (Huse and Ona 1996), TS measurements on captive adult herring (Ona 2003), avoidance to survey vessel using a submerged stationary acoustic transducer (Vabø et al. 2002), diurnal variability as observed from a moving vessel (Huse and Korneliussen 2000) and particularly for the aim of this paper; are diurnal dynamics correctly described by vessel acoustics? Acoustic surveys from research vessel (RV) are commonly used for assessment of clupeid species and are of major importance to the assessment of Norwegian Spring Spawning Herring (Mitson, 2003). Errors may have serious impact on the quality of the assessment.

Fréon et al.(1996) used acoustic data sampled from a moving RV to demonstrate, for pelagic fish ,a lower acoustic backscatter during the night (1900 to 0500) compared to a 2-3 times higher backscattering during the day (0500 to 1900). They also observed that the transition period from night to day is shorter than that from day to night.

Huse and Korneliussen (2000) used data from moving RVs to study diurnal dynamics of NSSP of wintering herring in the Ofoten area. They showed that the acoustic density was deep and dense during daytime (0700 to 1600), and shallow and more disperse at night (1600 to 0700). They found that the mean Nautical Area Backscattering Coefficient (s_A) for herring was 2-2.5 higher during the daytime.

On a short timescale there are three main factors influencing the acoustic backscattering from herring (Ona, 2003): Fish density, directivity of herring (tilt angle), and swim bladder volume. Variation in fish density on a location may occur due to natural temporal-spatial variations in distribution. The tilt angle (directivity) of herring varies naturally due to diurnal processes (Ona and Korneliussen, 2000).

Herring is a physostomous fish. Laboratory experiments suggest that herring may not be able to refill their swim bladder while submerged (Blaxter and Batty, 1984). Gas release has been observed for Pacific herring (*Clupea pallasi*) (Thorne and Thomas, 1990), herring (*Clupea harengus*) in the Baltic sea (Suuronen et al., 1997) and for over wintering Norwegian spring spawning herring (*Clupea harengus*) (Nøttestad, 1998). The swim bladder is the primary acoustic scatter for many fish species (Foote, 1980b, 1985; Furusawa, 1988). When herring swim to deeper water the swim bladder will be compressed according to Boyle's law (Ona 1984, 1990; Mukai and Kohji, 1996). As a consequence the backscattering is reduced and the herring will have negative buoyancy. A swim and glide strategy is obtain to avoid or reduce sinking speed (Huse and Ona, 1996), this also influences the tilt angle of the fish. It is believed that the swim and sink strategy can reduce energy expenses, theoretical studies has shown energy savings of 50 % (Weihs, 1974).

In October 2001 the Institute of Marine Research in Norway (IMR) deployed two bottom mounted acoustic transducers an Acoustic Doppler Current Profiler (ADCP) and horizontal sonar at the entrance of the Ofoten Fjord (Figure 1, Godø et al. in prep). The motivation was twofold. Firstly, if the cross section of a main migration route is covered it might be possible to assess stock abundance during the migration by integrating observed densities in the section over time. Further, when such a system is located in a dynamic central ecological area (ocean hub) key dynamic processes can be observed continuously and undisturbed. This feature is explored in this paper. It is assumed that the bottom-mounted system produces temporal unbiased data in contrast to the vessel data due to vessel avoidance as reported in (Olsen, 1990;Olsen et al., 1983;Olsen, 1971;Soria et al.,1996; Fréon et al., 1992).

The object of this study is firstly to demonstrate the potential of a stationary bottom mounted system and to compare it with data from a moving RV. The stationary of the system is also used to investigate the diurnal vertical migration. Investigation of acoustic diurnal variation as observed from a moving research vessel has been done in the same area and spices by Huse and Korneliussen (2000). In this work the acoustic diurnal variation from a moving RV and from a stationary platform is investigated and compared. Then layer depth and thickness, biological diurnal periods and duration is studied.

Material and Methods

Acoustic data on herring were collected by RV "Johan Hjort" (JH), RV "G.O Sars" (GOS) and RV "Sarsen" (SA) during the months November and December from 1998 to 2003. All data were collected in Tysfjorden, Ofotfjorden and Vestfjorden. Data from the stationary

transducers were collected from 30 November 2001 to 15 January 2002. Figure 1 shows the main survey area and the location of the bottom-mounted transducers.

JH and SA collected data using a 38 kHz EK500 scientific echo sounder while GOS used an EK60 scientific echo sounder for the acoustic sampling. All ships have the transducers mounted on a drop keel. The 3dB beam width was 7 degrees. Data were stored to file using the Bergen Echo Integrator (BEI) (Foote et al,1991). Calibration was done according to standard procedures (Foote et al.,1987).

The bottom-mounted system contains a 38 kHz transducer and a general-purpose transceiver (GPT) suspended in gimbals to maintain transducer surface parallel to sea surface. The system is attached to land with an underwater cable for data transmission and power. The data is collected in a cabin on land containing a PC running the EK60 software. The 3dB beam width is 7˚ for the along fjord direction and 23˚ for the transverse fjord direction. The inmost transducer was placed at a depth of 400 m and the outmost at a depth of 500 m. The transducers are separated with a distance of 415 m. Both transducers were calibrated in-situ. A remotely operated vehicle (ROV) with a suspended calibration sphere was piloted down to both the transducers. The data were recorded and used to calculate a correction formula. This was then used to correct the already sampled data.

The acoustic data collected from ship were used to compare with the data collected from the bottom-mounted system. The data were scrutinized using BEI and herring recordings were separated from other scatters before storing. Data were stored in 0.1 or 1 nautical mile and 10 m horizontal and vertical resolution respectively.

Data from the bottom-mounted transducers were stored ping by ping, one ping pr. 1.5 second. The data was stamped with GPS time. Due to the large amount of data the system gathered, methods to automatic process the data was developed. The first step was to reduce the data into larger time and depth bins. This reduces the amount of data and simplified the following processing steps.

The data reduction was done using an average box filter (McDonnell, 1981), spanning over 10 minutes and 5-meter depths. None of the boxes were overlapping. This resulted in one sampling value for each box.

Due to the different bottom depths and the horizontal separation distance the inner transducer interfered with the outer in the upper 20 m. This water layer was discarded from the data set. Noise in the data had the characteristic of randomly distributed high intensity spikes, also known as salt and pepper noise, and was removed by using a median filter (Tyan, 1981) of dimension 50 min by 25 meter. All data were corrected for acoustic extinction according to Zhao and Ona (2003).

In order to analyse diurnal variation in density and distribution the data were processed so as to make one average 24-hour echogram for each of the bottom systems and the research vessels. To test repeatability or potential small-scale geographic variation the two data sets was analysed separately. The effect of vessel avoidance of surface distributed fish (Vabø et al. 2002) was simulated by reanalysing the data after removing the distinct surface layer.

Light intensity and moon gravity are major driving forces of diurnal processes (see e.g. Neilson and Perry 1990;Orlowski, 2005). The observed diel dynamics are therefore related to

an “average” sun height at different hours during day and night. The sun height for 10 minute interval was calculated from UTC, position and date according to Smart (1977) and from this the minimum, maximum and average sun height through each 24-hour cycle for the sampling period was established.

Norwegian Spring Spawning Herring show extensive diel vertical migration (Huse and Korneliussen 2000). The physical day and night do not necessarily correspond to the timing of the “biological” day and night, i.e. the periods when the herring are adjusted to light and darkness. The mean acoustic depth (z_{cg}) of the nautical area scattering coefficient (s_A) with respect to depth was used as a proxy for depth of the herring at a certain time. To estimate more accurately the “biological” day and night the temporal variation of z_{cg} was studied. The data from the moving RV was given directly in s_A while the data from the stationary system was given in volume backscattering strength (S_v). This was converted to s_A using equation (1).

$$(1) \qquad s_A = 4\pi 1852^2 \int_{z=z1}^{z2} 10^{\frac{S_v}{10}} dz$$

where s_A is the area backscattering coefficient,S_v is the volume backscattering strength and dz the thickness of the depth strata. The mean acoustic depth z_{cg} is given in equation (2)

$$(2) \qquad z_{cg}(t) = \frac{\sum_{s=1}^{n} s_A(s,t) d(s)}{\sum_{s=1}^{n} s_A(s,t)},$$

where $z_{cg}(t)$ is the centre of gravity at time t, d(s) is average depth of the depth stratum s and $s_A(s,t)$ is the back scattering coefficient from stratum s at time t. Over the 24-hour cycle z_{cg} thus can be used to express vertical migration dynamics. The slope of the $z_{cg}(t)$ curve is used as a proxy for vertical migration speeds. To separate day and night a two-sided Kolmogorov-Smirnow test (KS2) on the $z_{cg}(t)$ curve distributions was used. Each 24-houre cycle is resampled into data points averaging a 10-minute interval. The data points were put into bins corresponding to the time of day. Since the data set totally contained 45 diurnal cycles, each bin contained 45 data points constituting one distribution. Performing the two-sided Kolmovgorov-Smirnow test test between all distributions trough a diurnal cycle resulted in a matrix of p-values between all the 10 minutes periods. The null hypothesis was that all bins had the same distribution, i.e. no diurnal variation exists. The alternative hypothesis was that the samples came from different diurnal periods. A hypothesis matrix was formed from the p-values, rejections was done with a 95% confidence interval. The hypothesis matrix was filtered with a 30-minute by 30-minute median filter to remove noise. All the columns in the matrix were summed constructing a vector containing the frequencies of hypothesis acceptance. The start and end of biological day and night were determined from pronounced local maxima in the frequency distribution. A day-night index ($I_{D/N}$) was calculated to compare echo intensity during night and day using equation (3),

$$(3) \qquad I_{D/N} = \frac{s_{A(day)}}{s_{A(night)}} = \frac{\int_{t=16:10}^{07:10} s_A(t) dt}{\int_{t=10:00}^{12:50} s_A(t) dt},$$

where $I_{D/N}$ is the night day index, $s_{A(day)}$ is the total nautical area scattering coefficient during daytime and $s_{A(night)}$ is the nautical area scattering coefficient night. Finally, to assess

similarity in temporal dynamics of the various data set a simple correlation analysis between the s_A time series from the ship and the bottom mounted system where preformed.

Results

Average echograms for the study period over the 24-hour time cycle are showed in Figure 2, for vessel data (Figure 2a) as well as for the outer (Figure 2b) and inner (Figure 2c) transducers. The black curve indicates z_{cg}. A common feature for all platforms is the stratification in a thin top layer and a thicker bottom layer. See also a summary of layer information in Table 2. Both layers ascend at dusk and descend during the dawn period. The maximum vertical migration speeds are calculated to 1-2 cm/s.

A closer study demonstrates some discrepancies among the diurnal echograms in Figure 2. For the ship (Figure 2a) the two distinct layers during the night can bee seen. At start of dawn both layers increase in intensity. At daytime the top layer resides around the same depth as the bottom layer at night. The acoustic z_{cg} curve is fairly stable during night and has its descent and ascent during dawn and dusk. Diurnal fluctuation in depth distribution of the biomass is also reviled by z_{cg}. For the bottom mounted system there is a tendency for the z_{cg} curve to sink during midnight.

The data from the bottom-mounted transducer and ship shows similar pattern. Two distinct layers (Figure 2a, Figure 2b and Figure 2c) can be seen trough the diurnal cycle. At dawn both layers sinks to deeper depths. The top layer settles around where the bottom layer was at nigh time. For the outer transducer the start of the descent of the bottom layer (Figure 2b) during dawn seems to start more rapid than the end of the ascent during dusk. Interaction between the layers can bee seen trough the cycle.

Timing of the diurnal cycle in relation to the vertical migration pattern needs to be determined. The p-value matrix, Figure 3a, is symmetric around the diagonal. The diagonal going from top left to bottom right compares data from the same hour and thus the p-values are all one along the diagonal. The matrix can roughly be divided into nine regions or squares as indicated in Figure 3a, these are numbered from top left (square 1) and to bottom right (square 9). Square 1,5 and 9 compares data close in time. Square 1 and 9 contain overall high p-values indicating that only small changes occurs in this period. Square 5 contain data regarding the transition periods the larger changes are reflected in the pattern of this region. In Square 4 data from daytime is compared to data from the night-morning transition, and in square 8 data from daytime is compared to data regarding the day-night transition. The lower p-values in the middle of square 7 indicate some asymmetry during the diurnal process. The median filtered H-values from the two-sided Kolmogorov-Smirnow test, Figure 3b and Figure 3c, are used to define shifts in the diurnal cycle. The local maxima at about 08 and 16 hours correspond to the start of dusk and the end of dawn. Similarly, the local maxima at 0950 and 1250 hours define the span of daytime. The diurnal bar on bottom of Figure 3b and Figure 3d is constructed from the local maxima. Visually, it can be seen from the diurnal bar on bottom of Figure 3b and Figure 3d that the dawn period is longer then dusk. This is indirectly statistical significant tested with the KS test. Figure 3d demonstrates that the diurnal migration (z_{cg}) is synchronized with sun elevation angle. The details about timing of the diurnal periods and corresponding sun altitudes are presented in Table 1.

It is typically assumed that diurnal processes are only time and not geographically driven. When comparing the integrated echo intensity from the various platforms and layers over the

diurnal cycle (Figure 4) an unexpected layer and geographic phenomenon appears. Due to the vessel avoidance effect on herring in the top layer, it is of particular interest to compare ship data with results from the bottom mounted system, with (Figure 4b, d) and without (Figure 4c, e) this layer. The research vessel echo intensity level during day (Figure 4a) is more than double the level observed during night. Note that the values are multiplied by ten to fit to scale. The increase and decrease in s_A are associated with dusk and dawn. It is apparent from Figure 4 that the data from the bottom transducers are far less dynamic over the diurnal cycle. Further, there is a striking difference between these transducers. Note the difference between day and night levels in s_A with top layer included or excluded. No day and night difference is recorded for the inner transducer without top layer and for the outer transducer with top layer. In contrast, the inner transducer with top layer have a minimum at night while the outer without top layer have a maximum at the same time. In Figure 5 s_A values as observed from research vessels and from the fixed transducers is compared. Ship data compared to inner transducer data (Figure 5a) are negative correlated. When removing the top layer (Figure 5c) the correlation is considerably reduced. The correlation with the outer transducer is positive but very weak r^2=0.06 (Figure 5b). When removing the top layer (Figure 5d) the correlation is still positive and much stronger: r^2=0.52.

Discussion

Fish are mobile organisms with pronounced predator – prey interaction behaviour. A moving observation platform, which often will be recognized as a predator, may affect target species behaviour, in a way that lead to a biased assessment of density and/or size composition (One & Godø 1990; Gerlotto & Freon 1992; Vabø, Olsen, et al. 2002). Further, a survey vessel may wrongly cover, spatio-temporal variation in distribution when unexpected stratification occurs. The focus of this paper is to use data from the stationary acoustic system in the Ofoten fjord (Figure 1) to study such effects on overwintering Norwegian spring spawning herring.

The data

Before going into the biological interpretation of our results there is a need to clarify the comparability of results from bottom and vessel mounted acoustic systems. The research vessel instruments observe the herring from the dorsal aspect while the signals received by the bottom-mounted system has a ventral aspect. Foote (1985) measured 15 gadoids in the dorsal and ventral aspects while varying the tilt angle from –45 to 45 degrees. For 38.1 kHz the results showed that backscattering in the ventral aspect was found to be generally less directional than in the dorsal aspect. Simulated probability density functions of target strength from both ventral and dorsal aspects were similar. Based on this, target strength is assumed to be independent of measurement aspect in this study.

The difference in beam form will introduce a negative bias for the bottom-mounted system. Fish are observed over a greater tilt angle, this is due to the wider beam in one direction of the bottom-mounted system. The methodology to compensate for this effect is outlined in Foote(1980a). This is not compensated for in this study, but the consequences influencing the conclusion will be discussed.

When gathering acoustic data from a moving vessel, spatial and temporal variance is captured. The bottom-mounted transducers capture only the temporal variance and the data are thus expected to be less variable. Further, the acoustic beams from the bottom-mounted system cover a larger volume than that from the ship. This will further smooth the stationary data and amplify difference in variation between vessel and stationary data.

Our study area is a fjord with strongly variable depth along the survey transects. This will most likely mask out some of the layer stratification at daytime, it also may induce other unknown effects. The two bottom-mounted transducers might capture some of the small-scale local topographic related variation due to their difference in depth and location related to the walls of the fjord.

Fish avoidance from vessels is negligible below 150 m (Vabø et al., 2001). Some vessel activity is expected over the bottom-mounted system but the biomass as observed from the bottom-mounted system is looked upon as unbiased in this context.

The echo sounder on ship is calibrated before or after a survey, some times both times. During a survey, temperature and salinity observations are used to assess the absorption and sound velocity for use in the software of the acoustic system. For the bottom-mounted system a constant sound velocity is used. The variation in sound velocity is limited and is not expected to induce any significant bias between ship data and data from the bottom mounted system.

The diurnal periods can be determined merely from time of day or from height of sun above horizon. The diurnal vertical dynamics of the acoustic signals from the bottom mounted transducers are stable and it is therefore possible to let the data determine the biological diurnal periods, and most important, the transition periods (dusk and dawn). This contrasts other analysis, see e.g. Huse and Korneliussen (2000), who used the light intensity to determine the diurnal periods. Despite the methodological differences the timing of day and night are in good agreement. Due to the high and excellent temporal resolution of our stationary data we regard our estimates to give the most accurate reflection of the biological "correct" diurnal cycle. Further, it should also be kept in mind that the vertical migration speeds calculated, correspond to the speed of the layers and not the individual fish as e.g. in Huse and Ona (1996).

Stratification

In general, the observations from the bottom-mounted system agree well with earlier study by Huse and Korneliussen (2000). Herring concentrate in dense schools in the deep of the fjord during the day. At dusk most of them migrate to shallower water and define two separate layers. Due to the higher depth resolution in the data from the stationary system the top and bottom layers of herring during nighttime are clearly seen from the stationary system. The same tendency can be seen in the ship data, but separation is not as clear and layer not as well defined due to varying bottom depth and coarser depth resolution in the data. It is important to note the larger depth span of high intensity values in the bottom layer as observed from the ship during night compared to the stationary system. Due to the lack of geographic variability, and hence a superb temporal resolution a third layer appears in the stationary data, which has not been described based on vessel data. It appears from 200 to 350 meters during night hours and may represent herring not undertaking the diurnal migration. The interpretation of this is uncertain. The layer separation is more distinct during transition periods and daytime. This shows that layer interaction is most pronounced during nigh time, in other words that most of the biomass exchange between layers take place during this period.

Biomass point of gravity

The z_{cg} for the two stationary transducers has resemblances with the hourly depth distribution of herring as presented in Figure 2 in Brawn (1960). This time series show the hourly depth distribution of herring in Passamaquoddy Bay in March and September. For Brawn's time

series and the corresponding time series presented here, the dawn and dusk migration is the dominating feature, but the sinking at midnight should also be noted. This contrasts the observation by Huse and Korneliussen (2000) of a midnight ascent. Midnight sinking in zooplankton is one of the five phases of nocturnal vertical migration according to (Cushing, 1951), and is given different explanations: Slowing of swimming speed due to darkness, satiation (Gauld, 1953), increase in density when satiated (Krause and Radach, 1989) and predator avoidance (Tarling et al., 2002). The sinking of the biomass for pelagic fish is less studied. One explanation could be that acoustic target strength at surface has a minimum at midnight during the culmination of the nocturnal migration due to a minimum in swimming activity followed by an increase tilt angle. The herring do not feed during the over wintering period, this means that the sinking could be explained by slow swimming in darkness. It is also interesting to note the similarities between the shape of the depth distributions from the bottom mounted transducers and from Brawn's time series. The over all shape is the same with fish higher in the water during night then day. The spike around 1100 can be found in both time series, although it is more pronounced in Brawns's data set. The same holds for the downward dip around midnight. In our case the spike at daytime is explained by denser accumulation of biomass and accumulation between the two layers. An ecological explanation may be formation of denser smaller schools during the daytime in response to predator activity (Nøttestad et al., 1999).

Acoustic diurnal variation

The diurnal variation in acoustic density as observed from the ship fits well with the observation from Huse and Korneliussen (2000) and has resemblances with plots in Fréon (1996). Axenrot et al. (2004) found differences in hydro acoustic backscattering of Baltic sea clupeids between day and night with their bottom-mounted system. The abundance was highest during the day. The same was observed for the outer transducer. The differences between the vessel and the two bottom mounted transducers is evident. Shipdata shows less backscattering and bigger variation between day and night than from the stationary system. The comparison is, however, not straight forward due to the differences between the two transducers. The difference between the two bottom mounted transducers indicates that there are systematic small-scale spatial differences between the two locations. It is interesting to observe a completely out of phase variation in s_A between the inner transducer compared to the ship. This results in a negative correlation. Removing the top layer gives a shape in more resemblance to the ship but shifted towards the night-day period. This results in a low correlation. The outer transducer has a more flat shape. Removing the top layer reveal a more similar structure as in the ship data and shows a grater correlation. Not only does this tell us that awareness of small-scale variation is of importance when using stationary systems. Also, systematic spatial variation of this magnitude need careful attention when surveying the population with traditional methods to minimise spatial-temporal biases. The comparative analysis further tells us that the outer transducer without top layer mirrors the survey situation best and may be a reflection of vessel avoidance of herring at surface (Vabø, 2002). As the similarity in diurnal variation and day-night index between the ship and the bottom transducers increase from the inner to the outer it can be speculated that an transducer even further out towards the middle of the fjord would give a better correlation with ship data.

Diurnal periods

The long night and short day is well synchronized with the light intensity cycle at these latitudes during wintertime. A discrepancy between the length of the dawn and dusk periods is not uncommon (see e.g. Fréon et al.1996).

The day-night index from the inner transducer indicates less backscattering at night than during daytime. The opposite is true for the outer transducer. This is interpreted to be due to diurnal biomass transportation across the fjord between the shores and mid-fjord during a 24-houre cycle. The greater day-night index for ship data are explained by the vessel avoidance of the top layer during daytime. A possible explanation for the high negative correlation between ship data and the inner transducer is that this transport is very significant and the survey is not able to pick up this important local biomass dynamics.

Stationary versus moving-vessel observations

Stationary and mobile observation regimes have its strengths and weaknesses. A stationary observation system gives good temporal resolution but is very sensitive to geographical local effects as demonstrated in this paper. It is hence necessary to study the area in detail before deployment and any conclusion is drawn from the sampled data. Mapping the biological behaviour and water current (Paper VI) can partially compensate the lack of spatial resolution. Another solution would be to construct platforms with scanning ability. Stationary equipment is ideal and cost effective for long-term operations, such operations also faces the risk of damage due to harsh environment and commercial fishing activities. It is possible to construct trawl safe platform but this equipment is often more expensive. The excellent temporal resolution reveals detailed structures and dynamics that would not be possible with mobile platforms. The simplicity of stationary equipment often gives it greater mean time before failure. Mobile platforms often need more resources to run, this is especial true for survey vessel, and surveys can sometimes be set to a halt due to weather. The geographical movement smooths the geographic local effects. It is clear that the observation regimes can compliment each other. The usage of these two regimes is highly task dependent. A powerful approach for biomass surveillance would be to combine the two methods. A mobile survey could be preformed to establish a model of the biomass dynamics over time, and then a stationary system could feed the model with data and forecasting the biomass for the next time steps. The model should routinely be updated, performing a mobile survey over the geographic aria. The essence is to establish a connection between mobile collected data and stationary data.

Conclusions

The conclusions of this study are the following:

- Observations from the bottom-mounted system agree well with observations from earlier studies from survey ships.
- A third layer appears in the data from the stationary system. This layer is located below the second layer and is not as dense as the two upper layers. At daytime this third layer is merged with the second layer.
- There exist systematic acoustic small-scale spatial differences between the two locations of the stationary systems.
- Removing the top layer form the data from the stationary systems reveal a more similar structure as in the ship data.
- A stationary observation system gives good temporal resolution but is very sensitive to geographical local effects. The distance between two stationary transducers is 415 m.
- Acoustic data collected from a vessel-mounted transducer shows greater difference between day and night then the data from the stationary system.

Acknowledgements

The work was partially funded by the Norwegian Research Council, grant number 143539/431. Terje Torkelsen is thanked for his great efforts in establishing and running the stationary acoustic system. The Transportation department at Ramsund Military base is thanked for their support in personnel transportation to and from the Ocean Hub site.

References

Axenrot, T., Didrikas, T., Danielsson, C., and Hansson, S. 2004. Diel patterns in pelagic fish behaviour and distribution observed from a stationary, bottom-mounted, and upward-facing transducer. ICES Journal of Marine Science, 61:1100-1104.

Blaxter, J. H. S., and Batty, R. S. 1984. The herring swimbladder: loss and gain of gas. Journal of the Marine Biological Association of the United Kingdom, 64:441-459.

Brawn, V. M. 1960. Seasonal and durinal vertical distribution of herring (Clupea Callarias L.) in Passamaquoddy Bay, N.B. Journal of the Fisheries Research Board of Canada, 17:699-711.

Cushing D. H. 1951. The vertical migration of planktonic crustacea. Biological Reviews, 26:158-192

Foote, G. K. 1980a. Averaging of fish target strength functions. Journal of Acoustical Society of America, 67(2):504-515.

Foote, K. G. 1980b. Importance of the swimbladder in acoustic scattering by fish: a comparison of gadoid and mackerel target strengths. Journal of Acoustic Society of America, 67: 2084-2089.

Foote, K. G. 1985. Effect of swimming on fish target strength. ICES CM 1985/B:29 (mimeo).

Foote, K. G., Knudsen, H. P., Korneliussen, R. J., Nordbø, P. E., and Røang, K. 1991. Postprocessing system for echo sounder data. Journal of the Acoustical Society of America, 90(1):37-47.

Foote, K. G., Knudsen, H. P., Vestnes, G., MacLennan, D. N., and Simmonds, E. J. 1987. Calibration of acoustic instruments for fish densety estimation: A practical guide. ICES cooperative research report, 144:69.

Fréon, P., Geirlotto,F and Soria, M. 1996. Diel variability of school structure with special reference to transition periods. ICES Journal of Marine Science, 53(2):459-464.

Fréon, P., Gerlotto, F., and Soria, M. 1992. Changes in school structure according to external stimuli: description and influence on acoustic assessment. Fisheries Research, 15(2):45-66.

Huse, I., and Korneliussen, R. 2000. Diel variation in acoustic density measurements of overwintering herring (Clupea harengus L.). ICES Journal of Marine Science, 57:903-910.

Huse, I., and Ona, E., 1996. Tilt angle distribution and swimming speed of overvintering Norwegian spring spawning herring. ICES Journal of Marine Science, 53:863-873.

Huse, I., Korneliussen, R. 2000. Diel variation in acoustic density measurements of overwintering herring (*Clupea harengus* L.). ICES Journal of Marine Science, 57:903-910.

McDonnell, M. J. 1981. Box-Filtering Techniques. Computer Graphics and Image Processing, 17(1):65-70.

Misund, O., Vilhjalmsson, H., Jakupsstovu, S., Rottingen, I., Belikov, S., Asthorsson, O., Blindheim, J., Jonsson, J., Krysov, A., Malmberg, S., Sveinbjornsson, S. 1998. Distribution, migration and abundance of Norwegian spring spawning herring in relation to the temperature and zooplankton biomass in the Norwegian Sea as recorded by coordinated surveys in Spring and Summer 1996, Sarsia, 83:117-127.

Mitson R. B. 2002. Report of the Northern Pelagic And Blue Whiting Fisheries Working

Group ICES Headquarters 29 April–8 May 2003. ICES CM 2003/ACFM, 23:1-229.
Mukai, T., Iida, K. 1996. Depth dependence of target strength of live kokanee salmon in accordance with Boyle's law. ICES Journal of Marine Science, 53:245-248.
Neilson, J. D., and Perry, R.I. 1990. Diel vertical migrations of marine fishes - an obligate or facultative process. Advances in marine biology, 26:115-168
Nøttestad, L., and Axelsen, B. E. 1999. Herring schooling manoeuvres in response to killer whale attacks. Canadian journal of zoology, 77:1540-1546.
Olsen, K. 1971. Influence of vessel noise on the behaviour of herring. In Modern Fishing Gear of the World, 3th ed., 291-294, Ed. by H. Kristjonsson. Fishing News (Books) Ltd. London. 537 pp.
Olsen, K. 1990. Fish behaviour and acoustic sampling. Rapportes et Procès-Verbaux des Réunions du Conseil International pour l'Exploration de la Mer, 189:147-158.
Olsen, K., Angell, J., Pettersen, F., and Løvik, A. 1983. Observed fish reactions to a surveying vessel with special reference to herring, cod, capelin and polar cod. FAO fisheries reports, 300:131-138.
Ona, E. 1984. In situ observations of swimbladder compression in herring. ICES CM 1984/B:18. (mimeo).
Ona, E. 1990. Physiological factors causing natural variations in acoustic target strength of fish. Journal of the Marine Biological Association of the United Kingdom, 70:107-127.
Ona, E. 2003. An expanded target-strength relationship for herring. ICES Journal of Marine Science, 60:493-499.
Ona, E., and Korneliussen, R. 2000. Herring vessel avoidance; diving or density draining. Prooceedings of the fifth European Conference on Underwater Acoustic, ECUA 2000, 1515-1520.
Orlowski, A. 2005. Experimental verification of the acoustic characteristics of the clupeoid diel cycle in the Baltic. ICES Journal of Marine Science, 62:1180-1190.
Røttingen, I., Foote. K. G., Huse, I., and Ona, E. 1994. Acoustic abundance estimation of wintering Norwegian spring spawning herring, with emphasis on methodological aspect. ICES CM 1994/B+D+G+H:1, 17pp.
S. Tyan. 1981. Median filtering, deterministic properties, in Two-Dimesional Digital Signal Processing.Ed. by Huang, TS, Berlin.
Slotte, A. 1999. Differential utilization of energy during wintering and spawning migration in Norwegian spring-spawning herring. Journal of Fish Biology, 54:338-355.
Smart, W.M. 1977. Textbook on Spherical Astronomy. Cambridge University Press, Cambridge, UK.
Soria, M., Freon, P., and Gerlotto, F. 1996. Analysis of vessel influence on spatial behaviour of fish schools using a multi-beam sonar and consequences for biomass estimates by echo-sounder. ICES Journal of Marine Science, 53:453-458.
Suuronen, P., Lehtonen, E., and Wallace, J. 1997. Avoidance and escape behaviour by herring encountering midwater trawls. Fisheries Research, 29:13–24.
Tarling G. A., Jarvis T., and Emsley, S. M., Matthews J. B.L. 2002. Midnight sinking behaviour in Calanus finmarchicus: a response to satiation or krill predation? Marine Ecology Progress Series, 240:183-194.
Thorne, R. E., and Thomas, G. L. 1990. Acoustic observations of gas bubble release by Pacific herring (Clupea harengus pallasi). Canadian Journal of Fisheries and Aquatic Science, 47: 1920-1928.
Toresen, R., and Østvedt, O. J. 2000. Variation in abundance of Norwegian spring-spawning herring (Clupea harengus, Clupeidae) throughout the 20th century and the influence of climatic fluctuations. Fish and Fisheries, 1:231-256.
Vabø, R., Olsen, T., and Huse, I. 2002. The effect of vessel avoidance of wintering

Norwegian spring spawning herring. Fisheries Research, 58: 59-72.
Weihs, D. 1974. Energetic advantages of burst swimming of fish. Journal of Theoretical Biology, 48:215-229.
Zhao, X., and Ona, E. 2003. Estimation and compensation models for the shadowing effect in dense fish aggregations. ICES Journal of Marine Science, 60:155-163.

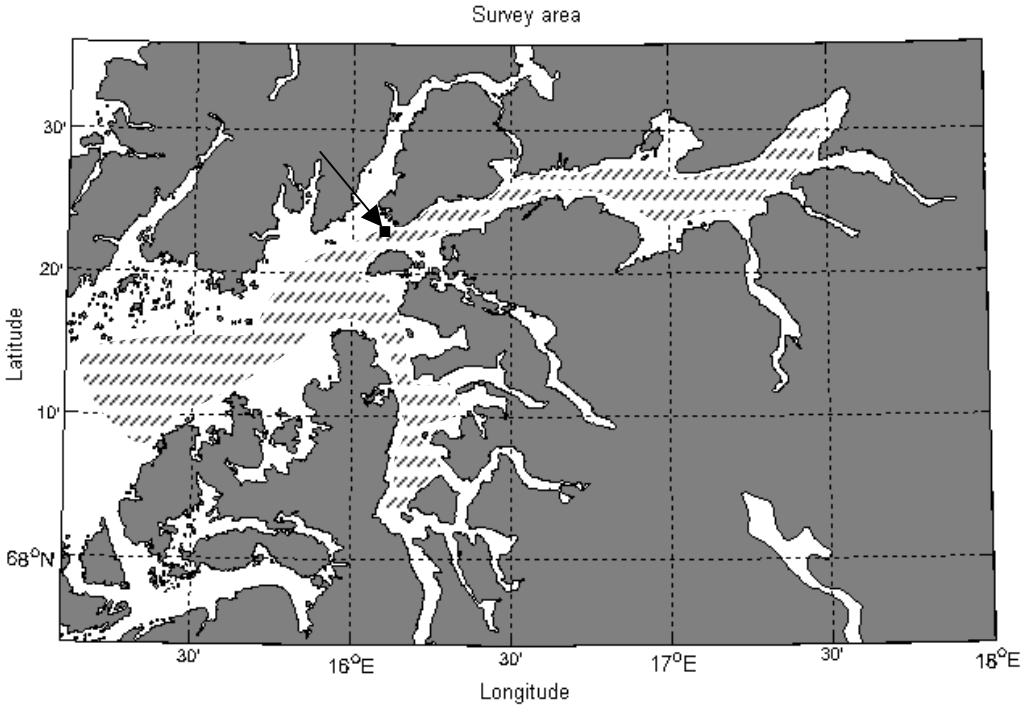

Figure 1. Map of survey area. Hatched region indicate area covered by ship survey. Arrow points at location of bottom mounted equipment.

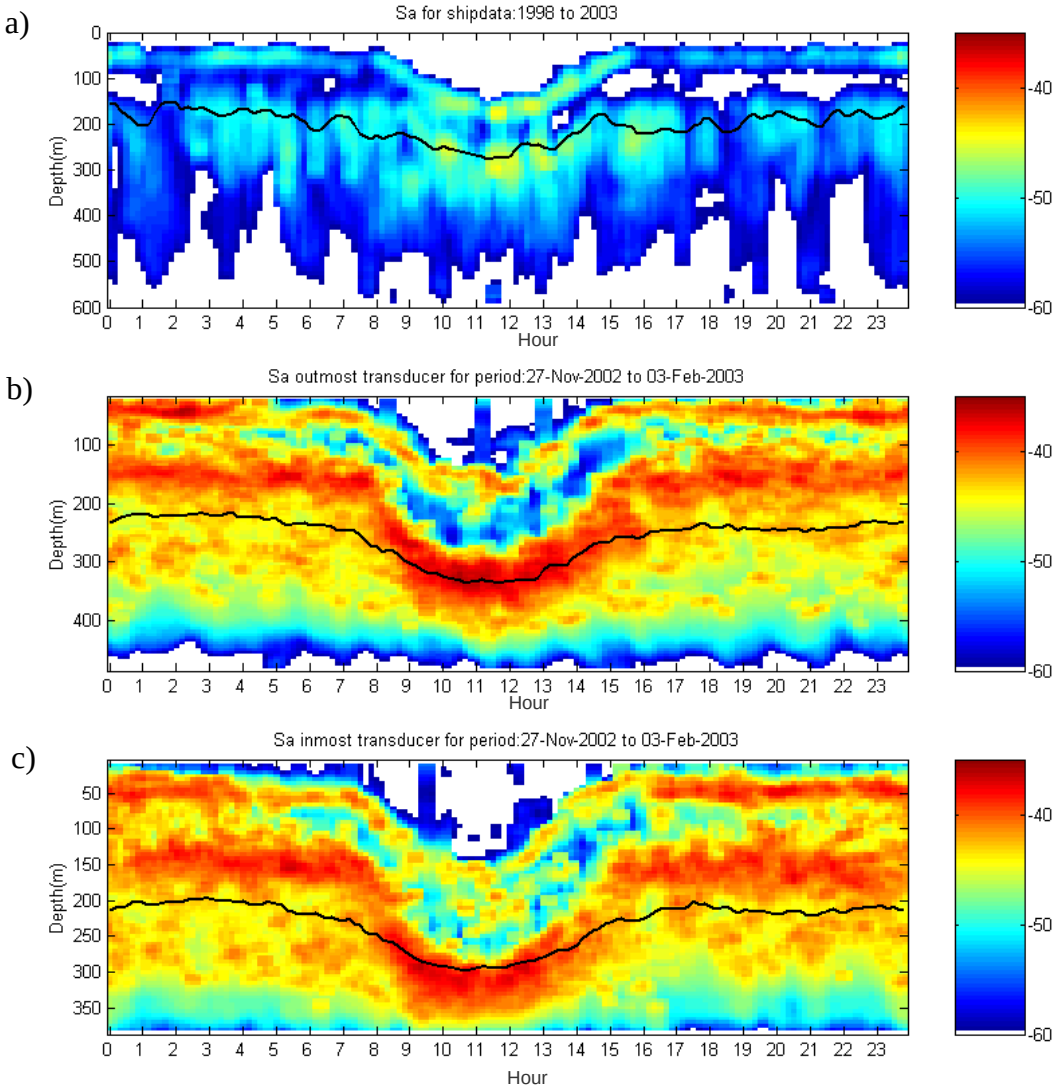

Figure 2.Vertical distribution of acoustic densities. z_{cg} indicated by black lines. a) From survey for 1998 to 2003. b) Outer transducer in period 27 November 2002 to 03 February 2003 c) Inner transducer in period 27 November 2002 to 03 February 2003.

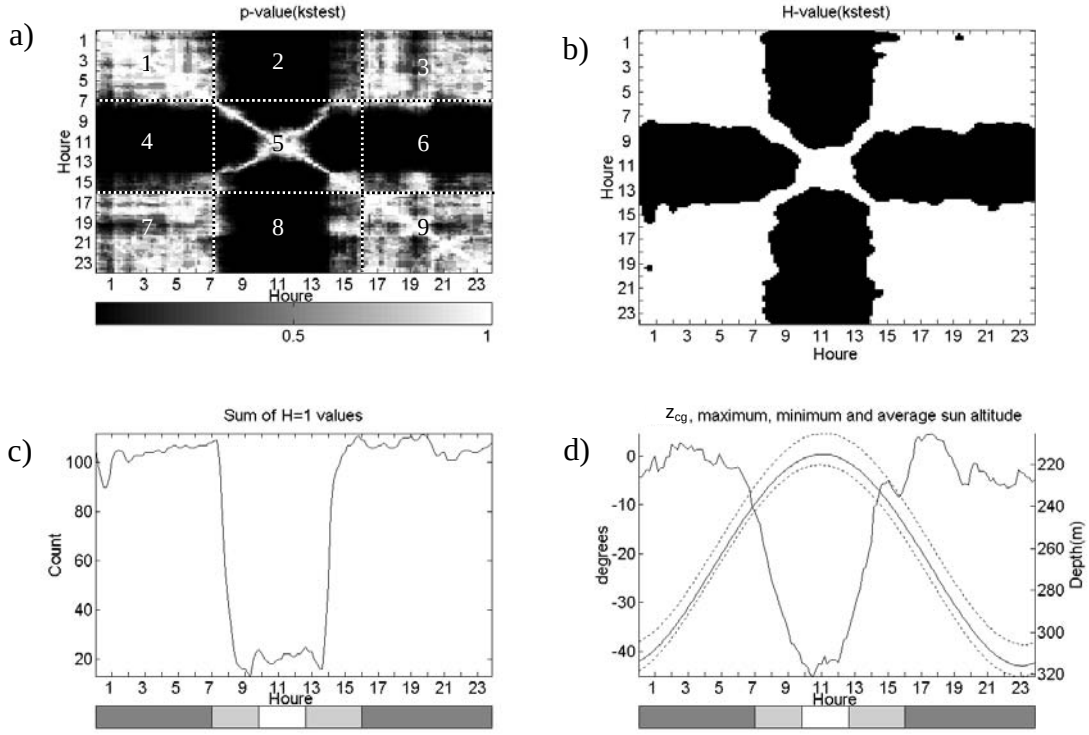

Figure 3. The calculations behind estimation of the biological diurnal periods. a) p- value matrix from two-sided Kolmogorov-Smirnow test. b) H- values from two-sided Kolmogorov-Smirnow test. c) Occurrence of Hypothesis acceptances. d) z_{cg} curve plotted with minimum, mean and maximum sun height during the sampling period.

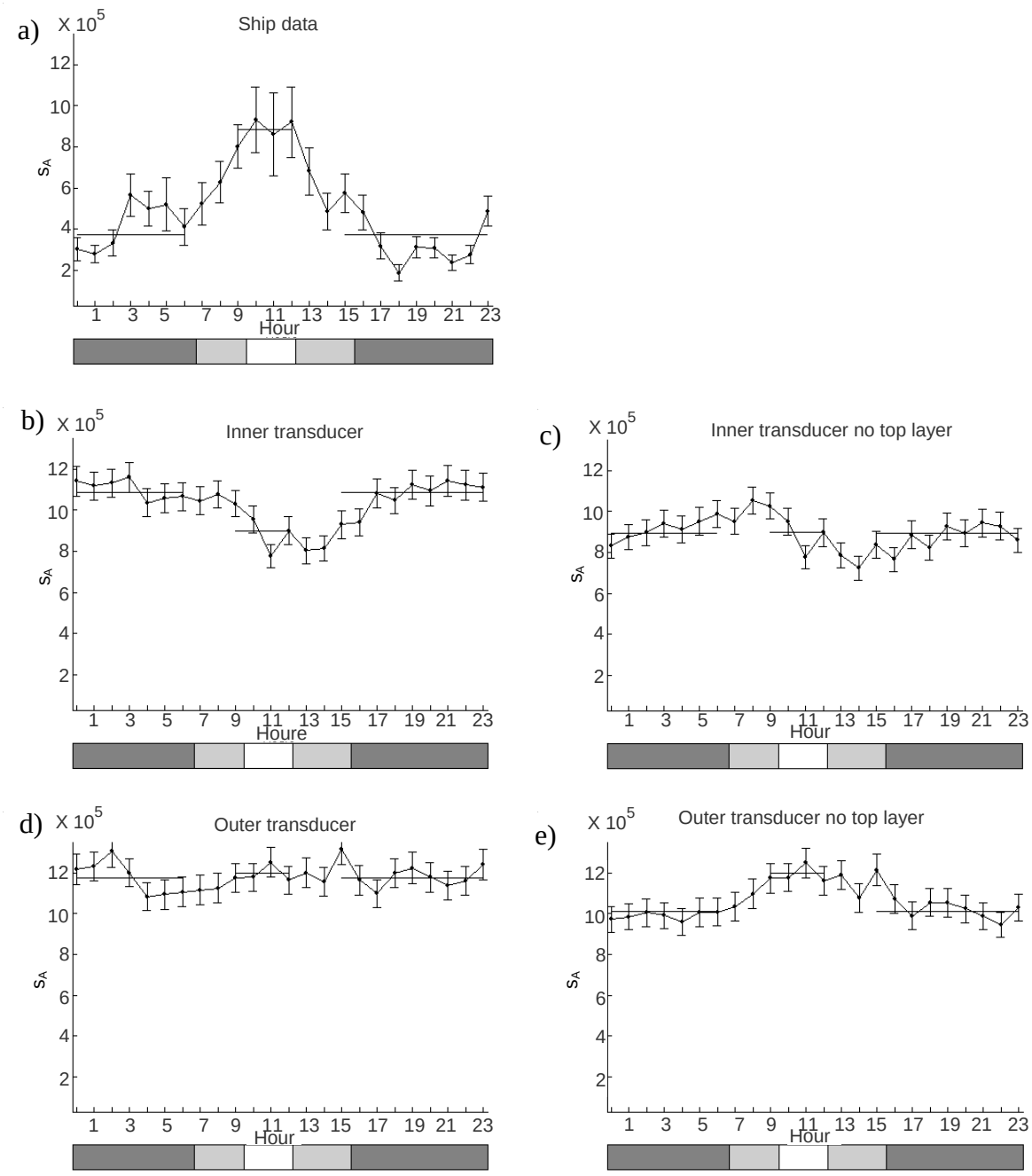

Figure 4. Average integrated acoustic density (s_A) by hour is described by the continuous line. Vertical lines indicate standard deviations. Day and night time levels are denoted by horizontal lines. a) A factor of 10 is added to the ship data to fit scale. b) Inner transducer. c) Inner transducer, no top layer. e) Outer transducer. e) Outer transducer, no top layer.

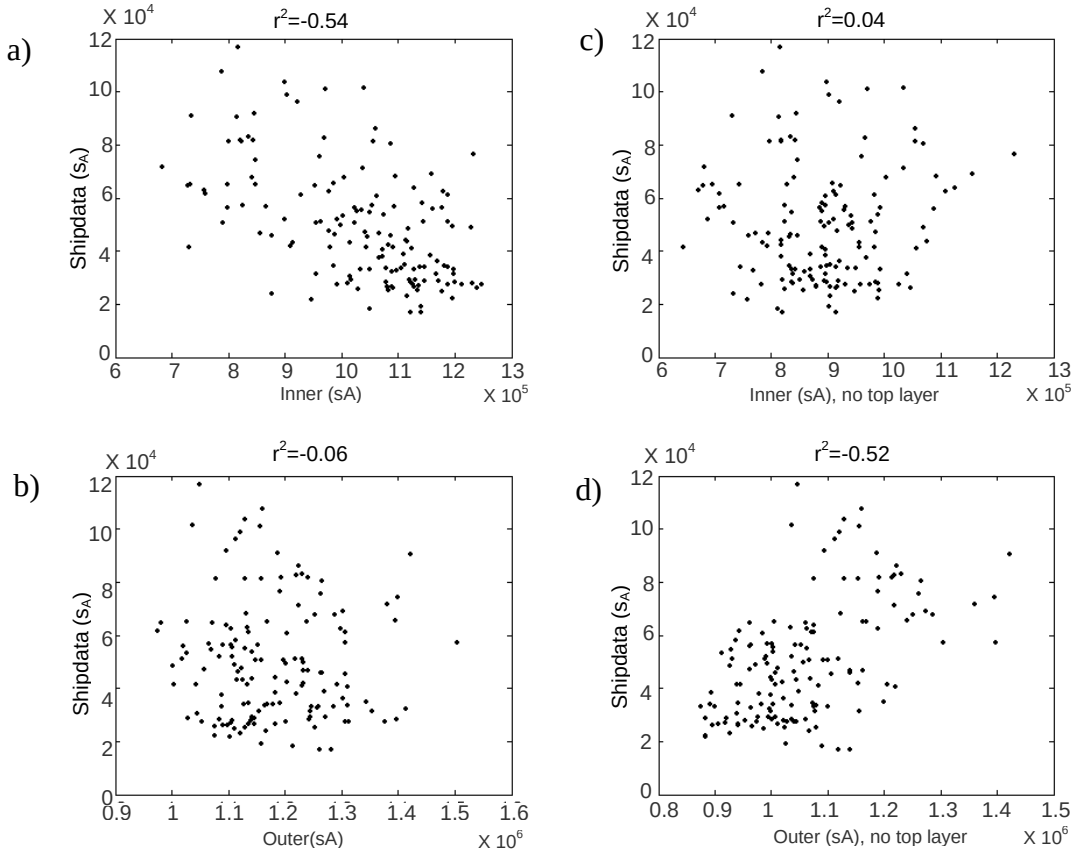

Figure 5. Correlation plot between acoustic densities (s_A) from the ship and from the bottom mounted system. The correlation coefficient (r^2) is shown on top of graphs. a) Ship and inner transducer. b) Ship and outer transducer. c) Ship and inner transducer, top layer excluded. d) Ship and outer transducer, top layer excluded.

Table 1. The diurnal periods as defined by local time and sun height.

	Time	Duration	Start and stop sun height (degrees)	Mean sun height (degrees)
Night	1550-0710	15h 20 min	-12.49, -9.78	-29.78
Night-Day	0710-0950	2h 40 min	-9.78, -0.96	-4.80
Day	0950-1250	3h	-0.96, -1.43	-0.25
Day-Night	1250-1550	3h	-1.43, -12.49	-6.29

Table 2. Depth span of the top and bottom layer as measured from the ship and stationary system.

	Top layer night (meters)	Top layer day (meters)	Bottom layer night (meters)	Bottom layer day (meters)
Ship	35-80	140-185	150-300	225-400
Outer Transducer	25-60	160-180	120-190	290-400
Inner Transducer	20-70	160-190	110-195	290-375

Table 3. Average relationship between day and night time values (day-night index). The values is calculated by dividing mean daytime s_A with mean night time s_A . Values > 1 indicates more backscattering at daytime then night time. Values < 1 indicates less backscattering during daytime then night-time.

	With top layer	Without top layer
Ship	2.26	-
Outer transduser	1.01	1.18
Inner transduser	0.82	0.99

Manuscript

Observing behaviour of over-wintering Herring (*Clupea harengus* L.) in Ofoten with Acoustic Doppler Current Profiler

Ruben Patel and Olav Rune Godø

Abstract

This paper present results and interpretation of velocity and signal strength data collected with the Nortek manufactured 'Continental' Current Profiler on over-wintering herring in the Ofoten Fjord in northern Norway. The instrument was lowered to a depth of 150 m and kept stationary with the transducer upward looking during a period of 14 days. In the same area and period we had two bottom-mounted echo sounder of the type EK60 at 500m and 400m depths. Data from the echo sounders were used to demonstrate that the Continental signal strength could clearly measure the backscattering of herring. First, we extracted the contours of herring schools from the EK60 data. The extracted contours were then overlaid the backscattered data from the Continental. The distribution and density dynamics of the two data sets matched very well. By using the extracted contours for analyzing the speed and direction, we concluded that herring behaviour could efficiently be observed from the Continental. We could not observe the diurnal vertical migration due to the lack of depth coverage of the migration range of herring. The horizontal speed and direction showed that the herring aggregations mainly followed the tidal current during the over-wintering.

Keywords: ADCP, echo sounder, Ofoten, over-wintering Herring, tidal current.

Ruben Patel: Institute of Marine Research, P.O. Box 1870 Nordnes, NO-5817 Bergen, Norway. Tel: +47 55 23 86 18, fax: +47 55 23 68 30, e-mail: ruben@imr.no. O.R. Godø: Institute of Marine Research, P.O. Box 1870 Nordnes, NO-5817 Bergen, Norway. Tel:+47 55 23 86 75, fax: +47 55 23 68 30., e-mail: olavrune@imr.no.

Introduction

Traditionally Acoustic Doppler Current Profiler (ADCP) is used for measuring water current and vessel speed by measuring the Doppler shift from the sea bottom or particles in the water. Although fish and other marine life with active movement are regarded as noise and biases the measurements. Some scientist has investigated the usage of ADCP on biology.

In an earlier study, echo frequency distributions were studied from three fish schools. The observed Doppler shift was related to the schools swimming direction, fish length, tail-beat amplitude and frequency (Holliday, 1974).

Freitag et al.(1992) compared data from ADCP with data from several Vector Averaging Current Meters (VACM) and Vector Measuring Current Meters (VMCM). The comparison shows that the ADCP is biased towards low velocities. This is proved to be due to contamination of fish echo in the ADCP signal. They use the beam-to-beam difference to implement a fish-bias rejection algorithm. The algorithm reduces the bias induced by fish,

an improvement of the rejection algorithm is reported in (Feritag et al., 1993). Mechanical Current Meters can be used to correct the bias in ADCP velocities (Plimton et al. 2000).

Roe and Griffiths (1993) demonstrate that different biological information can be obtained from routine ADCP operation. This includes horizontal and vertical Log Intensity Anomaly data and horizontal speed data. They conclude that ADCP can give additional valuable information about marine life.

In another study, biases in ADCP velocity estimates were reported as large residuals between the ADCP velocity data and a fitted tidal model (Wilson and Firing 1991). The authors suggest that coherent swimming activities, around sunrise, by a mesopelagic fish, which comprised the dense sound scattering layers in the study area, may have produced this apparent bias in the data. Other studies have documented diel periodicity in the ADCP echo amplitude. For example, Kaneda et al. (2001) observed a strong diel signal from the ADCP following a cold-water intrusion along the shelf slope region south of the Bungo Channel. They suggest that the change in ADCP signal strength resulted from immigration of zooplankton to the bay.

From these studies it is clear that the ADCP can provide information on animal movements and distribution patterns as well as information on ocean current velocities. The ADCP has to this date never been used as a standard tool for biomass surveillance although some experiments and attempts are reported. Some of them are reviewed in the following text.

A concurrent ADCP and SeaSoar survey calculated the volume backscattering (S_v) using real-time measurements of the absorption coefficient (Roe et al., 1996). The authors of the study conclude that ADCPs never can replace purpose-built, multi frequency, well-calibrated echo-sounders for biological purpose, but is suitable to map quantitative biology on the same scale as hydrography.

One of the difficulties in using an ADCP for biomass measurements is the difficulty in calibrating the ADCP. Brierley et al. (1997) suggested that one should avoid using ADCPs for abundance measurements despite the positive correlation with EK500 echo sounders. However, Griffiths and Diaz (1996) compared the calibration of an ADCP and EK500 echo sounder and reported that the difference between the two instruments is of less than 1 dB. They concluded that this level of accuracy is sufficient for many qualitative studies.

Several studies that used an ADCP and a Multiple Opening-Closing Net Environmental Sensing System (MOCNESS) found that net samples of Crustaceans, small fish and fragments of non-gas-bearing siphonophores exhibited a significant, positive correlations with the acoustic backscattering, whereas no significant correlations were detected in net samples of other gelatinous zooplankton, pteropods, atlantic molluscs, and gas-filled siphonophores (Ressler, 2002) . In another inter-calibration study done with a MOCNESS and a 307 kHz RD Instrument ADCP, zooplankton biomass was predicted with the ADCP data to approximately ±15 mg m^{-3} (Flagg and Smith 1988). Good results were only possible after careful calibration of the current profiler. Ressler et al. (1998) described a positive empirical relationship between s_v and the MOCNESS catches of zooplankton and micronecton. Thus, the ADCP measurements may be a useful index to describe zooplankton and micronecton biomasses.
Demer et al. (2000) reported that all the beams of the ADCP have to simultaneously ensonify coherent moving animal aggregations to be able to extract the three-dimensional

velocity vectors from the school. The authors also developed a fish velocity detection algorithm, which was used to separate velocities from fish and those from other non-coherent scatterers. By using these methods and instrumentation they were able to observe fish swimming in the opposite direction to the prevailing current.

Zedel et al. (2003) used a moored downward looking ADCP to observe over-wintering and migrating herring in the Vestfjorden and Ofotfjorden in northern Norway. They observe horizontal and vertical movements of the fish schools. Horizontal movements were estimated to range from 0 to 50 cm s^{-1} with highest speeds observed during daylight. No well-defined velocity was observed during night time although increased activity was observed at dawn and dusk.

Traditionally herring observations have been done using a Simrad EK500 or EK60 scientific echo sounder (Røttingen and Tjelmeland, 2003). These instruments are not capable of measuring Doppler shifts between the received and sent signal. However, swimming speeds and directions can be estimated for single fish by tracking the target through the acoustic beam (Ona and Hansen, 1991; Handegard et al, 2005). Because this method relies on non-over lapping echoes, the technique is limited to more dispersed fish aggregations than those that can be used with the ADCP. In this paper we investigate the ability of a 3 beam ADCP to record echo amplitude and velocity data from dense schools of herring. We then compare these measurements to the Simrad EK60 data to determine whether trends in the ADCP echo amplitude data are corroborated by the patterns that exist in the more quantitative EK60 data.

Material and Methods

The study took place in the Ofotfjorden in the northern Norway during 12/12/2002 - 12/16/2002 and 12/18/2002 - 12/28/2002. Figure 1a shows the location of the experimental area in Norway and Figure 1b shows a close up of the site. Mid-December is about midway through the herring over-wintering period. Two bottom-mounted Simrad EK60 38 kHz scientific echo sounders were deployed within about 400 m from each other. The north EK60 (N1) was deployed at a depth of around 400m and the south EK60 (S1) at a depth of 500 m (Figure 1b). A remote operated underwater vehicle (ROV) with a compass and high precision underwater positioning system (HiPAP) was used to determine the position and orientation of the echo sounders. The ping rate was 1.5 pings $second^{-1}$, pulse length was 1.024 ms, the transmit power was 1000W, along ship angle 7º and athwart ship angle 23º. In reference to the fjord, the along ship angel is along the fjord and the athwart angel is across the fjord. A 190 kHz Nortek Continental Current Profiler (ADCP) was placed around 800 m east of the two EK60 and 608 m from land (Figure 1b) at a depth of around 150 m. The ADCP receiver has a gain scaling accuracy of ±1dB over the instrument temperature range (-4º C to +40º C) and a resolution of 0.33 dB. Velocity is measured using narrowband auto covariance method (Medwin and Clay, 1998). The profiler uses 3 beams with a slant angel of 25˚. The velocity range is ±10m s^{-1} and has a resolution of 0.1cm s^{-1}. The accuracy is of 1% of measured value. The ADCP data bin depth was 5 m and a 2-minute average was sampled every 10 minutes. The ADCP was calibrated at the factory. The EK60 data were logged on land while the ADCP data were logged internally on a flash disk. A CTD profile was taken at 12/13/2002. To get an overview of the geographical extension of the herring schools, acoustic data was collected from the research vessel (RV) “G.O. Sars”. Using an EK60 with a 38 kHz transducer mounted in a drop keel with a ping rate of 1 ping $second^{-1}$, pulse length was 1.024 ms, the

transmit power was 2000W, along ship and athwart ship angle was 7º. The fjord is aligned East-West and we therefore expected the tidal current to be most evident in this direction.

Evaluation of Sampling locations

Because biological and physical processes occur at various temporal and spatial scales, the differences in the geographical locations of the instruments can potentially result in measurements of different processes. In this case there is an offset between the ADCP and the EK60s.

To verify that the biomass distributions measured by the moored instruments were from the same aggregation, backscatter values were collected from the research vessel for an area that included the moored instruments (Figure 1b). The data was collected from a larger survey started at 29/11/2003 and ending 10/12/2003. This resulted that the survey pattern and timing differed between each transect around the moored instrumentation. The timing of the data used from the survey is tabulated in Table 1. The data were averaged into 185.3 m (0.1 nmi) or 926.6 m (0.5 nmi) intervals and processed to create 2-dimensional representations of the herring aggregations, which were used to characterize the spatial dimensions of the schools during the study period. If the geographical offset had minor influence on the observations the next step was to verify if the ADCP actually could measure the target biomass. To evaluate if the geographical distance between the instrumentation would have any noticeable effect, the aria confined by the instrumentation was calculated and compared to the area of the herring distribution close to the instrumentation. The vertical distribution was also compared between one of the EK60 and ADCP.

Re-sampling and EK60 Contour extraction

At the time when this experiment was conducted there where no published accounts that describe the use of this ADCP to detect herring schools. To test whether this was possible, we compared acoustic backscatter from the EK60 with that from the ADCP. The EK60 data where resampled to match the ADCP data in time (10 minutes) and depth resolution (5 m bins). All data below –60 dB was defined as out-school and all data from –60 dB to 0 dB was defined as inn-school data. This was used to create a binary mask. All values below –60 dB was labelled as zero and all values from –60 dB to 0 was labelled as one. The radial sweep algorithm (Sonka et al., 1998) was used on the mask to extract a contour outlining the border between regions. This algorithm creates contours around labelled ones on a two dimensional mask. Although the algorithm ignores holes in objects and thus often requires the application of a hole detection algorithm, it was unnecessary in this study. The contour obtained from the EK60 data was plotted on top of the ADCP backscattering to visually inspect the correspondence between the two data sources. If the correspondence was good it indicated that the ADCP has the ability to detect dense herring schools reasonably well.

In-school and out-of-school threshold

Rather than use the EK60 data, a threshold was determined for distinguishing backscatter for data collected in- versus out- of the herring schools using the ADCP data itself. This also eliminated the effect of geographical offset. Because the ADCP and EK60 acoustic transmissions differed, the echo amplitudes were expected to differ for each of the two data sets. To calculate a separation threshold from the ADCP data, it was necessary to study the probability density function (pdf) of averaged backscatter from the tree ADCP beams. The pdf for ADCP backscatter is bimodal and represents the in-school and out-of-school values. The threshold was calculated by optimal threshold (Sonka et al., 1998). In short the

backscatter pdf was modelled by two normal distributions fitted using maximum likelihood. The optimal threshold is then calculated by finding the minimum probability between the maxima of the two normal distributions, this should result in minimum error segmentation (Chow and Kaneko, 1972; Rosenfeld and Kak, 1982;Gonzalez and Wintz, 1987). At the optimal threshold there is a probability to get in-school and out-school values. To reduce this, the in-school threshold was set to one standard deviation from the optimal threshold point according to the normal distribution corresponding to in-school values. The out-school threshold was set to one standard deviation from the optimal threshold point according to the normal distribution corresponding to out-school values.

Removing invalid ADCP data

Because the ADCP uses multiple beams (at least 3) to generate 3-d velocity estimates, violations in the beam separation and the homogeneity assumptions will produce bad data. These data need to be detected and removed. Typical, homogeneity violation occurs when a school covers some beams and the rest of the beams covers water. This results in high backscattering values in some of the beams and lower backscattering in the rest of the beams.

The homogeneity assumption was tested by calculating the max-min difference between samples in corresponding ranges from the ADCP from the different beams. Finding the maximum value and minimum value from a dataset and subtracting these two values define the max-min distance. This was done for backscattering strength. Increases in homogeneity should give corresponding decreases in the differences between maximum echo amplitude values. The threshold for homogeneity was calculated by generating the cumulative probability density function (cpdf) for the max-min values. The invalid data were defined as the data containing 10% of the largest distances. This resulted in 20% of the data being classified as invalid, and thus removed from the data set. This filtering procedure reduced the noise content of the remaining data, which were used in the subsequent analyses. Interpreting data as function of time and depth can be complicated. The data were simplified for further analysis by constructing time series and probability density functions (pdf), which are described below.

Tidal current

To identify the tidal current signal in the ADCP data, the recorded surface height from the EK60 was used. We assumed that the water height is an indicator of the tidal phase. The change in sea level generally ranges between 83 cm and 243 cm in Ofotfjorden. (Statens kartverk sjøkartverket, 1997). When the surface height is at its minimum or maximum the tidal should be turning and the current at its weakest. This means that the current speed is phase shifted around 90º in relationship to the surface height. To verify this, the phase shift between the two signals is calculated. Taking the Fourier transform and finding the dominating frequency component from each signal do this. The phase from each of the components are then subtracted. The result is the phase difference between surface height and tidal flow.

Time series

Ideally time series from in-school and out-school regions should be constructed and compared to separate water flow form fish swimming speed. Since the time series constitutes velocities from different depths they can only be compared if there is barotropic flow, an indication of this is a homogen density trough depth. However, density structure will imply the presence of a baroclininc flow and the time series cannot be compared. This

is verified by looking at the calculated density profile form the CTD profile. The density calculation was based on the algorithms described in (Fofonoff and Millard, 1983).

Probability density functions

To get an overview of the speed distributions, pdfs were constructed from the time-depth data. In-school regions were mainly used to extract the data, however the vertical speed component out-school data was also used. The datasets were then used to calculate the pdfs. In addition, key statistics such as mean, standard deviation, maximum and minimum velocity were tabulated.

Results

Evaluation of Sampling locations

The effect of the differences in the geographical locations of the EK60s and ADCP in describing the spatio-temporal patterns in the herring aggregations was negligible in our analysis. Scattering layers of marine organisms, trawl catches shows mainly herring. The patch size based on the vessel data extended beyond 4 km^2. This is large enough to cover all three instruments, witch is confined within an area of 0.25 km^2, although densities vary across the patch. Thus, the density above the southern EK60, witch is located more within the patch, is relatively greater than densities above the northern EK60 and ADCP that are located more towards the perimeter of the patch (Figure 1b). In addition the same structure is evident in the EK60 and ADCP echograms.

Re-sampling and EK60 Contour extraction

The ADCP has the ability to measure schools of herring. Visual inspection of the ADCP and EK60 show good agreement between the schools and the extracted contour for both data sets (Figure 2) except in one case (around. 23/12) when the radial sweep algorithm did not distinguish between the shallow and deeper patches (Figure 2a). This was not critical because the contour is only used for visual inspection. In the EK60 data one can see that the there is herring under the ADCP. This was not measured due to the range of the ADCP. When the EK60 contour is overlaid on the ADCP data, there is overall good agreement between the schools in the ADCP data and those identified in the EK60 contour. Exception is around 21/12 where it is less herring registered by the ADCP than for the EK60. The opposite case is true for 25/12.

In- and out-of-school threshold

The threshold values for the ADCP data where estimated to [<-, -47.2] dB for the out-school data and [-30.4,0] dB for the in-school data. Figure 3 shows the calculation of the threshold. The school contours as extracted from the ADCP backscattering (Figure 4a) superimposed on the velocity and direction data. In the east west direction (Figure 4b) one can see periodical speeds in both directions. There is no evident pattern matching between school contours and the velocity data. But it is clear that different speeds dependent on depth exist inside the schools. This is also clear from the horizontal speed direction (Figure 4d). Studying Figure 4d one can also see that there exists different current directions at the same time, dependent of depth. This can bee seen at the 12/22 around 1500 hours. Between the surface to 65 m and from 100 m to 140 m depth the speed direction is around 270º. While between 65 to 100 m the speed direction is around 140º. Different speed directions also occur at the 23/12 around 0300 hour. For the vertical direction one can see burst of higher speeds, especial inside the schools and in the upward direction (Figure 4d).

Removing invalid ADCP data

The error threshold for the backscattering values was 10.64 dB. Filter mask calculated from the beam backscattering Figure 5 shows error values along the school borders. Inside the school in the upper layers less errors can bee seen. Sporadic errors are distributed around in the dataset.

Tidal current

Tidal currents likely explain the velocity trends in the ADCP data Figure 6. For example, the sea surface height is generally at a minimum or maximum when current velocities are minimal. The length of the two data sets was 1265 samples and the length of the Fourier transforms was 631 samples. A phase difference of around 93º shows that the water current is dominated by the tidal flow.

Time series

The calculated density profile (Figure 7) from the CTD profile indicates baroclininc flow. This imply that the horizontal velocities cannot be averaged trough depth and compared for in-school and out-school regions. The gaps in the time series are due to lack of data. At some time the herring schools are completely absent from the ADCP view. This is typically at daytime when the herring reside at deeper depths. This produces gaps in the in-school velocity series. Key maximum and minimum speeds is presented in Table 2. The east(positive) west velocity is dominated by the tidal current. The north(positive) south speed is dominated by a south speed component and 2 large spikes can bee seen at the 22/12 and 23/12. The vertical in-school out-school difference shows that the in-school regions sinks relative to the out-school regions.

Probability density functions

The East velocity distribution (Figure 9a), north velocity distribution (Figure 9b) and vertical velocity distributions (Figure 9c) take the form more similar to a normal distribution. There is a decrease in standard deviation from Figure 9a to Figure 9c (difference distribution), this can bee seen in Table 2. The Horizontal speed distribution (Figure 9d) has a tail to the right while the vertical direction distribution (Figure 9e) is bimodal with mode peaks around 90 and 270 degrees.

Discussion

In this paper we have studied the ability of an ADCP to observe behavioural characteristics of schools of herring. The fish mainly follow the tidal current and show a southeast direction. The vertical velocity of fish is negative relative to the water. The instrumentation used to observe is geographical separated. This means that the typical school size should be larger than the area covered by the instrumentation. Survey data shows that this is the case in this area. The stability of the readings over long periods suggests that this is the prevailing condition.

The horizontal water current velocity and fish swimming velocity was not compared due to indication of baroclininc flow. This might have been possible using a mechanical current meter. The aria covered by the schools is much larger than the distance between the beams of the ADCP. There for the homogeneity statement in Demer et al. (2000) should also hold for the data used in this study. In contrast to Demers study there was no clear indication of

movement against the current. This is reasonable since the herring is in a non-feeding state and energy minimization is important (Slotte, 1999).

The overlaid contour shows that there is a good correspondence between EK60 and ADCP backscattering. Some exceptions exists, this is most likely due to the geographical offset and not that there exists measure difference between the instruments. The contour on the horizontal speed and horizontal direction shows that speeds inside schools can have different direction and velocity. One can speculate if these differences have something to do with the school stratification or purely due to baroclininc flow. In either case this shows that the fish in large schools might move in opposite direction depending on depth. We observe a greater downward in-school speed relative to the out-school speed.

This means that the school is sinking to deeper depths in this area. Further deployments of ADCP at different position should be done to find the upward fish movement. The error values along the school border was as expected.

The border represents an area where the larges in-homogeneities occur. The fact that error values can bees seen along the top edge of the school is due to the in-homogeneities and the geometry of the ADCP beam. The farther from the ADCP the greater is the distance between the beams. This increases the probability that some beams cover in-school region or single fish while other covers water voids.

The phase difference between the east – west velocity and the surface height demonstrates the dominating tidal forces setting up the current. The horizontal directions pdf has peaks at 98 and 266 degrees which is close to the east (90 degrees) and west (270 degrees) direction. This also agree with the along direction of the fjord. The maximum speed of 24.4 cm s^{-1} agrees with the maximum speed of 20 cm s^{-1} found by Zedel et al. (2003) in the over wintering period in the Ofoten fjord.

The overall fish speed direction over the observation point is east, in to the fjord. The in-school velocities tend to dominate in the east direction.

For the north-south direction the main transportation direction is south, away from the shore.

The observations also suggest a circular movement of the herring mass. The upper layer moves from shore and out into the fjord while it slowly descents into deeper waters. Fish closer to the bottom moves into the shore and to the upper layer, this still has to be verified closer by deploying ADCP at different locations.

Acknowledgements

We thank Terje Torkelsen at the Institute of Marine Research for designing the mooring and deploying the ADCP. Nortek for lending us the Continental Current Profiler. This work was financed by the Norwegian research council grant 143539/431. Chris Wilson is thanked for comments and suggestions.

References

Brierley, S. A., Brandon, A. M., and Watkins, L. J. 1998. An Assessment of the utility of an acoustic Doppler current profiler for biomass estimation. Deep-Sea Research I, 45:1555-1573.

Demer, D. A., Barange, M., and Boyd, A. J. 2000. Measurements of three-dimensional fish school velocities with an acoustic Doppler current profiler. Fisheries Research, 47:201-214.

Chow, C. K., Kaneko T. 1972. Automatic boundary detection of the left ventricle from cineangiograms, 5:388-410.

Falgg, C. N., Smith, S. L. 1998. On the use of the acoustic Doppler current profiler to meassure zooplankton abundance. Deep-Sea Research, 36(3):455-474.

Freitag, H. P., Plimpton, P. E., and McPhaden, M. J. 1993. Evaluation of an ADCP fish-bias rejection algorithm. Proceedings from Oceans 93, Victoria, Canada, 8-21 October 1993 , Vol 2, 394-397 pp.

Fofonoff, N. P and Millard Jr, R. C. 1983. Algorithms for computation of fundamental properties of seawater. Unesco Technical Papers in Marine Sciences ,(44):53.

Gonzalez, E. C., Wintz, P. 1987. Digital image processing. Addison-Wesley Reading, MA, 2nd edition.

Griffiths, G., and Diaz, I. J. 1996. Comparison of acoustic backscatter measurements from a ship-mounted Acoustic Doppler Current Profiler and an EK500 scientific echo-sounder. ICES Journal of Marine Science, 53:487-491.

Handegard, N.O., Patel, R., Hjellvik, V. 2005. Tracking individual fish from a moving platform using a split-beam transducer. The Journal of the Acoustical Society of America, 118(4):2210-2223.

Holliday, D. V. 1974. Doppler structure in echoes from schools of pelagic fish. The Journal of the Acoustical Society of America, 55(6):1313-1322.

Huse, I., and Ona, E. 1996. Tilt angel distribution and swimming speed of overwintering Norwegian spring spawning herring. ICES Journal of Marine Science, 53:863-873.

Kaneda, A., Takeoka, H., and Koizumi, Y. 2002. Periodic Occurrence of Diurnal Signal of ADCP Backscatter Strength in Uchiumi Bay, Japan. Estuarine, Coastal and Shelf Science, 55:323-330.

Ona, E., and Hansen, D. 1991. Software for target tracking of single fish with split beam echo-sounders. User manual. Institute of Marine Research, Bergen, Norway, October. 1991.

Plimpton, P. E., Freitag, H. P., and McPhaden, M. J. 2000. Correcting Moored ADCP Data for Fish-Bias Errors at 0., 110.W and 0., 140.W from 1993 to 1995.17. NOAA Technical Memorandum OAR PMEL-117.

Ressler, P. H., Biggs, D. C., Wormuth, J. H. 1998. Acoustic estimates of zooplankton and micronekton biomass using an ADCP. The Journal of the Acoustical Society of America, 103(5):3000.

Roe, H., and Griffiths, G. 1993. Biological information from an Acoustic Doppler Current Profiler. Marine biology, 115(2):339-346.

Roe, J. S., Griffiths, G., Hartman, M., and Crisp, N. 1996. Variability in biological distribution and hydrography from concurrent Acoustic Doppler Current Profiler and SeaSoar surveys. ICES Journal of Marine Science, 53:131-138.

Rosenfeld, A., Kak, A. 1982 Digital picture processing. Computer science and applied mathematics. Academic Press, New York, 2nd edition.

Røttingen, I., and Tjelmeland, S. 2003. Evaluation of the absolute levels of acoustic estimates of the 1983 year class of Norwegian spring-spawning herring. ICES Journal of Marine Science, 60(3):480-485.

Slotte, A. 1999. Differential utilization of energy during wintering and spawning migration in Norwegian spring-spawning herring. Journal of Fish Biology, 54(2):338-355.

Sonka, M., Halavac, V., and Boyle, R. 1998. Segmentation in Image Processing, Analysis, and Machine Vision. Second ed., pp. 142-143. Ed. by Jeans, S. PWS Publishing, USA. 770 pp.

Statens kartverk sjøkartverket. 1997. Den norske los 1. Alminnelige opplysninger. 6 edition. ISBN 82-90653-12-3.

Vabø, R. 1999. Measurements and correction models of behavorial induced biases in acoustic estimates of wintering herring (Clupea harengus L.). University of Bergen, PhD Thesis, Bergen. 161 pp.

Wilson, C. D., and Firing, E. 1992. Sunrise swimmers bias acoustic Doppler current profiles. Deep-Sea Research, 39(5):885-892.

Zedel, L., Knutsen, T., and Patro, R. 2003. Acoustic Doppler current profiler observations of herring movement. ICES Journal of Marine Science, 60:846–859.

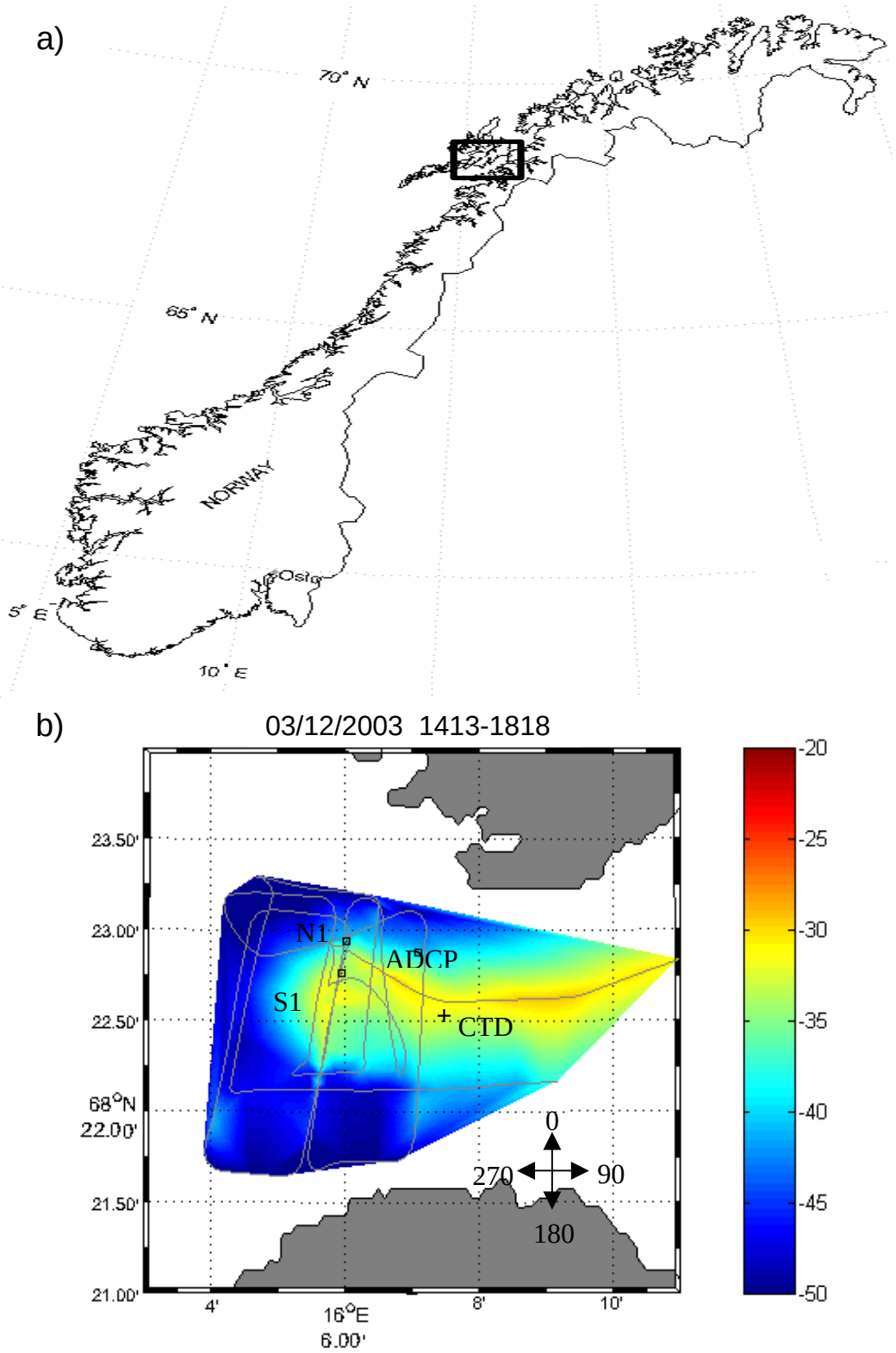

Figure 1. Geographic location of the experimental aerial. a) Location of the Ofoten in Norway. b) Location of the Simrad echosounder (N1 is North EK60 and S1 is South EK60), acoustic Doppler current profiler (ADCP) and spatial distribution of herring biomass based on survey data. Survey track is seen as grey solid line. The colour bar is in S_A (dB). Squares indicate position of the instrumentation. Some anomalies can be seen due to the triangulation and interpolation of the ship data between the ships.

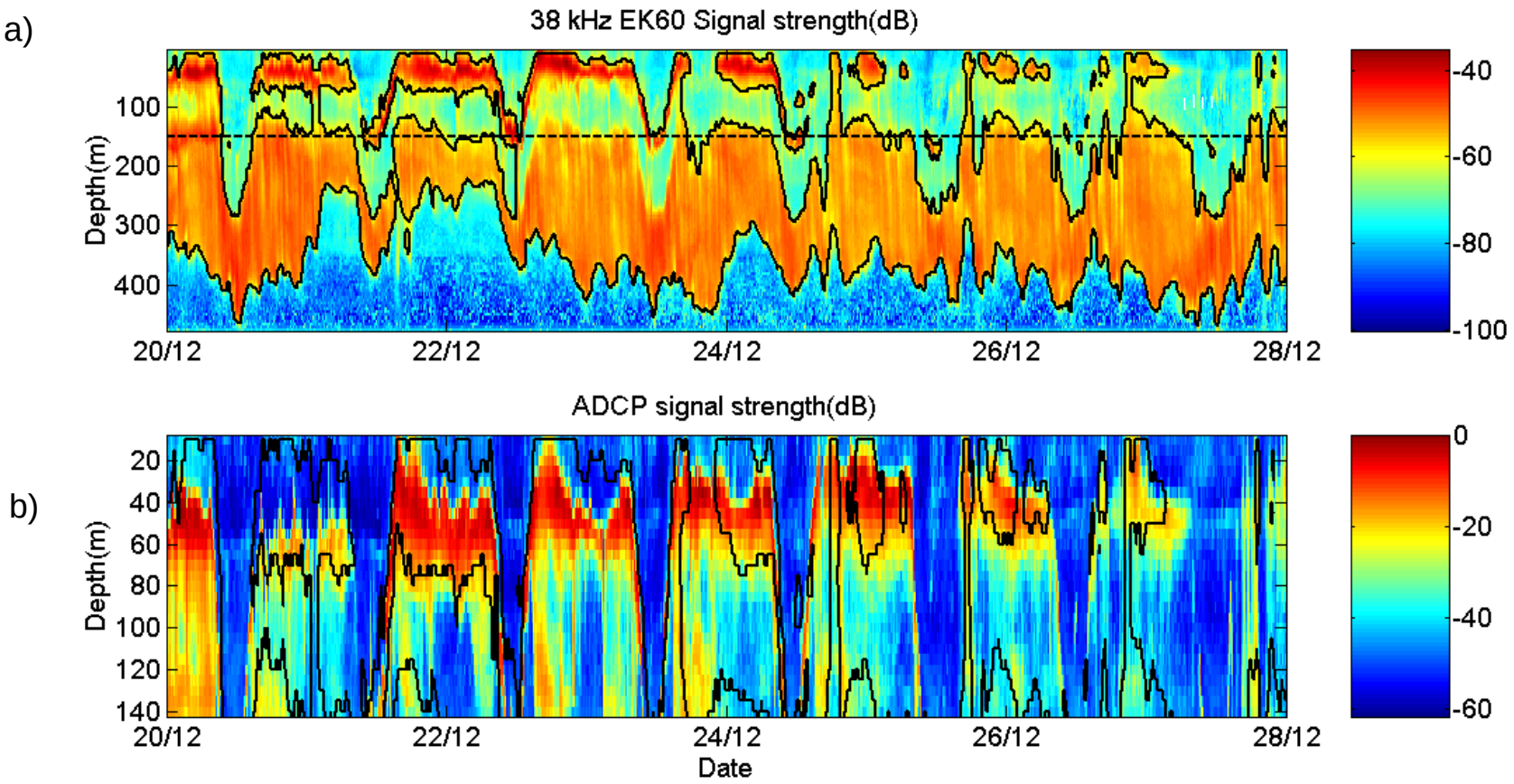

Figure 2. Echograms based on the EK60 (a) and ADCP (b). The solid black line shows the extracted contour based on the EK60 data, which represents the border between backscatter classified in-school versus that classified out-of-school. This line is displayed on both plots. The dashed line shows the depth of the ADCP. The colour bars give volume scattering strength in (dB rel 1 m^{-1}). All volume backscattering values are in relative terms.

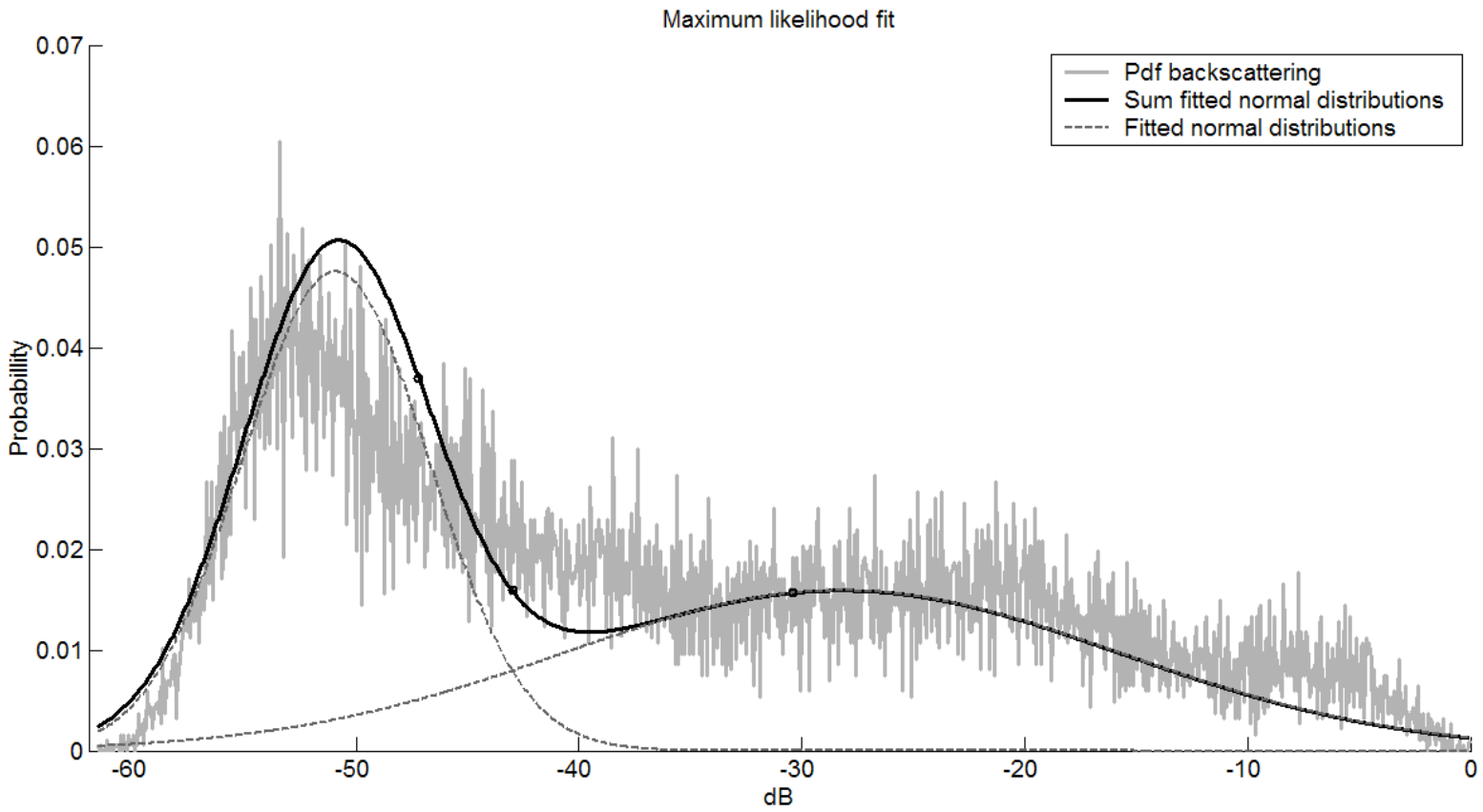

Figure 3. Calculating threshold for in-school data and out-school data. Light grey curve is pdf of ADCP backscattering data. Hatched curves is fitted normal distributions and black line is the sum of fitted normal distribution. Middle marker shows the optimal threshold value at –43.0 dB. Left marker is threshold for out-school data and has a value of –30.4 dB. Right marker is threshold for in-school data and has a value of –47.2 dB.

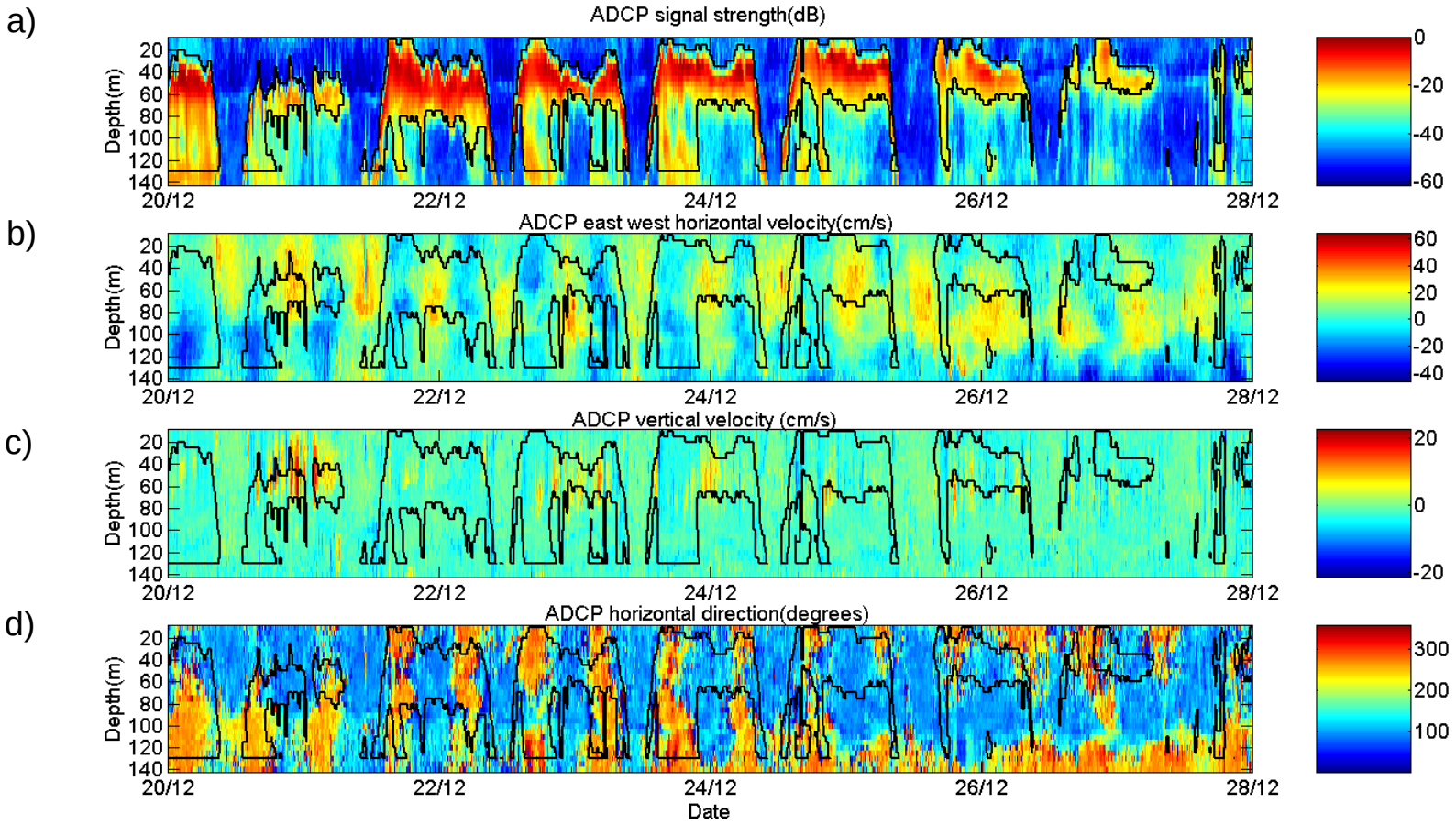

Figure 4. ADCP data with in-school contour (black lines) based on ADCP backscattering data (see text for explanation). a) ADCP echo amplitudes. The colour bars give volume scattering strength in (dB rel 1 m^{-1}). b) East-west velocities. Negative values are to the east. Colour bar gives speed in cm s^{-1} c) Vertical velocities, Positive values are toward the surface. Colour bar gives speed in cm s^{-1} d) Horizontal velocity direction in geographical degrees where 0 = north. Colour bar gives direction in degrees.

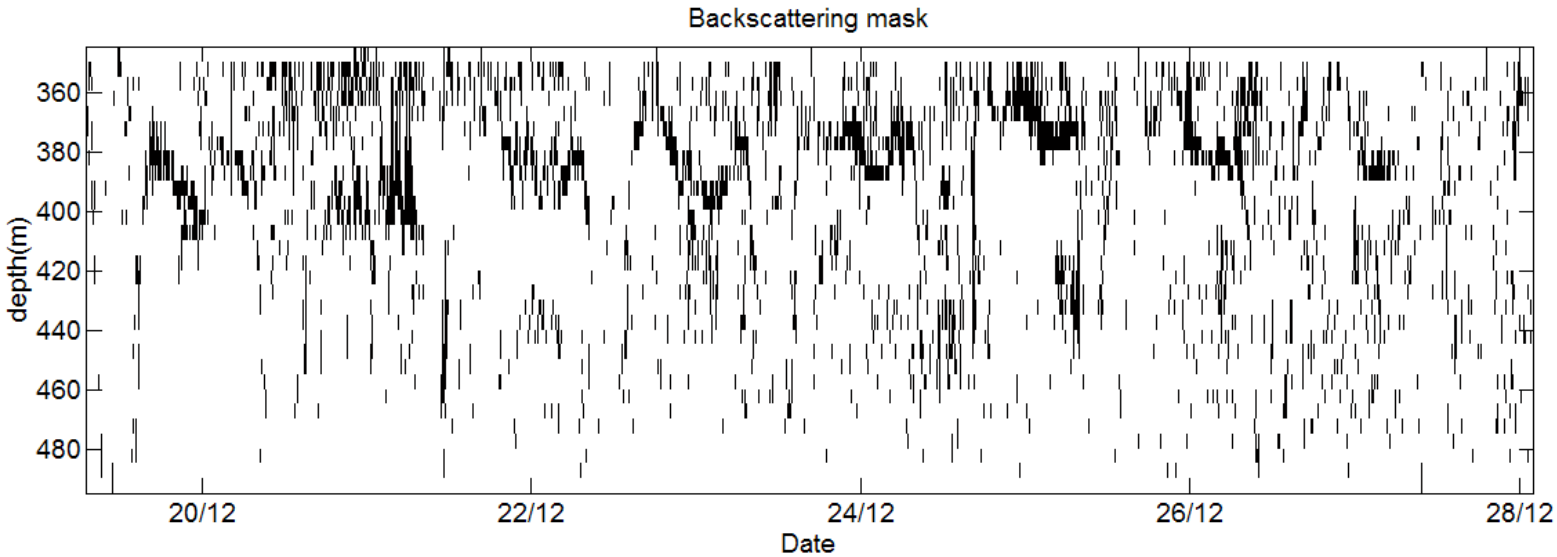

Figure 5. Mask for valid backscattering values. Black dots indicate invalid values.

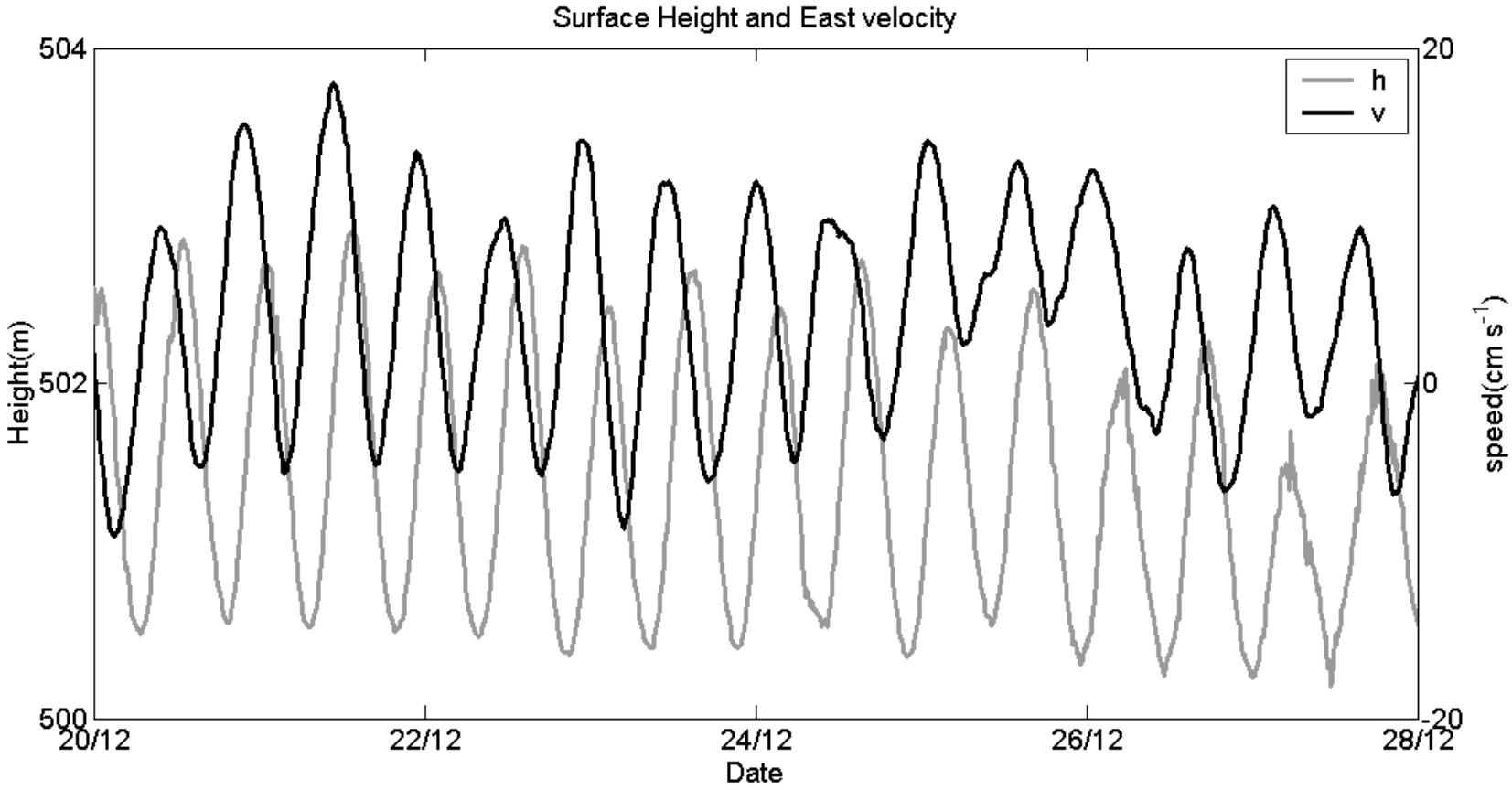

Figure 6. Tidal current and sea surface height relative to sea floor. The phase shift between the dominating frequency components is 93º.

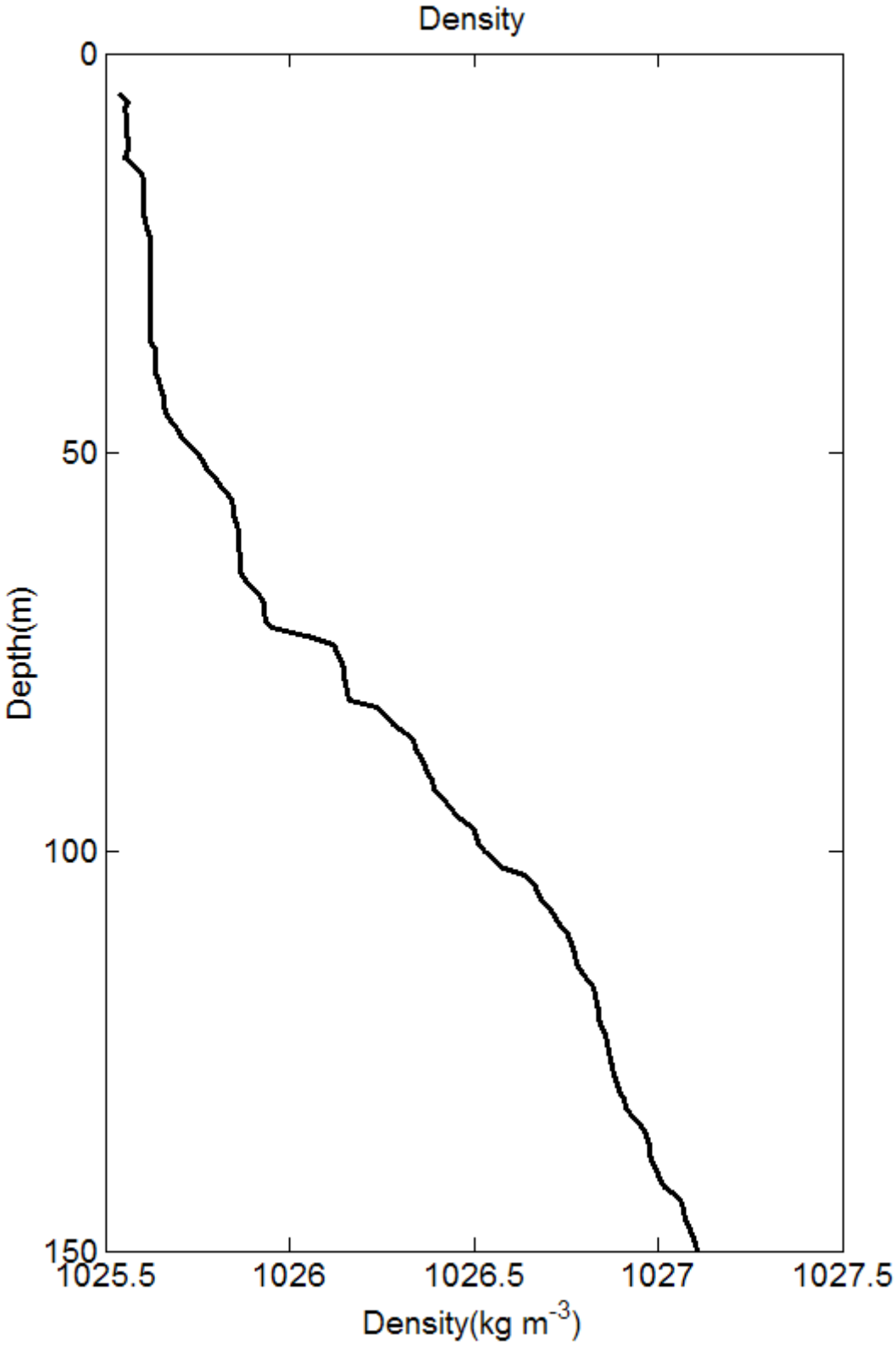

Figure 7 Calculated density profile from the CTD profile

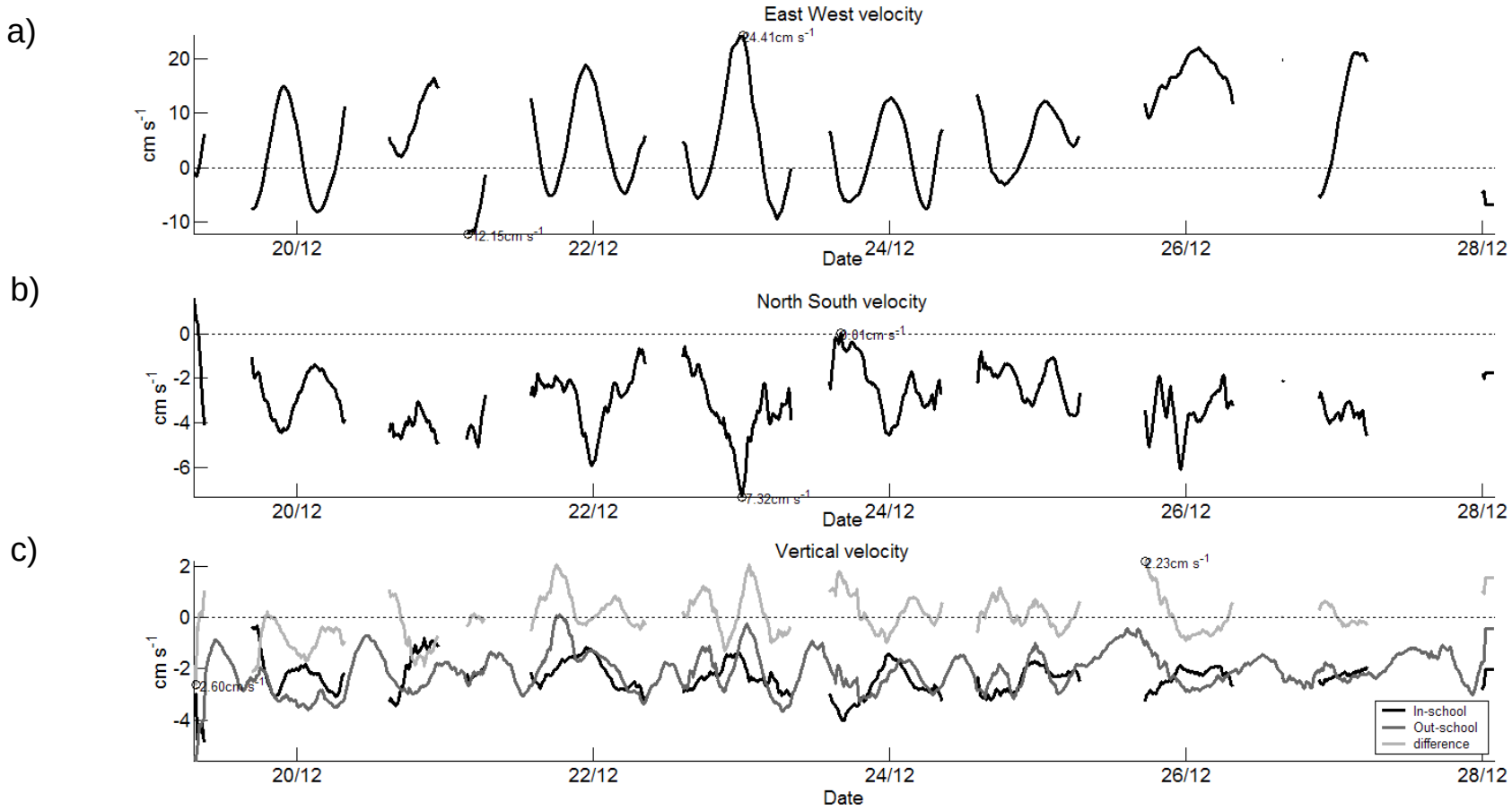

Figure 8. Velocity of in-school, out-school, and difference between in-school and out-school speeds. a) East-west velocity, u. b) North-south velocity, v. c) Vertical velocity, w.

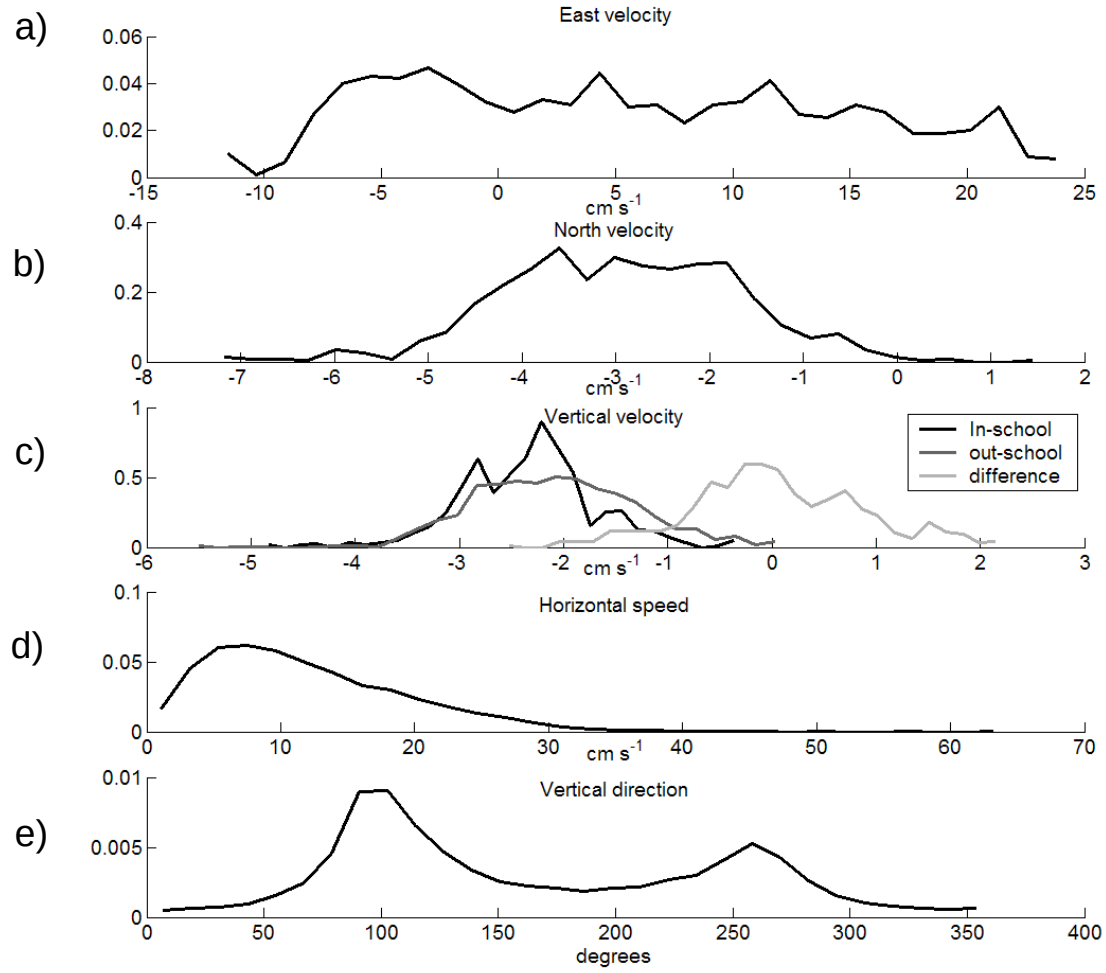

Figure 9. Probability density functions of in-school (solid line) and out-school (dashed line) data based on entire data set. a). East-west velocity where east is positive. b) North-south velocity where north is positive. c) Vertical velocity where upward is positive. d) Absolute horizontal speed. e) Geographical direction of absolute horizontal speed.

Table 1. Timing of data used from the survey to study geographic dispersion of Herring at the instrumentation area.

Date	Start Time	Stop Time	Duration (h:mm)
29 Nov 2003	0732	0934	2:02
29 Nov 2003	1050	1348	2:58
02 Dec 2003	0645	0738	0:53
03 Dec 2003	1413	1818	4:05
08 Dec 2003	1247	1616	3:29
09 Dec 2003	0005	0309	3:04
10 Dec 2003	0011	0059	0:48
10 Dec 2003	0132	0241	1:09
10 Dec 2003	0241	0343	1:02
10 Dec 2003	0424	0526	1:02

Table 2. Key maximum and minimum speeds from time series in Figure 8.

	East West in-school speed (cm s^{-1})	North South in-school speed (cm s^{-1})	Vertical velocity in-out-school difference (cm s^{-1})
Maximum speed	24.4	0.0	2.2
Minimum speed	-12.2	-7.3	-2.6
Mean speed	5.4	-3.0	-0.3
Std speed	9.1	1.3	0.8